University of Stellenbosch

Masters Thesis

Options to reduce sediment build-up in a surf zone trench protected by an open-ended cofferdam

Author:
Jacobus Johannes Müller

Supervisor:
Mr. Geoffrey Toms

A thesis submitted in fulfilment of the requirements
for the degree of Master of Engineering
in the

Department of Civil Engineering

March 2015

Declaration of Authorship

By submitting this thesis electronically, I declare that the entirety of the work contained therein is my own, original work, that I am the authorship owner thereof (unless to the extent explicitly otherwise stated) and that I have not previously in its entirety or in part submitted it for obtaining any qualification.

Signed: _____

Date: _____

UNIVERSITY OF STELLENBOSCH

Abstract

Port and Coastal Engineering
Department of Civil Engineering

Master of Engineering

Options to reduce sediment build-up in a surf zone trench protected by an open-ended cofferdam

by Jacobus Johannes Müller

When constructing a submarine pipeline, construction teams must work in the hostile environment in the ocean known as the surf zone. The surf zone is the area along a shoreline stretching between the first evident point of wave breaking and the beach line. In order to ensure that the pipeline is shielded from the imposing forces within the surf zone, engineers use a burial technique which leaves the pipeline length in the surf zone buried underneath the active seabed once construction is finished.

Thus a temporary surf zone trench is dredged and protected by an open-ended cofferdam built using iron sheet piles. As a result of the incoming wave climate and the surf zone currents created by this wave climate, sedimentation in and around the trench becomes problematic. In this study alternative geometric layouts for the open-ended cofferdam protecting the surf zone trench are investigated, attempting to minimize the sediment build-up in and around the trench.

This was done by using both a 3D qualitative physical model conducted at the CSIR in Stellenbosch, and numerical model using MIKE developed by DHI. However, this study only considers sediment build-up and not structural integrity and constructability of the cofferdam designs.

Combining the observations of both the physical- and numerical models, a conclusion was drawn that a structure built perpendicular to the shoreline with a 45^oextended arm built from the upstream edge of the cofferdam wall, is the most effective. No dimensions are given as the cofferdam design will change depending on the site specific characteristics. Also an increase in structure length will result in the mouth of the structure being located outside the active sediment zone, which leads to a longer period of time before the pipeline pathway is compromised by sediment.

STELLENBOSCH UNIVERSITEIT

Opsomming

Fakulteit van Siviele Ingenieurswese
Kus en Hawe Ingenieurswese

Meesters in Ingenieurswese

Options to reduce sediment build-up in a surf zone trench protected by an open-ended cofferdam

deur Jacobus Johannes Müller

Tydens die konstruksie van 'n onderwaterse pyplyn, moet konstruksie spanne in 'n gevaarlike gedeelte van die see werk naamlik die brandersone. Die brandersone kan gedefinieer word as die area tussen die eerste punt waar branders breek en die strandlyn. Om die pyplyn te beskerm teen die kragte wat branders op dit uitoefen, gebruik ingenieurs 'n installasietegniek waar hul die brandersone seksie van die pyplyn onder die aktiewe seebodem begrawe.

Om die tegniek te bewerkstellig, grawe kontrakteurs 'n sloot deur die brandersone en beskerm dit met 'n tydelike struktuur bekend as 'n kofferdam. As gevolg van die inkomende branders en die strome wat deur die branders aangedryf word, kan die opbou van sediment in, en rondom die sloot in die brandersone problematies word. Hierdie studie ondersoek alternatiewe uitlegte vir die tydelike kofferdam struktuur met die oog daarop om die opbou van sediment in, en rondom die struktuur te verminder.

Die doel was nagestreef deur gebruik te maak van beide 'n 3-dimensionele fisiese model, gebou en gebruik by die WNNR in Stellenbosch, en 'n numeriese model wat op MIKE, ontwikkel deur DHI gedoen was. Let wel die studie het slegs die sediment beweging in die nabye area van die tydelike kofferdam struktuur in ag geneem en nie die praktiese implimentering en strukturele integriteit van die struktuur nie.

Deur die observasies van beide die fisiese- en numeriese modelering in ag te neem, is die volgende gevolgtrekkings gemaak. 'n Struktuur wat loodreg met die strandlyn gebou is en met 'n 45^o arm wat na die stroom-op kant toe uitstrek, was die mees effektiewe een. Geen dimensies is deurgegee nie aangesien die ontwerp sal verskil afhangende van die spesifieke area waar die projek aangepak word. Daar is ook gesien dat indien die struktuur langer gemaak word, sal die kontrakteur langer tyd hê voordat daar sediment probleme in die brander sone sloot ondervind sal word.

Acknowledgements

- First I would like to acknowledge our Heavenly Father for the strength he gave me in order to complete this study.
- The support I received from my family and close friends were of immeasurable value to me and without them this would not have been possible.
- I want to acknowledge Mr Geoffrey Toms for the guidance and knowledge he gave me as my supervisor over the past 2 years. I wish him the best of luck on his journey to the Middle East.
- I would like to acknowledge the following companies and individuals for their support and resources which allowed me to complete my study the way I did:

  From Clough Murray & Roberts Marine (Cape Town)

  Frederik Theron

  Alec Dixon

  Karl Heath

  From the CSIR (Stellenbosch)

  Kishan Tulsi and his team

  From PRDW (Cape Town)

  Stephen Luger

Contents

List of Figures

List of Tables

Symbols

A	Dean formula scale parameter; Empirical coefficient
C	Chezy coefficient
c	wave speed or also denoted as wave celerity or phase speed
c_f	friction coefficient
d	water depth
d_1	depth of closure
d_b	water depth at breaking
D	sediment particle diameter
$D_{50}; d_{50}$	median grain size
E	wave energy
E_b	dissipated energy as a result of wave breaking
F_x	wave induced radiation force in the x-direction
F_y	wave induced radiation force in the y-direction
g	gravitational acceleration
h	Dean formula water depth
H	wave height
H_o	deep water wave height
H_b	wave height at breaking point
H_e	nearshore significant wave height
H_{max}	maximum wave height
H_s	significant wave height
$I_1; I_2$	Einstein Integrals
k_s	bed roughness
k	constant
L	wavelength; structure length
L_o	deep water wavelength
n	ratio of group wave velocity over phase speed
p	porosity
P	hydrostatic pressure

$Q_{breaking}$	momentum due to wave breaking
Q_{total}	total momentum
Q_x	horizontal momentum
q_b	Bijker bed load transport
q_s	Bijker suspended load transport
q_t	Bijker total load transport
S_b	beach slope
S_{down}	sediment transport in the downward direction
S_{gross}	gross longshore sediment transport rate
S_{net}	net longshore sediment transport rate
S_{up}	sediment transport in the upward direction
S_{xx}	normal radiation stress in the x-direction
S_{xy}/S_{yx}	shear radiation stress
S_{yy}	normal radiation stress in the y-direction
S'_{xy}	turbulent shear stress
T	wave period
T_e	nearshore significant wave period corresponding with H_e
T_p	peak wave period
T_s	significant wave period
T_z	zero crossing wave period
u	particle velocity
V	longshore current velocity
$V_{*,cr}$	critical bottom shear velocity
v_t	eddy viscosity
W	surf zone width
w_s	structure width
y	Dean formula cross-shore distance
β	incidence angle
ζ	Iribarren number
η	water surface elevation relative to SWL
γ	breaker index
ρ	mass density
ρ_s	density of sediment grains
μ	ripple factor
σ	standard deviation
τ_{cw}	critical bottom shear stress
$\tau_{b,y}$	longshore bed shear stress
θ	dominant wave direction
ω	angular frequency

Chapter 1

Introduction

1.1 Background

The ocean is one of the world's largest and most diverse of natural resources. The ability to access natural oil and gas fields lying within the oceanic boundaries are very important despite the fact that the search for alternative energy sources continues. Also as the need for fresh water increases all over the world, intake structures are required to obtain salt water as a resource to be used in desalination plants. In order to transport these resources via pipeline, safe construction into and beyond the hostile area between the shoreline and the initial point of wave breaking, called the surf zone, is a prerequisite. Construction projects in these areas are referred to as shore crossings.

Over the last 10 years various projects involving shore crossings have been completed, such as the seawater intakes at Mossel Bay (2011) and at Trekkopjes in Namibia (2010) [1] where it was necessary to lay pipelines through the surf zone[2]. Obstructions in the surf zone can have drastic consequences in a short amount of time due to the interference of currents and sediment transport along the shoreline. If these consequences are not understood, they can cause serious problems to both the construction team and the environment. Consequences include the accretion of sand in, and upstream of the structure and also erosion processes downstream of the structure. The method that is used to build a pipeline through the surf zone requires the construction of a trench through the surf zone, protected by using a sheet pile structure to form a cofferdam. The cofferdam not only protects the trench but also ensures a safe working environment for the construction team.

It is thus quintessential to know what type of structures to design, both temporary and permanent, to optimize the construction process and to minimize the interference, due to sediment infill and scour problems. The continuous maintenance of the construction

[1] For exact locations refer to Chapter 3

[2] Throughout this report the locations of the two case studies will be referred to as Mossel Bay and Trekkopje

site is also very expensive and as such, the financial gain from finding a solution to this problem poses as a big incentive for this study.

In this study, research is done in order to find the optimal geometric layout for the temporary structures (cofferdam) in the surf zone to minimize the sediment build-up in the surf zone trench. The coastal processes will be taken into account and the different geometric layout options will be investigated by means of physical- and numerical modelling.

1.2 Problem Statement

Clough Murray & Roberts Marine is one of the major contractors in marine construction. In recent projects around the coast of southern Africa they were required to install submerged pipelines running from the on-land facilities into the ocean, where the pipelines are used as intake structures for sea water. In order to install a pipeline in a hostile surf zone, protection is provided by an open-ended cofferdam constructed from sheet piles driven into the seabed. The goal of the cofferdam is twofold. Firstly it protects the working environment from the incoming wave climate, thereby creating a safe construction area for the people at work. Secondly it protects the surf zone trench, that was dug through the surf zone, from sediment build-up as a result of sediment transport mechanisms. Although the cofferdam can provide temporary protection against sedimentation, in time the sediment build-up at the mouth of the structure is inevitable.

1.3 Objective

The objective of this study is to improve the geometric layout of an open-ended cofferdam in the surf zone to reduce the sediment build-up at the mouth of the cofferdam which is caused by continuous wave processes and longshore currents.

1.4 Solution Approach

Following from the problem statement in Chapter 1.2 and the objective in Chapter 1.3 a solution approach was determined. This approach was determined to fit both the availability of resources and time. A literature study will be done explaining the processes at hand and identifying other studies with similar characteristics and will also investigate other projects where cofferdams have been used inside a shore crossing project. After a brief discussion of the two case studies that served as primary motivation for this study, a solution will be proposed after using both physical and numerical modelling. Both modelling types have their own goal and will reinforce each other to make sure that the conclusion is made with an informed base of knowledge and understanding.

Initially a qualitative physical model will be built at the CSIR's hydraulic laboratories in Stellenbosch. The goal of the physical model is twofold. Firstly it serves as a visual aid in the understanding of sediment movement and the processes at hand around a surf zone trench protected by a cofferdam structure. Secondly, the sensitivity of changes to sedimentation processes due to changes in the wave climate is investigated to determine what effect the water level, wave direction and wave height will have on surf zone sediment movement. The same trends will be observed and further investigated using a numerical model.

MIKE 21/3 Coupled Model (FM) will be used to investigate alternative options to the cofferdam layout. Due to the vast number of possible structural forms, a number of scenarios will be chosen to model and investigate. As the aim is to better understand the geometric layout of the structure, all input parameters will be kept the same leaving only one variable, which is the shape of the structure itself. A qualitative validation of the numerical model will then be done using the physical model and literature study to judge the accuracy of the model runs based on the formulation of the surf zone processes. Sedimentation problems are unique to each area and for that reason the numerical tests of a somewhat idealised situation will be compared with each other and no specific quantities and rates will be determined from them.

1.5 Report Outline

The report will investigate the processes in the surf zone by means of a literature study in Chapter 2. This will provide a good background of the processes responsible for the movement of sediment around surf zone structures. Also included in Chapter 2 is a brief discussion of the design and construction of surf zone structures and other studies done on hard surf zone structures. This also includes the investigation of past projects where surf zone cofferdams have been used within a shore crossing project.

A brief description of the two case studies which fostered the research in this report is given in Chapter 3.

The scope of work, setup and results of the physical modelling undertaken in this study will be discussed in Chapter 4, followed by a brief discussion on the numerical model and its results in Chapter 5.

Chapter 6 concludes the study by combining the concluding remarks of both the physical and numerical modelling and gives a full study conclusion.

Recommendations for future studies are provided in Chapter 7 .

Chapter 2

Literature Review

2.1 Literature Introduction

The literature review will cover two main aspects. It will primarily focus on the description of the surf zone and the processes therein, such as sediment movement and surf zone currents. In order to understand these processes, a brief background on the driving forces responsible for them will be discussed, explaining their relevance to this study. In the second part of the literature review a brief description of submarine pipelines and cofferdam construction is given and past research on surf zone structures is reviewed.

2.2 Surf Zone Processes

The area of concern for this study is the *surf zone* where sediment movement is most prominent. It is for that reason that this literature study will start by assuming that the waves arriving at the edge of the closure depth have already undergone certain processes by which they have been generated, sorted and the wave condition applicable to the specific area is fully developed. This literature review will thus start by explaining the processes from a point just beyond the seaward extent of the *storm surf zone*.

Wave particle velocities, both horizontal and vertical, and their displacements follow circular motions in deep water. As the wave enters shallower water, energy starts to dissipate on the seabed as a result of bottom friction. This bottom friction is the transference of energy and momentum from the water particles to the boundary layer, the rate of which is dependent on the particle velocity and the shear stress directly above the boundary layer (Holthuijsen, 2007). Once this starts to happen the wave particle motions are no longer circular but takes on an elliptical shape. This effect is shown in Figure 2.1 below.

Note: This image is not drawn to scale. It is mere an interpretation of the explained phenomenon.

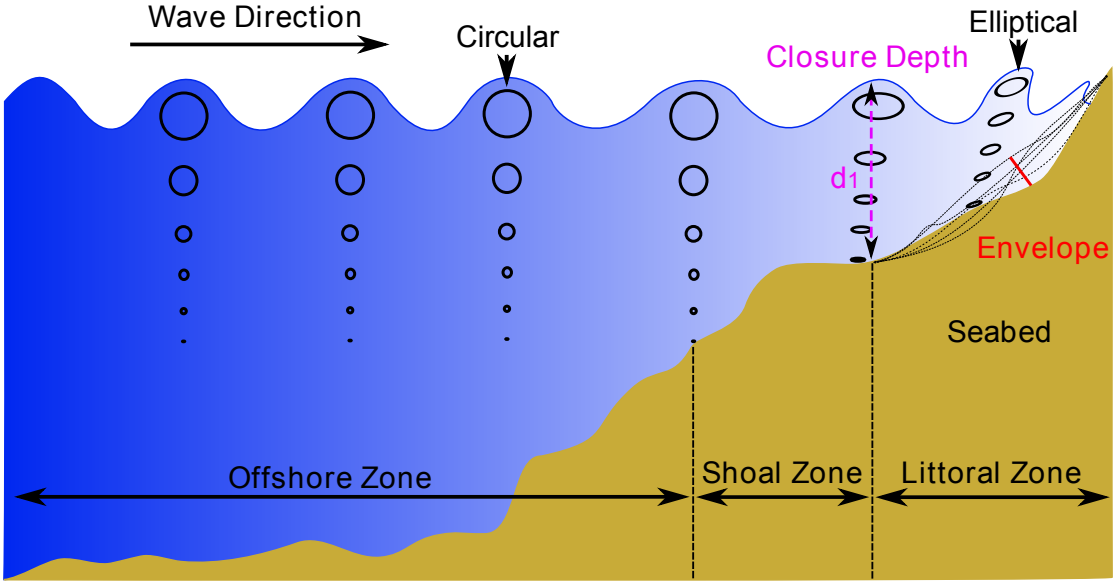

FIGURE 2.1: Water Particle Motions and Closure Zonation (Adapted from Hallermeier (1981))

The seabed also undergoes significant changes in this area close to the shoreline as indicated by the dashed lines in Figure 2.1. The point where the seabed becomes more stable and where these bathymetric changes do not occur any more is known as the *closure depth*. As the bathymetry inside the closure depth is quite variable in shape and depth, the distance between the lowest recorded seabed and the highest recorded seabed is known as the *envelope*. The closure depth which is the most seaward point of significant wave driven sediment transport, does however take storm events into account and can be situated a long distance offshore. The phrase contains the statement "significant" for a reason, as it needs to be made perfectly clear that there will still be sediment movement outside of this boundary but on a very small scale. Outside of this boundary sediment particles will move side to side as a result of the wave energy interacting with the seabed but the sediment will not move great distances as a result of wave energy or wave induced processes. In summary, sediment movement will still be visible seaward of this boundary, especially during storms, however on a much smaller scale than on the shoreward side of it (Wright et al., 1991).

In earlier research by Capobianco et al. (1997) and Nicholls et al. (1996), it was identified that different closure depth formations apply for different time scales. Four time scales were identified, namely: a small time scale for single events to seasons, a medium time scale for a time period ranging from one year to one decade, a large time scale ranging from a decade to a century and then a very large time scale for a time period of

centuries to millennia. Hallermeier (1981) suggested that the depth of closure (d_1) can be calculated using the following formula :

$$d_1 = 2.28H_e - 68.5(\frac{H_e^2}{gT_e^2}) \tag{2.1}$$

where H_e is the annual nearshore significant wave height exceeded 12 hours per year, T_e is the corresponding wave period and g is the gravitational acceleration. H_e in this case is a statistical parameter which can be calculated by using a formula derived by fitting a modified exponential distribution as seen in Hallermeier (1981):

$$H_e = \bar{H_s} + 5.6\sigma \tag{2.2}$$

where $\overline{H}_s$ and σ are the mean annual significant wave height and the standard deviation respectively. This limit is set and defined as the boundary of significant sediment movement as seen in Figure 2.1[1] The shoal zone also contains some sediment movement but the significance of this is unimportant as the amount of sediment moved in this zone is too small and can be ignored. Thus the area of concern will be the shoreward part of the littoral zone as defined in Figure 2.1.

Although Hallermeier's equation delivers a reasonable estimate of the closure depth, Birkemeier (1985) used the equation in a previous study and compared it to field measurements documented. The result of this study was the recalibration of the coefficients used in the Hallermeier equation and hence delivering a more accurate estimate of the closure depth. The improved formula is:

$$d_1 = 1.75H_e - 57.9(\frac{H_e^2}{gT_e^2}) \tag{2.3}$$

The understanding of this energy transfer boundary is most important when designing temporary works for a submarine pipeline. This will be thoroughly discussed in this study's results. Note that if the mouth of an open-ended structure is situated within this boundary, it will be exposed to much more sediment movement than that of one situated outside of this boundary.

[1]Note: The boundary of sediment movement may move as a result of water level changes or the changes in wave height.

The closure depth however, is not a set depth all the time. It will shift around due to an increase of wave height or water level. For example, a study done by Bruun (1962) envisioned the closure depth of east Florida at a depth of 18 m. However, a nourished beach design done in the same area in 1991 revealed that the closure depth of this same area is believed to be as shallow as 4 m. This variation in closure depth can have a major effect on the transport of sediment in the surf zone. No studies have been done in recent years to indicate what the closure depth is of the specific locations of the case studies considered in this study, but a study done by Mather and Strech (2012) shows an average closure depth of 15 m around the eastern coast of South Africa. This can be explained by looking at the characteristics of the eastern coast of South Africa. The coast is exposed to deep sea wave conditions as there is no protection in the form of bays in this area. The exposed sites combined with deep water areas, lead to a deep closure depth result. However, when considering the wave climate around the southern coast of South Africa, the closure depth at Mossel Bay and around the southern coast of South Africa is believed to be much less as the nearshore wave climate is not as violent as that of the eastern coast. The waves at Mossel Bay for example are waves reaching the nearshore zone in a sheltered area. Deep sea wave conditions are blocked and diffracted around the headland resulting in a much calmer and smaller wave condition at the shoreline. If the western coast is considered, the closure depth is once again believed to be much deeper as the wave climate here is much larger. The western coast, for example the coast of Namibia, is exposed to larger wave conditions as the shoreline is not sheltered.

The calculated Hallermeier closure depth for the Mossel Bay site location (refer to Chapter 3 for site location) is 6.5 m. Nearshore wave data that was recorded by the CSIR's (Stellenbosch) waverider buoy off the coast of Mossel Bay, at a sheltered location well inside the bay, over the last 7 years was used to calculate this value and the calculations can be found in Appendix A. The data was collected on behalf of the Transnet National Port Authority (TNPA). As expected, this closure depth is shallower than that of the east coast of South Africa, as shown by Mather and Strech (2012). A closure depth of 11.84 m was calculated for Trekkopje, Namibia. Nearshore wave data from Clough Murray & Roberts Marine (2010) was used to calculate this value and can be found in Appendix A. As expected this is a much larger value than the calculated closure depth of the Mossel Bay site. Landward of this point we can refer to the waves as being *depth limited* waves. Depth limited waves entails that the wave characteristic (wave height, wave breaking, etc.) is now a function of the water depth. This means that the wave height is limited by the water depth and as the wave moves beyond a certain water depth the wave becomes unstable and breaks. For breaking criteria refer to equation 2.5 and 2.6 on page 12.

Although it will be ideal for temporary structures with the purpose of blocking sediment transport, such as a cofferdam, to be built to a depth that surpasses the closure depth, this is an unrealistic request for contractors with short duration operations (eg. weeks or months, not years) due to economic constraints. At some locations, for instance the coastline at Trekkopje, the closure depth could be several hundred meters offshore and the cost and time it will take to build the temporary cofferdam to this depth will not be justified considering the cost of the project or maintenance of a far shorter structure. Also, the closure depth is based on the historical movement of the seabed meaning that major storm events are included in the calculations thereof. For a temporary structure, not typically erected for longer than 4 months, it will be over conservative to design for major storm events such as a 1 in 10 year, or bigger, storm. It is for these reasons that the surf zone becomes the realistic boundary to surpass when considering the use of a temporary cofferdam in the pipeline installation process.

The surf zone can be properly defined in the following manner. Consider a coast with a seabed and beach consisting of sand. The bed slope will usually be fairly shallow. Waves will therefore start to break at some distance from the shoreline. At this initial point of breaking the wave will have a wave height H_b and be orientated at an angle β to the beach line. The region between this initial breaking point and the beach is known as the *surf zone* for that wave condition (Chadwick, 1989).

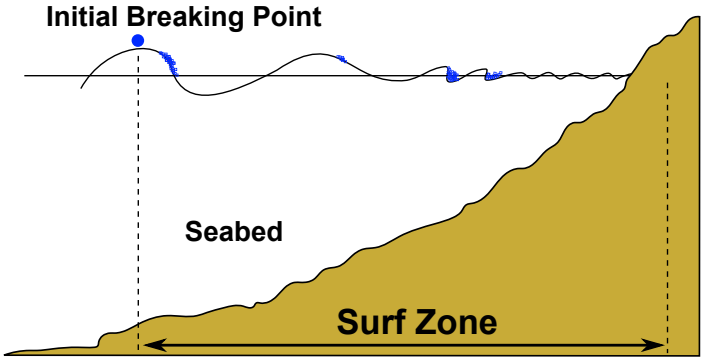

FIGURE 2.2: Surf Zone Definition

At this point waves have already experienced modifications which will progress even faster from this point on. Modifications such as shoaling, refraction and breaking are mainly due to bathymetric changes, or changes in water depth, and modifications such as diffraction and reflection are due to obstacles (such as cofferdams) in the path of the propagating wave condition. These processes defines the characteristics of a wave condition, which is responsible for the driving forces of surf zone sediment transport.

Shoaling is the increase of wave amplitude as a result of energy being bunched up near the coast. When a wave propagates in shallow water the wave velocity [2] (a.k.a. wave celerity) decreases and gets closer to that of the wave group velocity. Such variation in group velocity causes variations in the local wave energy, hence an increase in local amplitude (Holthuijsen, 2007). Shoaling is best visualised by looking at a linear sloped seabed with a contour parallel to that of the propagating wave crest, and consequently the wave will have an incidence angle (β) of 0^o. A wave's *incidence angle* is the angle at which the wave energy makes contact with an obstacle or the seabed as seen in Figure 2.3.

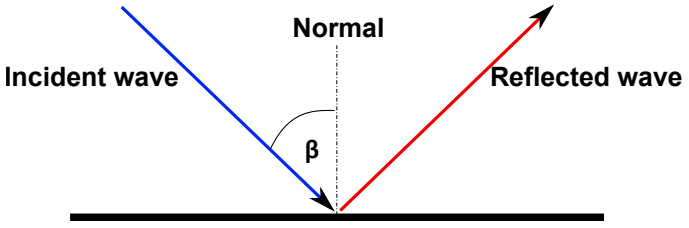

FIGURE 2.3: Incident Wave Angle

If the contour of the seabed is not parallel to the crest of the propagating wave, then the wave has an incidence angle other than 0^o and a process called *refraction* will occur (Figure 2.4) (Chadwick et al., 2004). As the wave energy is affected by the seabed, the wave velocity decreases as it is a function of the water depth. It is important to remember that the period is unchanged. The angled contour causes a lateral difference (different points on the same wave crest) in the wave velocity. This lateral change will cause the wave crest direction to change and will cause the wave to bend towards the shallow water. This can be illustrated using wave rays[3] and is also known as Snell's law of refraction:

$$\frac{sin\beta_1}{d_1} = \frac{sin\beta_2}{d_2} = k \tag{2.4}$$

Where β is the incidence angle and different points along a wave ray as indicated by the subscripts $_1$ and $_2$, d is water depth at respective points, and k is always constant.

Diffraction on the other hand is the change of wave direction due to an interruption by obstacles (such as surf zone structures) in the path of a propagating wave. It can be defined as the process by which the energy is interrupted and spread along the wave's crest, leading to the presence of waves in the shadow zone, leeward of the obstruction (Holthuijsen, 2007).

[2] The wave speed/velocity/celerity is the speed at which the wave moves across the seabed.
[3] Wave rays are lines orthogonal to the wave crest.

FIGURE 2.4: Showing wave crest refraction at Trekkopje, Namibia (2010)(Photo: Clough Murray & Roberts Marine)

Reflection is the rebound of energy in the opposite direction to that of the incidence wave due to the presence of an obstruction. Reflection occurs on the exposed side of an obstruction whereas diffraction will occur on the protected side of the obstruction. Both the processes of diffraction and reflection are illustrated in Figure 2.5 (Hugo (2013) cited Bosboom and Stive (2012)).

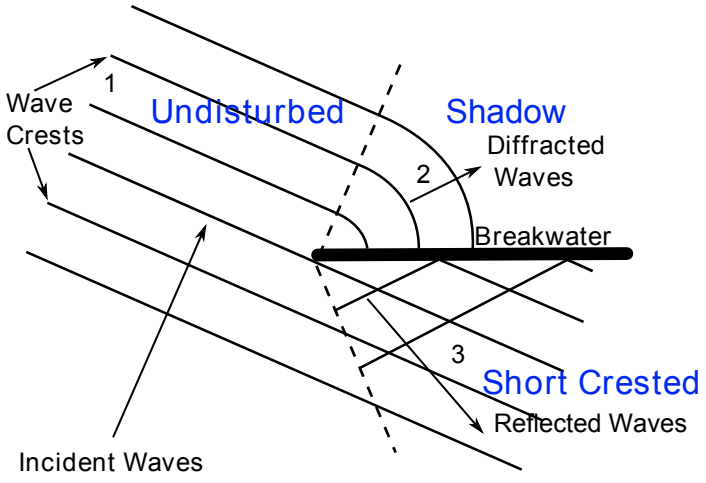

FIGURE 2.5: Diffraction and Refelction

In regard to this specific study on sediment movement around a surf zone structure, the above mentioned mechanisms are of great significance as waves are the primary driving force of sediment movement. If the wave field is altered by the above mentioned

mechanism it will consequently alter both the characteristics of the currents and in effect the sediment movement.

As waves move into shallower water, energy dissipation through wave breaking occurs. Wave breaking is very important as it influences the coastline and the processes in the surf zone to a great extent, but unfortunately it is possibly the most difficult wave phenomenon to describe mathematically. Theoretically, wave breaking can be determined as a function of the wave steepness (H/L). The wave height will keep increasing due to shoaling, and when the wave becomes unstable, it will break. This breaking height (H_b) occurs when the particle velocity at the crest of the wave exceeds the phase speed of the wave. The theoretical steepness limit for shallow water according to the linear wave theory is presented as such (Hugo (2013) cited Bosboom and Stive (2012)):

$$\frac{H_{max}}{L} \approx 0.88\frac{d}{L} \tag{2.5}$$

Where H_{max} is the maximum wave height, L is the wavelength and, d is the water depth. It can also be presented using the breaker index (γ):

$$\gamma = (\frac{H}{d})_{max} = \frac{H_b}{d_b} \approx 0.88 \tag{2.6}$$

A breaker index value of 0.78 was adopted in 2002 as suggested by the U.S. Army Corps of Engineers (2002) but is based on the solitary wave theory and is more applicable to tsunami waves or single waves. A breaker index value of 0.88, is a more recent suggested value. The point of depth induced wave breaking defines the breaking line and the seaward boundary of the surf zone.

The wave characteristics and phenomena in the surf zone have now been described. The phenomena mentioned above have a great effect on the coastal shoreline. All of these processes are responsible for forming and creating the type of wave condition present at the specific coastline under consideration. This wave condition is responsible for the generation of various coastal processes. These processes shape and form the shoreline and are responsible for the stability of the beach line, the surf zone seabed and the processes around any structures located within the surf zone.

2.3 Coastal Processes

Soft shorelines are very sensitive to obstructions within the surf zone. By interrupting the natural flow of water and also the sediment being transported along with it, the shoreline will be introduced to processes such as erosion and accretion. It is therefore important to understand the processes responsible for the transport of sediment in the surf zone.

As indicated in Chapter 2.2, the orbital motion of the water particles in a deep water wave can be seen as a circle. When the wave passes into the shoal zone these orbital motions become more elliptical as a result of bottom friction. Bottom friction on the seabed will result in the movement of sediment particles and then the turbulence created by wave breaking will bring larger amounts of sediment into suspension. The sediment in suspension is then transported by a combination of different currents. In order to understand the process of sediment transport and in return the build-up of sediment against structures built in the surf zone, it is important to know the function of each of these currents, and what effect each of them have on the total sediment budget.

When waves propagate through the surf zone towards the shoreline, they transfer both energy and momentum. This is due to the orbital motions of the water particles between the crest of the wave and its trough. For waves not under the influence of energy dissipation (such as wave breaking) the horizontal momentum (Q_x) is represented by the mass density (ρ) multiplied by the particle velocity in the x-direction (u), integrated over the depth and then averaged over time (Bosboom and Stive, 2012):

$$Q_x = \overline{\int_{-d}^{\eta} \rho u_x dz} \tag{2.7}$$

Where η is the surface elevation above the Still Water Level (SWL) and d is the water depth. For waves that are affected by wave breaking, such as the ones in this study, this formula will change. When a wave breaks, the mass transported towards the shore is enhanced significantly. This extra momentum needs to be added to the horizontal momentum and will be denoted as breaking momentum ($Q_{breaking}$) . Thus the total amount of momentum will be denoted as (Hugo (2013) cited Bosboom and Stive (2012)):

$$Q_{total} = Q_x + Q_{breaking} \tag{2.8}$$

When a mass of water hits an obstacle, the mass of water needs to be diverted or returned. In the case of waves in the surf zone the obstacle in the way is the shoreline. To honour the mass flow law which states that mass equilibrium needs to be maintained,

a return flow is established. This return flow is called an *undertow*, and can form below the waves in the surf zone or in the form of a *rip current*[4]. This process of mass transport is called a *cross-shore current*. The cross-shore current is mainly responsible for seasonal changes in the shoreline. In studies done by various researchers around the world including Doria and Guza (2013) & Wang et al. (2014), it is shown that when the wave climate is smaller, as it is in the summertime around southern Africa, sand is transported towards the shoreline and accretion is achieved which creates a broad beach front at the shoreline. In opposite fashion, when the wave climate is bigger and more violent, as it is during the winter season around southern Africa, the sand is transported offshore and settles on an offshore sandbar. These are short-term changes which will not have a dramatic long term effect on the permanent shape of a shoreline, although it can cause a dramatic change in the short term sediment budget, especially in the case of a storm event and shallow water construction such as a cofferdam and trench.

In the same manner as the return flow (*undertow* or *rip current*) is created, if a wave train is reflected from an obstacle (the shoreline), its momentum must be reversed. Conservation of momentum once again then requires that there is a force exerted on the obstacle, equal to the rate of change of the wave momentum. This force is a manifestation of the *radiation stress*. Thus it can be said that due to the presence of waves, the transport of the above mentioned momentum and mass will result in an excess of momentum and this momentum flux is called radiation stress (Longuet-Higgens and Stewart, 1964) ,(Longuet-Higgens, 1970).

Radiation stresses have the ability to cause variations in the mean sea level and are thus responsible for processes such as longshore currents. These stresses can be taken to be in the direction of the propagating wave (S_{XX}) or at a right angle to the direction of propagation (S_{YY}). If the wave propagates towards the shore at an angle (β), a non-zero shear stress component is also created which can be denoted as S_{XY}. It is this shear stress in the longshore direction which causes the manifestation of a longshore current.

In order to understand the change in shorelines in the longshore direction due to obstructions in the surf zone, and also the build-up of sediment, more knowledge is needed of longshore currents and gradients.

The *longshore current* is the movement of water along the shoreline in a certain direction. The longshore current can flow in either direction along the shoreline depending on the direction of the wave field driving the current.

[4]Rip currents are the seaward return flow of water concentrated at points along the beach. They are caused by a longshore variation of wave height, and hence wave set-up, which provides the necessary hydraulic head to drive them (Swart and Fleming, 1980).

Due to the geographical location of southern Africa, the current directions vary depending on which side of Cape Point the site location is. Harris (1978) shows that around the southern coast of South Africa (Mossel Bay), the dominant oceanic current direction is down the coast from north east to south west. Yet it also reveals that the longshore current direction is in the opposite direction. This is because the longshore current is driven by the wave field which is generated by the storm systems coming in from the south west. Bowditch (2002) shows that the dominant longshore current direction of the Namibian coast is from south to north. This makes sense as the dominant wave field is generated by the same storms coming from the south west.

The longshore current has many contributing factors depending on the layout of the specific location. A longshore current can be caused or enhanced by the variation in wave characteristics, bathymetry layouts or obstructions sheltering certain areas along the beach from wave energy. However, the two main contributing factors are; a longshore gradient caused by the longshore force ((Fredsoe and Deigaard, 1992),(Longuet-Higgens, 1970)), and the turbulent shear stresses which are proportional to the turbulent motions caused by waves breaking in the surf zone (Hugo (2013) cited Bosboom and Stive (2012)).

By considering the above mentioned factors, the longshore current velocity can be written as a function of the cross-shore position (Hugo (2013) cited Bosboom and Stive (2012)).

$$\frac{sin\beta}{c}E_b + \frac{\partial}{\partial x}(d\rho\nu_t\frac{dV}{dx}) = \tau_{b,y} \tag{2.9}$$

where:
$\frac{sin\theta}{c}$ = Snell's law (constant)
with c as the wave celerity and β is the incidence angle.

E_b = energy dissipated through wave breaking
d = water depth
ρ = mass density of water
v_t = eddy viscosity
V = longshore current velocity
$\tau_{b,y}$ = longshore bed shear stress

If the longshore current velocity is to be calculated through all the positions in a cross-shore profile of the surf zone, it will be found that the longshore current velocity has a distribution that is always the same when considering a gradual slope. The current velocity will start to increase just outside the breaker line as the flow of energy is spread past the initial generation point which is the breaker point. The velocity will then reach its maximum velocity at a distance of approximately two thirds of the total distance

away from the shoreline (U.S. Army Corps of Engineers, 2002). This is an area of high sediment activity and must be kept in mind when designing sediment sensitive structures. The longshore current velocity will then decrease until it reaches the zero mark at the shoreline. This distribution is represented in Figure 2.6 in a schematic manner and is not derived from any mathematical formula. In various studies done on longshore current velocity distribution it is possible to see that this distribution profile can differ if there are abnormalities in the bathymetry. ((Hamilton and Ebersole, 2000),(Kuriyama and Sakamoto, 2014), (Reniers and Battjes, 1996)).

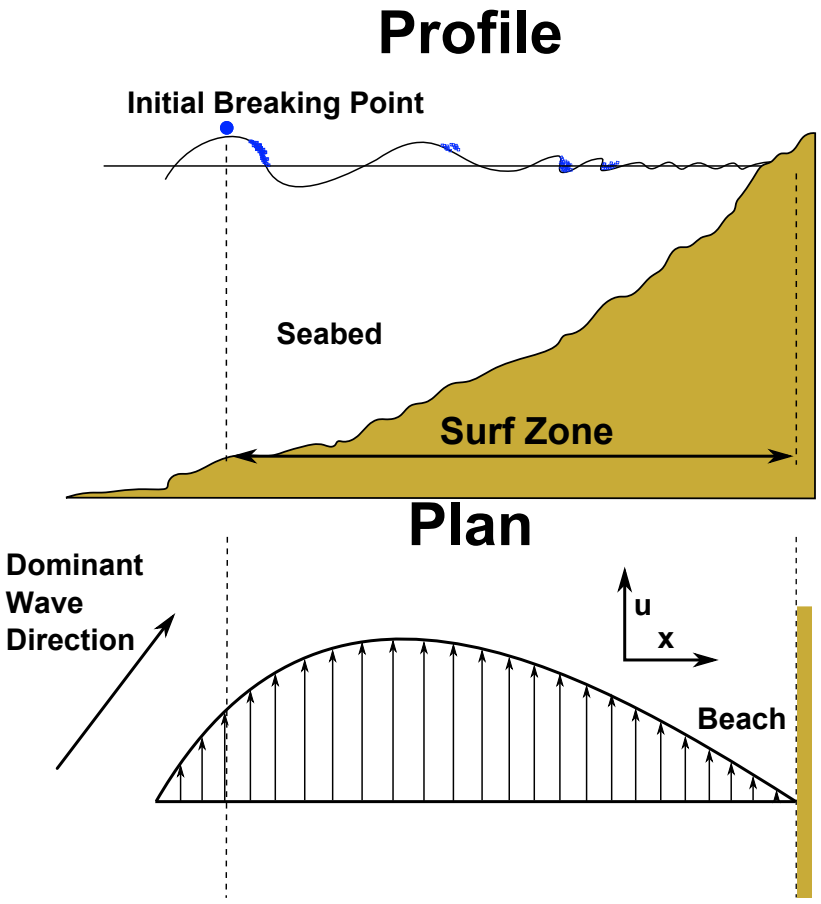

FIGURE 2.6: Longshore Current Velocity Distribution **(Adapted from U.S. Army Corps of Engineers (2002))**

2.4 Sediment Transport

Considering the mechanisms of waves and currents in the surf zone the basic characteristics of sediment transport can be described.

The process by which sediment is transported along the shoreline due to currents and wave action is called *longshore sediment transport* or *littoral transport* (Schoonees and Theron, 2002). This process is utterly important to understand even though it is a daunting task to calculate the rate of sediment transport accurately. The rate of sediment transport is usually expressed as a volume of sediment transported per unit time for example m^3/s, or more common $m^3/year$. Knowledge of the longshore transport rate is essential for the design of surf zone structures, whether they are permanent or temporary.

Sediment transport can occur in a number of different modes. Starting from the sediment transport that occurs closest to the seabed, sediment can be moved by a transport mechanism called *Bed Load Transport*. This type of transport refers to the movement of the more coarse material in such a manner that the particles are almost in constant contact with the seabed. Thus the particles have a motion that resembles rolling or jumping in the direction of the flow. Bed load transport can thus be expected to occur due to the bed shear stress acting on the sand surface (Fredsoe and Deigaard, 1992).

Moving away from the seabed, sediment is moved by a transport mode called *Suspended Load Transport*. This mode of transport refers to finer material that is agitated by the orbital and turbulent motions of the waves and brought into suspension. Once the particles are in suspension they are moved forward in the direction of flow by the longshore current.

The third and final mode of transport is called *Wash Load Transport*. This mode of transport moves very fine sediment particles. The particles are so fine that they are almost always in suspension due to the agitation caused by the turbulent water. Wash load is thus not considered part of the total transport load as it is not represented on the seabed (Hugo, 2013).

Sediment transport is usually represented either by mentioning the direction of flow, for example northern transport or southern transport, or by describing the sediment movement as upstream (S_{up}) or downstream (S_{down}) relative to the net transport direction. Once a convention is set the transport rate can be defined as two different rates, the *gross transport rate* or the *net transport rate* (Schoonees and Theron, 2002). The gross sediment transport is the total sediment that is transported past a certain point, regardless of which direction the flow:

$$S_{gross} = |S_{up}| + |S_{down}| \tag{2.10}$$

The net sediment transport can be seen as the calculated excess sediment transport in a certain direction and can be calculated as such:

$$S_{net} = S_{up} + S_{down} \tag{2.11}$$

Depending on the nature of the problem, a choice will be made on which definition or type of transport will be used in the calculations as the design transport rate, net or gross. In case of dredging volumes, as in this study, the gross transport is used as this volume will represent the total volume of sand captured in the area between the sheet piles or in the trench. In case of beach nourishment the net transport rate will be used as nature will return a certain volume of sand to the area of interest at a later stage in time. It should be borne in mind that the shift in longshore sediment movement direction is usually as a result of a change of seasons when the weather patterns change. For temporary structures, such as cofferdams, longshore sediment transport is usually unidirectional. A study done by Ribas et al. (2013) on shoreline sand waves on the south west coast of Africa (Namibia) shows a very oblique wave angle encouraging a very active coast in terms of sediment transport. Schoonees (2012) indicate that the net longshore sediment transport rates along the coast of southern Africa, from Saldhana up to Walvis Bay, is between 270 000 m^3/year and 860 000 m^3/year and are in a north west direction.

The interaction between water processes and sediment is still poorly understood. The chance of calculating sediment transport rates accurately is therefore small. Various longshore transport rate formulae have been developed and they can be classified as either bulk or detailed formulae (Swart and Fleming, 1980). *Bulk formulae* are determined in such a way that a single transport rate is obtained for a certain wave condition. Meaning that the total sediment load, wash load excluded, which is moved parallel to the coastline, at different depths, in a certain time step past a set line perpendicular to the shoreline, is calculated. Thus no information about the distribution of the transport rate is given in the bulk formulae (Schoonees and Theron, 2002). *Detailed formulae*, as the name implies, supply much more information of the transport rate distribution throughout the cross-shore profile. Schoonees and Theron (2002) state it well on page 13 of their journal article: "Detailed formulae (or predictors) provide information on the transport rate at different depths at each location. The local transport rate is the transport rate at the particular depth. Each of these local transport rates is multiplied by the

cross-shore (horizontal) distance that it represents to obtain the local transport product. These local transport products are then added up to acquire the total (integrated) transport rate at the specific location (or line perpendicular to the beach). By dividing the the local transport product at each depth by the total transport rate, the so-called cross-shore distribution of the longshore transport is obtained." These formulae requires a much more detailed input, such as the seabed characteristics, but in return can give you a more detailed output and information on aspects the bulk formulae cannot.

The fact that over 50 different sediment transport rate formulae exists can bring other problems forth. Questions need to be answered before the calculations can be done. Which formulae provides the most accurate answer? Have the formulae been calibrated? Is a specific formula applicable to the specific circumstances of the site under consideration? Research has been done for many years and these formulae are still at a stage where a factor of 3 is acceptable when interpreting the results.

In an attempt to improve the accuracy of these formulae, Schoonees and Theron (1996) did a study by testing the sediment transport rate formulae in order to know which is best. In this study they discovered that the 3 most accurate bulk transport formulae, in descending order are:

I. Kamphuis, 1991(Dimensional Analysis) (Kamphuis, 1991)

II. Van Hijum, Pilarczyk and Chadwick, 1989 (Energetics, "Energy flux")(Chadwick, 1989)

III. Van der Meer 1990(Empirical)(Van der Meer, 1990)

Although this is the case for bulk formulae, the numerical model used in this study (Chapter 5), uses a well renowned detailed formula known as the *Bijker total transport load* formula.

The Bijker formula (Bijker, 1967, 1971), is one of the earliest formulae developed for the calculation of sediment transported under the influence of both waves and currents. It is able to determine both the sediment transport rate and the transport distribution throughout the surf zone. The formula is based on a formula proposed by Frijlink (1952), developed for the calculation of river transport, and calculates the sediment transport as a function the specific wave condition and longshore current. Bijker identifies two types of transport in his formula, bed load transport and suspended load transport, and after extensive algebra he shows the suspended load transport as a function of the bed load transport. After some modifications to his formula, Bijker proposed a formula that is applicable for both breaking and non-breaking waves. However, the calculations needed in order to use the final formula are quite complex. The final bed load, suspended

load and total sediment load transport formulae are shown below. The mathematical derivation of these formulae is given in Appendix B. The bed load transport is:

$$q_b = \frac{Ad_{50}V\sqrt{g}}{C} \exp\left(\frac{-0.27\triangle d_{50}\rho g}{\overline{\mu\tau_{cw}}}\right) \tag{2.12}$$

where q_b is the bed load transport, A is an empirical coefficient (1.0 for non-breaking waves and 5.0 for breaking waves), d_{50} is the sediment particle diameter, V is the mean current velocity, C is the Chezy coefficient, $\triangle$ is the relevant apparent density of the bed material, ρ is the mass density of the water, g is the gravitational acceleration, μ is the ripple factor and τ_{cw} is the time averaged bed shear stress due to currents and waves. The suspended load transport can be written as:

$$q_s = 1.83Qq_b \tag{2.13}$$

where Q is a function of the water depth d, the bed roughness k_s and two Einstein integrals I_1 and I_2, all of which are defined in Appendix B.

And then the total transport q_t, can be written as:

$$q_t = q_b + q_s = q_b(1 + 1.83Q) \tag{2.14}$$

All sediment transport formulae have their differences as the assumptions made by the researchers that proposed them are different. A study done by Anıl Arı Güner et al. (2011) shows the Bijker formula to overestimate the sediment transport when compared to other detailed formulae and site measurements. This shows that there is still much to learn when it comes to the accurate calculation of the longshore sediment transport rate.

Longshore transport is not always constant and can be enhanced by certain factors. For instance, sediment transport rates are enhanced during the duration of a storm. During a storm a number of natural phenomena are present, such as pressure differences and strong winds which cause the still water level to rise and the wave condition to grow. When a low pressure is present, the water level directly below it will rise. This is called a *barometric tide* (Dean and Dalrymple, 2002). The water level can also increase through wind shear stress. When strong winds blow across the water surface, a horizontal shear stress is present between the wind and the water surface. Not only is this responsible for the generation of waves but if these winds are directed onshore, water is forced towards the shoreline leading to a raised water level. These effects combined are referred to as a *storm surge*. This is an important phenomenon to keep in mind when trying to protect

a surf zone trench from sedimentation. If a protective structure is designed for a certain short term wave condition and a storm is present, it can increase the wave condition to a level which will cause difficulties in the installation process.

Sediment can also be transported by means of the wind, and is known as *Aeolian transport* (U.S. Army Corps of Engineers, 2002). However, sediment transported by wind occurs on land and will not be regarded in this study.

2.5 Pipeline Construction

2.5.1 Construction Methods

Submarine pipeline construction involves a wide range of activities and each of them can be seen as a specialised field in their own. Different activities require different setups or different construction equipment, not to mention that some of the activities require specialist inputs before construction can commence. A good example of such activities in construction are tasks which do not take place over dry land and require specialist divers to carry out, or a welding team for the linking of pipe sections. Although this study concentrates on two aspects, specifically the trench and temporary cofferdam construction, it is important to understand what activities and tasks lead up to this phase of the construction process.

The first step in offshore pipeline construction is to investigate the project specifications and choose an installation technique which suits the specific project criteria best. Gerwick (2007) has outlined that the following 5 aspects are of importance in the decision making phase of identifying an offshore pipeline installation technique:

1. Environmental conditions during construction.
2. Availability and cost of equipment.
3. Length and size of the pipeline.
4. Constraints of adjacent lines and structures.
5. Depth of the water.

If these 5 steps lead to a pipeline installation technique that requires the surf zone burial of the pipeline (as was the case for this study), the contractor must choose a method to bury the pipeline. Some of the options a contractor can choose from are the horizontal directional drilling (HDD) method where a tunnel is drilled underneath the surf zone from a land based position and the other end of the tunnel appears outside of the active surf zone. The pipeline is then guided trough the tunnel and out to deeper water. This method is however more expensive than an open excavation method such as a surf zone trench (Tideway Offshore Construction, 2011). For this reason, methods such as HDD, are only considered when an open excavation is not possible for instance when environmental laws do not permit it. Another method implemented is where the contractor dredges a surf zone trench and allows it to fill up again after the installation

of the pipeline is complete. Depending on the variation of the above aspects, a number of different techniques can be chosen to install a pipeline. The following methods are some of the most commonly used pipeline installation methods that may be employed for the surf zone burial of a pipeline:

Method	**Description**
The Reel Barge Method	In this method a pipeline is wound on a hub of a reel, mounted on a conventional lay barge which is dragged to an offshore position. From here the pipeline is spooled between the land based position and the barge. (PetroMin Pipeliner, 2012)
The on-Bottom-pull/tow Method	This method requires the pipeline fabrication to take place onshore whereas it is conventionally done on the lay barge before the pipeline is installed. The fabricated pipeline is then towed from its onshore position by sea going vessels along a planned route. (PetroMin Pipeliner, 2012)
Surface Float Method	This method entails that a pipeline, buoyed with floats or pontoons, is towed on or near the surface of the water, to the position where the pipeline is planned to be installed. Then, with consideration of the environment, the pipeline is lowered by one of many techniques, for example, coordinated release of the floats. (Fernandez, 1981)

TABLE 2.1: Pipeline Installation Techniques

There are various other methods not mentioned which were designed and implemented subject to the characteristics of specific projects. For the case of this study, and the case studies on which it is based on, only two of these method are applicable, the *Surface Float Method* used by Clough Murray & Roberts Marine at Mossel Bay and the *On-Bottom-Tow Method* used at Trekkopjes in Namibia.

Although the above mentioned methods are different in nature, both of them have a common aspect which ties them to this study. At both locations a surf zone trench was implemented and protected by an open-ended cofferdam. Both of these aspects are part of the temporary construction and are removed and filled up once the pipeline installation is complete. Once the trench is back filled by the surf zone processes, the pipeline is protected from the forces in the surf zone. Beyond the closure depth the pipeline rests on the seabed as this area is not as hostile and the pipeline is not as vulnerable.

2.5.2 Surf Zone Trenches

Pipeline construction through the surf zone requires contractors to dig a trench from the shoreline through the surf zone in order to install the pipeline and to protect it from the natural elements once the installation is complete. The construction of a surf zone trench involves dredging activities which are also used to remove some obstacles in the way of the pipeline. An example of such obstacles is undulations on the bathymetry (Kaergaard and Fredsoe, 2012). It is important to flatten these undulations. By reducing the areas where the pipeline is in free span, the tension on the pipeline sections is reduced, ensuring a safe and successful installation.

Due to the fact that a non-cohesive soft seabed is so active and levels in the bathymetry profile can vary in a short amount of time, the burial depth of the pipeline is very important (Dean and Maurmeyer, 1983). If the pipeline is not buried deep enough, the surf zone processes will expose the pipeline at some stage in time, thus exposing it to all the surf zone forces. On the other hand, if the pipeline is buried too deep, the load of the sediment on top of it can cause the pipe section to fail. To determine the burial depth, designs are drawn to ensure that the pipeline is beneath the active surf zone depth which is ideally equal to the depth of closure as shown in Figure 2.7 below.

Note: This image is not drawn to scale. It is mere an interpretation of the text explained above.

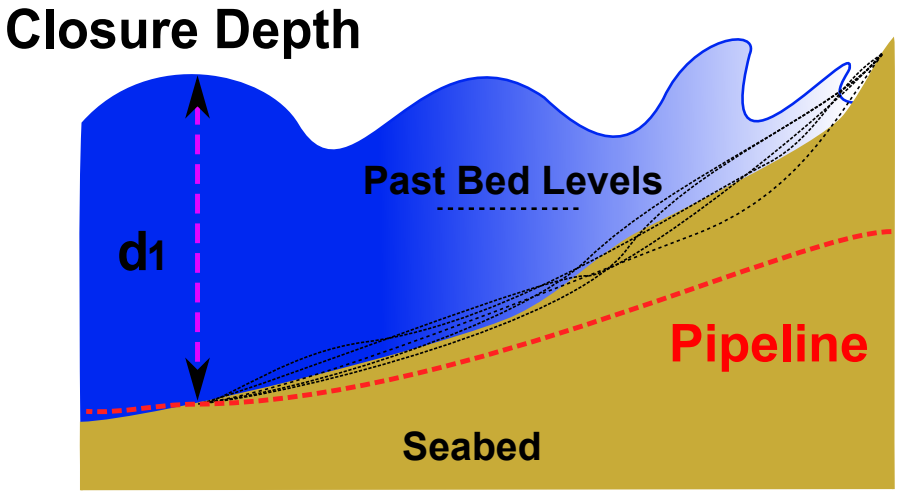

FIGURE 2.7: Pipeline Burial Depth (Adapted from Hallermeier (1981))

The method by which this trench is constructed depends on the soil characteristics of the seabed at the area of construction. Various dredgers are available to use for different soil types, for example, in some situations the seabed will be solid rock which makes the digging of the trench more difficult (Vlasblom, 2003). In situations such as this a cutter dredger is needed or as an alternative the hard rock can be broken up by implementing

blasting. Once the solid seabed has been blasted into removable pieces, a bucket dredger will be used to remove the debris. In the case of a soft seabed an alternative method may be followed and a suction dredger can be used to remove the sand. If the wave condition is calm and the water is shallow enough a simple bucket excavator on a barge can also be used to remove sediment. This is also more cost effective than using floating dredging vessels. If the water is too deep and dredging is required, the options become more limited and floating dredging vessels needs to be implemented.

A good example of a difficult dredging situation is the one of the desalination plant that was constructed by Clough Murray & Roberts Marine in Namibia at Trekkopjes (2010). At this location the seabed consisted of hard rock. In order to remove it, blasting was required. Once the seabed was broken up, a bucket dredger was used which was situated by a temporary jetty to remove the debris and dig the surf zone trench (Dixon et al., 2014). Photos of this process can be seen in Appendix C.1.

This surf zone trench was dug in a hostile environment and required protection from currents and the incoming wave condition. It is instances such as this where the temporary working protection via a cofferdam structure becomes relevant.

2.5.3 Temporary Stringing Yard

In order for a construction project to move forward, temporary working quarters need to be established. The temporary quarters in pipeline projects are called the *stringing yard*. Within the stringing yard, different areas are allocated depending on which type of pipeline installation method is used. Usually for pipelines which are deployed from land the stringing yard consists of a *receiving area*, a *welding area*, a *weight coating area* and a *waiting area*. These are all planned and used to ensure maximum efficiency. An example of a typical stringing yard is the one that was erected at Trekkopjes (Dixon et al., 2014). The different areas are explained in Figure 2.8. Keep in mind this stringing yard was constructed for a project which used the bottom-tow method to install the pipeline. Photos of this process can be seen in Appendix C.2.

As the pipe sections arrive at the construction site they are unloaded at the receiving area (Figure 2.8 Point A). From here they will be moved and placed on place holders in the welding area (Figure 2.8 Point B) to ensure that the welding team can attach sections together accurately. A number of sections welded together form a pipeline length, and this length is moved on to the weight coating area (Figure 2.8 Point C) using a hydraulic jack system. Here they receive a coating of protective material specified by the design. Once the coating is complete the pipeline lengths will be moved on to the waiting area (Figure 2.8 Point D) where they will remain until the pipeline is pulled through the pipe launchway out to the ocean.

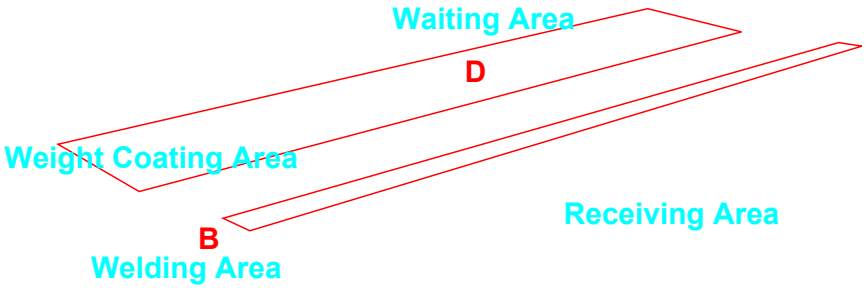

FIGURE 2.8: Trekkopje Temporary stringing Yard

The pipe launchway consists of a series of rollers over which the pipeline is pulled in the direction of the ocean. The launchway is designed to have an "S" shaped profile with a specific bent radius to ensure that the pipeline is not over stressed during installation. Figure 2.9 shows the pipe launchway that was constructed at Trekkopjes (Dixon et al., 2014). Photos of this process can be seen in Appendix C.3.

FIGURE 2.9: Trekkopje Pipe Launch Way

As seen on the Figure 2.9, the 1st curve had a vertical radius of 2.4 m and the second curve a vertical radius of 2.1 m.

2.5.4 Cofferdams

A cofferdam is a temporary structure designed to keep water and/or soil out of the excavation in which a bridge pier, foundation, pipeline or other structures are built. Pipeline cofferdams in the surf zone become open-ended cofferdams as they do allow water to enter at the mouth of the structure and are built only to protect the surf zone trench and not always to create a dry working environment. In some situations a dry working environment can be created depending on the specific site characteristics. The word "cofferdam" comes from "coffer" meaning box, in other words a dam in the shape of a box. When it comes to coastal cofferdams this definition can be misleading as coastal cofferdams in the surf zone are not always dry inside. Cofferdams are constructed using a variety of sheet piles by implementing a wide range of different methods (Nemati, 2007). Due consideration must be given in the design and construction of cofferdams and the environment wherein they are built as the forces imposed on the structure may vary with different circumstances. The erection process is not the only phase that needs attention as the removal of a cofferdam can be just as dangerous if the loads and water masses are not handled in the correct manner.

A few types of cofferdams exist in the construction of bridges and piers. Of the many types only two are of relevance when considering coastal surf zone cofferdams.

Cofferdam Type	**Description**
Braced Cofferdam	A cofferdam formed from a single wall of sheet piling which is driven into the ground to form a "box" around an excavation site.
Double-Walled Sheet Pile	Double wall cofferdams comprising of two parallel rows of sheet piles driven into the ground and connected together by a system of tie rods at one or more levels.

TABLE 2.2: Cofferdam Construction Methods (Nemati, 2007)

Coastal cofferdams are mainly constructed using the double-walled sheet pile method, but the design usually incorporates elements of the braced cofferdam method to enhance the design.

According to Nemati (2007) the success of any piling scheme requires satisfactory completion of the following stages:

1. Competent site investigation, sampling and relevant testing to get an informed picture of the task.

2. Adequate design of all the stages of the construction.

3. Placing and installing of the sheet piles.

Due care must be taken in all of these steps as there are a number of imposed loads that work in on a cofferdam, as listed in Table 2.3.

Load	**Description**
Hydrostatic Pressure	The water level on either side of a cofferdam sheet piling is not always the same. This level difference creates a force that is proportional to the mass of the water and is known as the hydrostatic force or pressure force.
Soil Loads	As excavation is done inside a cofferdam the soil that rests against the sheet piling on the outside impose a force on the cofferdam. These forces are known as soil loads.
Current Forces	As currents hit the cofferdam structure they need to be diverted. As the sheet piling is not permeable this imposes a force on the cofferdam. These forces do not only work in a normal direction but are also responsible for drag forces alongside the cofferdam. The magnitude of this force is also affected by the corrugation of the sheet piles used.
Wave Forces	Waves hit the cofferdam and that energy is transferred onto the cofferdam.
Ice Forces	Only applicable in certain locations. There are two types of ice forces, static ice forces as a result of the expansion of a closed-in solidly frozen-over water surface, and dynamic ice forces as a result of the breakup and movement of ice pieces.
Seismic Loads	These are not as important with temporary structures but it should be taken into consideration that in certain areas of the world seismic activity can have an effect on the integrity of temporary structures.
Accidental Loads	These loads are usually caused by construction equipment working alongside the structure for example, a barge bumping into the cofferdam that is being used to excavate a surf zone trench.

TABLE 2.3: Imposed Loads on a Cofferdam (Nemati, 2007)

These components and loads are important to take into consideration in the investigating and design phase of a project. Also along with the loads imposed on the structure, coastal processes need to be taken into account. *Scour* is a major process and can be defined as the erosion of sediment against the foot of the structure due to tidal or wave-induced currents. If this process is not taken into consideration, it can result in a loss of structural integrity. When scour is present at the foot of a structure, sediment is removed on one side of the structure leaving a larger piece of foundation exposed. The sediment against the exposed foundation is needed to balance out the soil loads on either side of the structure. If the sediment is removed, the soil load on the opposite side of the structure will become too large and force the structure to collapse. Examples of cofferdam failures include the Marmot cofferdam, Sandy River, Oregon, USA (Grant et al., 2008) and the Gladstone cofferdam failure (Komarek, 2014). These are not further explained as they are not surf zone coastal cofferdam projects.

Once the design has commenced, it is important to consider all the components that are involved in the construction of a cofferdam. These will include the two main physical components of the cofferdam and the equipment used to install them. These physical components comprise the sheet piling and the bracing system. The first component, *sheet piling*[5] can be defined as iron sheets that are driven into the seabed using pile driving equipment. The sheet piling can take different forms depending on the site and project specifications. The first sheet pile is installed at a strategic location and interlocking sheet piles are then driven into the ground to form a continuous wall. The shapes of sheet piles differ in two manners, the overall shape of the sheet pile itself and the interlock at the edges. The following shapes are the most commonly found sheet pile configurations:

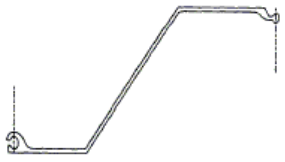

FIGURE 2.10: Z Shaped Sheet Pile (PILEBUCK, 2014)

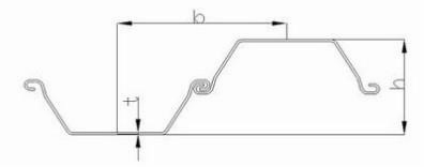

FIGURE 2.11: Larsen U Shaped Sheet Pile(PILEBUCK, 2014)

[5]Sheet piling is a manufactured construction product with a mechanical connection or "interlocks" at both ends of the section. These mechanical connections interlock with each other to form a continuous wall of sheet piling.

Some of the more commonly found interlock configurations includes the following:

Name	**Layout**
Double Hook Interlock	
Thumb & Finger (One Point Contact) Interlock	
Thumb & Finger (Three Point Contact) Interlock	
Single Jaw Interlock	
Hook & Grip Interlock	

TABLE 2.4: Sheet Pile Shapes (ThyssenKrupp, 2014)

The second component, the bracing system, is designed to fit each unique cofferdam to support and uphold it against imposed loads. When the cofferdam is removed the bracing system will be de-constructed from a strategic point to ensure that the structure does not fail.

The equipment used to drive the sheet piles into the seabed can be one of a number of different machines designed to install sheet piling in the most effective and efficient way possible. The two common methods are the use of an impact hammer or a vibratory pile driver. An impact hammer as seen in Figure 2.12, is a giant machine that lifts and drops a weight onto the sheet pile to drive it into the ground. The speed at which it drives the pile is depended on the amount of force which can be applied. This force is governed by the buckling force of the sheet pile itself, the force required to make effective progress with each blow and the soil characteristics.

FIGURE 2.12: Impact Hammer(ISCHEBECK, 2014)

A vibratory pile driver such as the one seen in Figure 2.13, is a piece of machinery that is elevated using a crane. The head of the pile driver is then clamped onto the upper end of the sheet pile. The sheet pile is then sunk into the ground using vibrations. By vibrating the sheet pile, the pile driver loosens the soil around it which allows it to sink to the design depth under its own weight. It is not always possible to use this method as its success depends on the soil characteristics

FIGURE 2.13: Vibratory Pile Driver (Sandhurst Equipment Rental, 2014)

2.6 Design Specifications and Layouts from past Studies for Surf Zone Structures

2.6.1 Introduction

Following extensive review of the literature, no published studies could be identified on the specific topic of minimizing sedimentation problems by finding possible alternative geometric layouts for surf zone cofferdams. However, some major engineering firms have documented their comments and reasons for using specific layouts or construction techniques when it comes to surf zone crossings. Also, research has been done on other hard surf zone structures such as jetties, groynes and harbour breakwaters, which will give a some relevant insight into what problems to expect when designing a temporary cofferdam inside an active surf zone.

An informed background on surf zone sediment transport processes has already been manifested with the first part of this literature review. This knowledge can be used to make an educated prediction of what will happen when the different structures interfere with these processes and also why the structures in the case studies experienced the problems they did.

2.6.2 Past Cofferdam Shore Crossing Projects

Although no sedimentation problems are documented in the reports of the past case studies, they do inform one of how cofferdams look and function in the real world.

2.6.2.1 Lower Churchill Project, Turkish Coast Cofferdam

In a Shore Approach Feasibility Study published by Tideway Offshore Contractors, they explain their entire methodology of shore crossing projects with reference to the Lower Churchill Project or generally referred to as the Labrador-Island Transmission Link. The project comprised of a 1100 km High Voltage Direct Current (HVDC) link from Gull Island to the central region of Labrador to Newfoundland's Avalon Peninsula and had various shore crossings(Tideway Offshore Construction, 2011). Figure 2.14 shows the location of the project as indicated by Tideway Offshore Construction (2011).

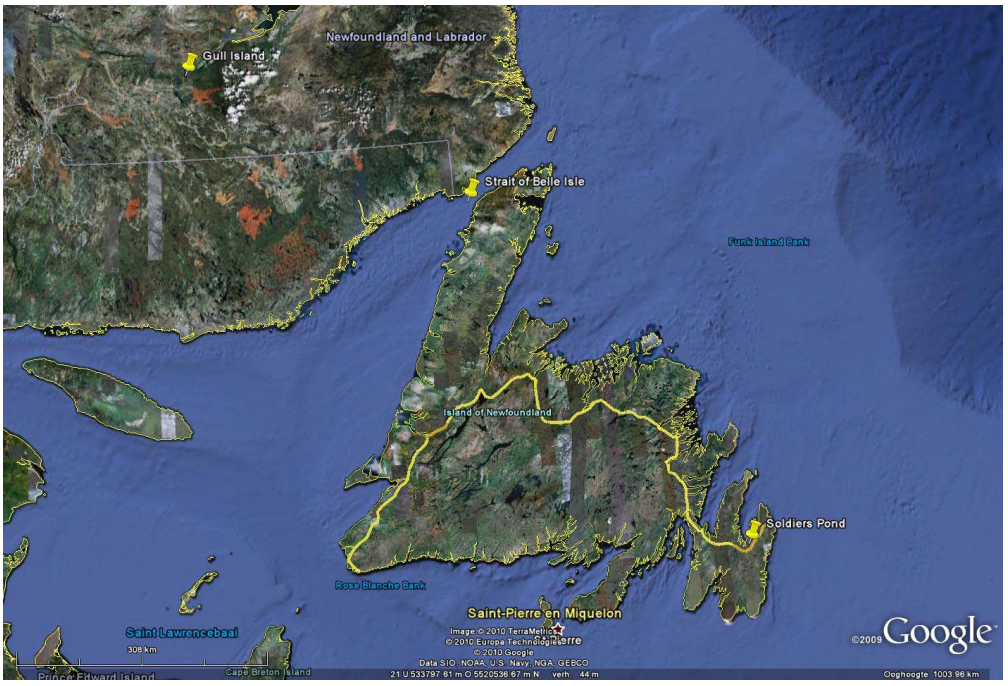

FIGURE 2.14: [Lower Churchill Project Location (Tideway Offshore Construction, 2011)

In this feasibility study Tideway clearly states that when possible, an open excavation (surf zone trench) is the most common and effective technique to use to install a pipeline. Depending on the soil characteristics they use either a cofferdam to protect the trench,in case of soft seabed material, or in the case where the soil is too hard to install a cofferdam, they build a protecting groyne. Also depending on the project specifications they either dredge, blast or excavate the trench using either sea going vessels or land based equipment. In a project in Turkey, in the order to prevent the near-shore seabed material to run into the surf zone trench, they provide the cofferdam with horizontal wings as seen in Figure 2.15.

When considering the wave and current data reported for the specific site on the Turkish Coast, it is evident that the coast will be exposed to moderate to large sediment transport near the shoreline (Tideway Offshore Construction, 2011). An average near bottom current speed of 3.1 m/s, along with a deep sea significant wave height of 5.5 m was recorded as part of the project specifications. These wave and longshore current conditions are quite extensive and can be expected to cause difficulties during the implementation of the project. The other shore crossing were done using protecting groynes and not cofferdams.

FIGURE 2.15: Bluestream, Turkish Coast (Tideway Offshore Construction, 2011)

2.6.2.2 New Langeled Pipeline at Easington,UK

Jan De Nul Group undertook a pipline project in order to get access from Norway's gas-rich fields and connect them to the UK (Figure 2.16). The project details show a cofferdam layout on the Easington coast shore approach (Figure 2.17). The project required both a tunneling technique in order to maintain unstable cliffs which are subject to high erosion processes and a cofferdam for protection in the surf zone. The cliffs are believed to retreat landward up to 1-2 m per year (Vercruysse and Fitzsimons, 2006).

FIGURE 2.16: Langeled Pipeline, Easington,UK (Vercruysse and Fitzsimons, 2006)

A 220 m straight cofferdam with no alternative geometric extensions was built in the surf zone in order to grant protection against incoming waves and to create a safe working environment during high tide. The cofferdam extended from a tie-in-pit on the beach to 60 m beyond the low water mark (Figure 2.17). The cofferdam was built by land-based equipment working at low tides from a causeway constructed alongside the cofferdam as

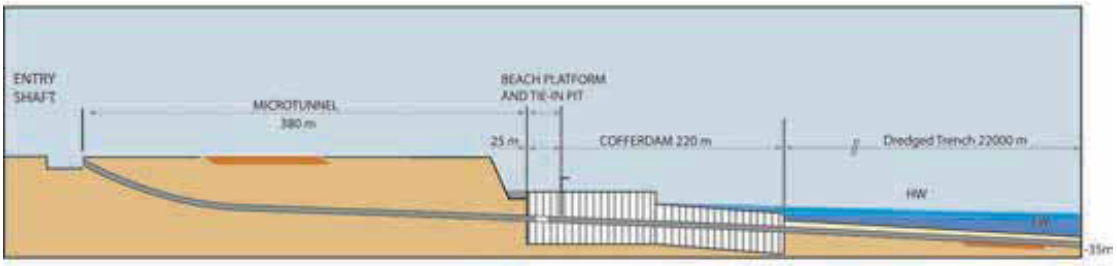

FIGURE 2.17: Langeled Cofferdam Layout (Vercruysse and Fitzsimons, 2006)

seen in Figure 2.18. The soil consisted of a stiff clay and it proved to be problematic for the installation of the sheet piles. Some pre-auguring was needed in order to install the sheet piles to the required depth. In this project, the Jan De Nul Group scheduled both the tunnelling and the cofferdam to be completed in advance of the arrival of the pipe laying vessel in order to save time (Vercruysse and Fitzsimons, 2006). This is an option that will only be possible in an area exposed to small volumes of sediment transport as the surf zone trench will be more exposed to sediment build-up the longer it is in the water waiting for the pipeline section to be installed. The trench would have been backfilled by natural processes if it was made in an active surf zone such as the one at Trekkopje, Namibia (Clough Murray & Roberts Marine, 2010). However as a result of the nature of the soil and wave climate at Easington, this method proved to be a success.

FIGURE 2.18: Langeled Cofferdam Construction (Vercruysse and Fitzsimons, 2006)

2.6.2.3 Balgzand-Bacton Pipeline (BBL)

Boskalis Dredging and Marine Experts in collaboration with Saipen UK Ltd. undertook a gas pipeline project running from Balgzand (The Netherlands) to Bacton (UK)(Figure 2.19).

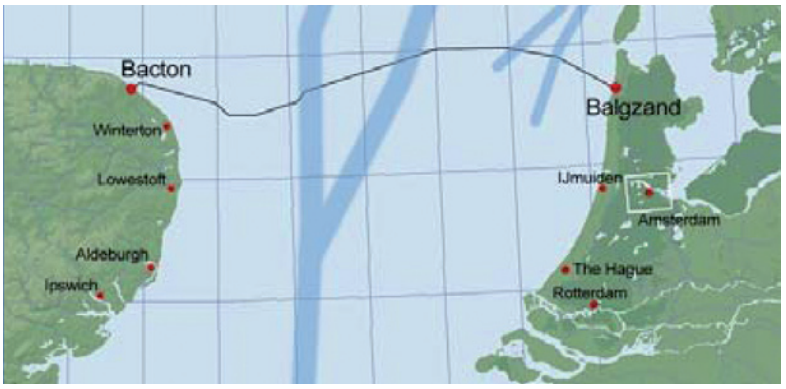

FIGURE 2.19: Balgzand to Bacton Pipeline (Boskalis Dredging and Marine Experts, 2012)

The shore crossing consisted of a 300 m cofferdam which was installed using a 300 m long and 5 m wide temporary jetty as seen in Figure 2.20 below. A 5 m wide trench was excavated within the cofferdam by using a specified dredging apparatus that worked from the temporary jetty (Boskalis Dredging and Marine Experts, 2012). At the shoreward side of the cofferdam was a tie-in-pit where the pipeline was connected to the land-based pipe which was passed underneath the dune zone by means of Horizontal Directional Dredging (HDD). Because of the calm weather climate and low wave height, no significant sediment transport was noted. This was not documented but can be gleaned from the fact that the dredged sediment was stored on the outside of the cofferdam, and returned to the surf zone trench once the pipeline installation was completed. If sediment transport processes were present at the location, this would not have been possible. The cofferdam and temporary jetty can be seen in Figure 2.20 and Figure 2.21.

FIGURE 2.20: Balgzand to Bacton Cofferdam and Temporary Bridge(Boskalis Dredging and Marine Experts, 2012)

FIGURE 2.21: Balgzand to Bacton tie-in-pit(Boskalis Dredging and Marine Experts, 2012)

2.6.3 Other Hard Structures in the Surf Zone

2.6.3.1 Introduction

In the absence of information on studies that have been done on the geometric layout of cofferdams specifically, studies related to other hard structures in the surf zone will be used instead. By studying the proposed design specifications , understanding the reasons for them and observing the effect they have on longshore sediment transport, a better design can be proposed for a temporary cofferdam.

Van Rijn (2013) confirms the statements in the first part of the literature review with the following factors that favours coastal sediment transport processes and erosion:

- Exposure
- Persistent oblique wave attack
- Unconsolidated sediments
- Absence of offshore energy dissipation through bars, banks or shoals

Keeping this in mind, two main shore-normal structures will be looked at:

- Groynes
- Jetties or Harbour breakwaters

2.6.3.2 Groynes

Groynes are long thin structures, built perpendicular to the shoreline and extending into the surf zone (Figure 2.22). In general they extend beyond the low water mark

but usually not by far. They are built with the purpose of reducing longshore currents, longshore sediment transport and to stabilize, extend or maintain beach lines. Another, but not as common purpose of groynes, is to deflect currents in order to calm or stabilize relatively deep tidal channels. This type of groyne is known as a current groyne (Van Rijn, 2013). It is evident from the above definition that groynes are hard surf zone structures with a similar purpose to that of the temporary cofferdams erected during a shore crossing. These structures are also found in areas with a predominant longshore current and therefore areas with a significant longshore sediment transport rate. The difference is that groynes are designed as permanent structures and to maintain the downstream shoreline, where in the case of cofferdams long term downstream shoreline erosion is of no real concern as the beach will return to its natural shape when the cofferdam is removed.

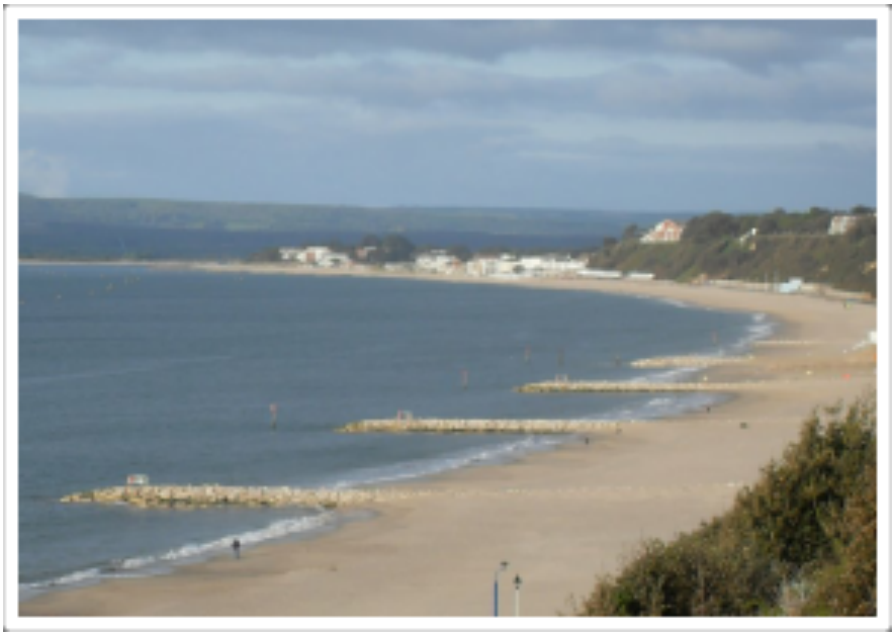

FIGURE 2.22: Groynes at Branksome Chine(Poolebay Coastal Management, 2014)

Different shapes of groynes, such as straight, T-head, L-shaped and Y-shaped have been considered in past studies. The effectiveness of these shapes were compared and documented. However, because of the nature of a groynes purpose, a successful groyne should allow sediment to pass by it at a certain rate or in certain circumstances in order to maintain downstream shorelines. The purpose of a cofferdam on the other hand is to block the sediment completely. For this reason the findings of the past studies shall be interpreted with reference to the purpose of a cofferdam and not a groyne.

Van Rijn (2013) states that the effectiveness of groynes relies mostly on their length in relation to the surf zone width and their spacing in relation to each other. As a cofferdam is a single structure on its own, the length of the structure is where the

attention will be focussed and not on the spacing of the structures. Van Rijn (2013) gives general guidelines for the most effective design of groynes regarding their length and crest level. These guidelines are given in Table 2.5 and then interpreted with reference to the situation as pertaining to a cofferdam.

Design Specification	**Effective Groyne**	**Effective Cofferdam**
The crest level at the dune toe of the groyne should be slightly lower than the local beach, and at the tip/mouth of the groyne it should be slightly higher than mean low waterline.	These levels are prescribed for groynes as they should allow sediment to pass over the structure under storm wave conditions and do not care for both overtopping and water passing by at the shoreline side of the structure.	A cofferdam's function is to provide a safe working environment and to block sediment from entering the surf zone trench, especially under storm wave conditions, and can not allow overtopping anywhere along the structure. For this reason a cofferdam is designed and installed with a crest level far higher than that of the mean sea level watermark.
The tip of a groyne should be within the surf zone to allow sediment to pass around its tip.	For a permanent groyne structure this is essential as the downstream shoreline should be maintained.	A cofferdam structure is temporary and should stop all sediment making its way towards the surf zone trench. Thus the length of a cofferdam should surpass the active surf zone.
Maximum groyne length is roughly determined by the low water spring line in tidal environments	As water and sediment is allowed to pass the structure under storm wave conditions this guideline is set in order to make the structure more cost effective.	A cofferdam can not permit water and sediment to enter the surf zone trench from the shoreline side and the design should consider the mean high water spring tide watermark as a cut off line.

TABLE 2.5: Groyne Design Guidelines

Nairn and Dibajnia (2004) investigated the different shapes of groynes (T-shaped, L-shaped and straight-angled) in a study done on a project in west Africa. The wave conditions were unidirectional and had a wave height (H_s) in the range of 0.5 m to 2.5 m. A dominant longshore current was present and caused a net longshore transport of between 300 000 m^3/yr to 500 000 m^3/yr. These conditions are similar to that of Trekkopje, Namibia. The study found the effectiveness of the structures to be quite similar but the straight structure was deemed to be the most efficient groyne structure as the difference in outcome was to small to justify the extra mass of the L-shaped and T-shaped groyne structures.

Other studies ((Kana et al., 2001), (Basco and Pope, 2004)) have also confirmed similar design guidelines. Depending on the environmental data and site location, the guidelines differ in nature but the general design specifications stay more or less the same.

2.6.3.3 Jetties, Harbour Breakwaters and Sand Bypassing

Jetties are long and narrow structures, a geometric shape similar to groynes, but is built to stop migrating sediment from reaching entrance channels or modified natural inlets (Van Rijn, 1998). Jetties, unlike groynes, do not allow sand to bypass at all. *Harbour breakwaters* are similar structures but usually larger and built to withstand and divert the incoming wave condition in order to protect the inner harbour area against intruding waves (Van Rijn, 2013).

These structures generally extend past the surf zone and beyond the outer breaker line, and are impermeable. They have a characteristic effect on the surrounding shoreline with sediment accretion upstream of the structure and sediment erosion on the downstream side. In view of the fact that these structures are permanent structures and that the associated sediment effects will not restore naturally, mechanical sand bypassing must be implemented (Van Rijn, 2013).

From the definitions above, it is clear that these structures and a temporary cofferdam in a shore crossing, have similar goals. The difference between these structures and a cofferdam are the time period over which they are interfering with the natural longshore current and sediment transport processes. Jetties and harbour breakwaters are specifically designed and built for each unique location and the environmental data associated with that location. For this reason, and the fact that they are permanent, large scale sediment bypassing systems can be implemented at these locations as it is part of the maintenance of a major permanent structure. For temporary cofferdams this is not the case. If a large scale bypassing system is implemented, the project will no longer be economically viable. However, some of these bypassing systems may have aspects which could be modified in order to make them suitable for a temporary cofferdam scenario.

Bypassing solutions include (Van Rijn, 2013):

- Digging a sand trap upstream of the structure. Usually a sand trap is used in combination with land-based or ship-based dredging equipment.

  Clough Murray & Roberts Marine implemented a sand trap at the Trekkopje project by digging a sand trap upstream of the structure every low tide using land-based equipment (Dixon et al., 2014). After high tide, the sand trap was filled up and the sediment had to be removed again. No dredging equipment was paired with the sand trap as this would have been too costly. The maintenance of the sand trap also proved to be a non-economical solution for the temporary structure.

- Sand trap at the entrance of the channel or in the case of this study, at the mouth of the cofferdam.

  Once again this solution needs to paired with dredging equipment otherwise the sand trap would only serve as a very short term solution.

- A sophisticated jet-pump system connected to a bypassing pipeline which deposits sand downstream of the structure.

  This solution is very sophisticated and has only been implemented at a couple of locations around the world for permanent structures (Tweed River Entrance , Australia (NSW Government, 2014); Nerang River Entrance , Australia (Cowper and Thomas, 2014); Ngqura Port, South Africa(Coastal Environmental Services, 2001))

All of these solutions are very effective if implemented in the correct manner, but all of them are expensive and not that plausible for a temporary cofferdam structure.

2.6.4 Past Case Study Summary and Conclusion

Chapter 2.6 embodies work done in the past on both temporary cofferdam structures and other hard structures built within the nearshore area.

After extensive literature review, limited information on the design specifications of temporary cofferdams could be found. For this reason permanent hard structures with the goal to interrupt longshore sediment transport was researched in order to get a better understanding of the most important design specifications of surf zone structures.

Four main design elements were identified, namely the structure length considering the surf zone width, structure height, shape and if there are multiple structures, there spacing in regards with each other. From these four element only two were deemed applicable for the design of temporary cofferdam structures, the structure length considering the surf zone width and the structure shape. Temporary cofferdams are designed in an over conservative manner regarding their height and they are also single structures so their spacing are of no concern for this study.

Taking the above mentioned into account, and also the goal of a temporary cofferdam, which is to block longshore sediment from entering a surf trench in a economically viable manner, due consideration will be given to the shape and length of the cofferdam structure when considering alternative designs for this study.

2.7 Literature Summary

In order to complete a submarine pipeline project successfully and efficiently, a vast variety of coastal- and construction design knowledge is needed. The above literature study attempts to define this knowledge and apply it to this study by linking all of these aspects to the objective mentioned in Chapter 1.2. This will be done by investigating the influence they will have on a surf zone trench protected by an open-ended cofferdam.

Once a wave field enters coastal waters, the wave field is altered more and more as the waves become a function of the water depth. This means that the bathymetry has an effect on the wave form. Waves bend, grow higher, break and cause water levels to change which in return is responsible for radiation stresses and forces in the surf zone. Depending on the specific wave field and bathymetry, different radiation stresses, and in effect the forces, are developed and these stresses and forces are responsible for creating currents in both the cross-shore and longshore directions. Cross-shore currents exist in the form of an undertow or rip currents and mainly have short term effects on the shoreline. A structure such as a cofferdam in the surf zone has a larger effect on the longshore current, as it changes the flow pattern of this current. An accurate definition of a longshore current and the understanding of its characteristics, for example the velocity distribution through the surf zone, is of paramount importance for it is this current which is responsible for the movement of sediment in the direction of the structure.

Sediment is brought into suspension through the working of turbulence caused by wave breaking, and transported by means of both the cross-shore current and the longshore current. If structures, both temporary and permanent, are built in the path of these currents, changes will be visible at the shoreline. Accretion and erosion will occur around the structure and if not understood, sedimentation can make such a project very difficult if not impossible.

Once the coastal processes are understood, knowledge of construction design is needed. This study concentrates on the design and building of the temporary structures. The equipment and methods to design and install both the pipeline and the temporary cofferdam structure in a submarine pipeline project is described in Chapter 2.5. It does however take into account how permanent structures have been designed in the past and how they overcame sedimentation problems. This knowledge is then applied to the possible designs investigated during this study.

Chapter 3

Description of Case Studies

The two past projects providing the motivation for this study have been taken into consideration as the same dominating problem was experienced in both instances at different locations. The processes in the prototypes were not replicated precisely but it was attempted to replicate the same coastal mechanisms at work.

3.1 Desalination Plant at Wlotzkasbaken Trekkopje Namibia (2010)

One of the prototypes under consideration was the Trekkopje desalination plant constructed in 2010. The salt water intakes and brine outfall pipelines of this plant are situated 1 km north of Wlotzkasbaken which is 30 km north of Swakopmund, Namibia. The desalination plant was built to supply fresh potable water for a new uranium mine approximately 65 km north of Swakopmund.

The geotechnical surveys at the site indicated hard rock covered in fine to medium grained sand. Excavation of the surf zone trench required blasting in order to loosen the sediment until it was possible to excavate it using a bucket dredger. As a result of the hard rock, it was difficult to set the sheet piles for the temporary cofferdam to a satisfactory depth. This enhanced the effect the waves and longshore current had on sedimentation in and around the structure as it could not be extended further out to sea. A sand trap was dug upstream of the trench with each low tide in an attempt to protect the trench from sediment build-up in the high tide period. As a result of the active surf zone the project became very expensive. At this site the pipeline was installed using the bottom-tow method.

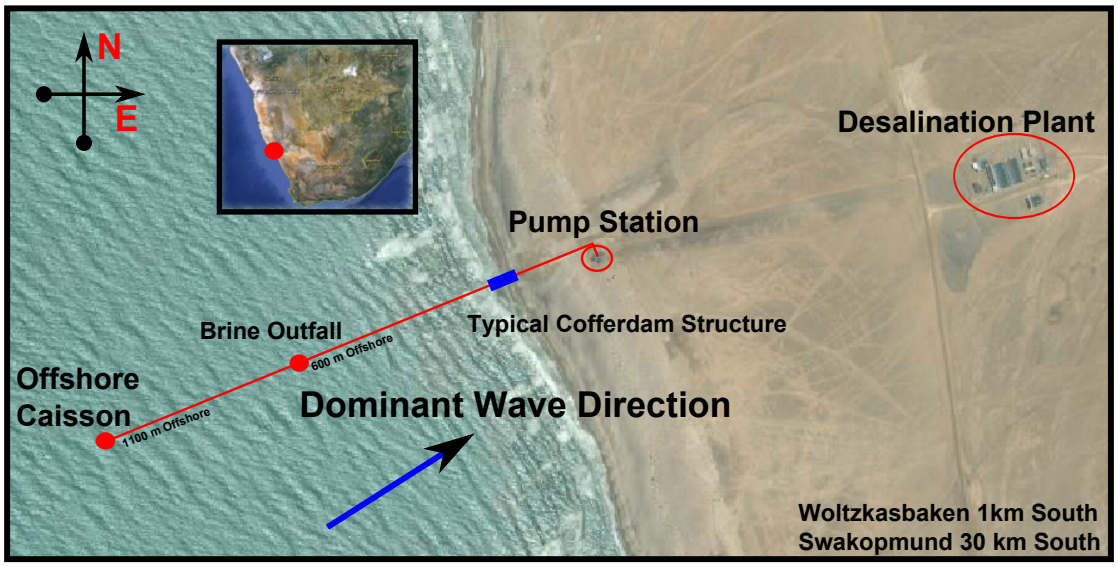

FIGURE 3.1: Trekkopje Desalination Plant Project Namibia 2010 (Image from Google Earth)

3.1.1 Environmental Data at the Trekkopje Construction Site

- Water Levels

The following water levels are as indicated on the SA Navy Tide Tables (2005).

Parameter	**Water Levels (m)**	
	Relative to Mean Sea Level	Relative to Chart Datum
Highest Astronomical Tide (HAT)	+1.004	+1.97
Mean High Water of Spring Tide (MHWS)	+0.724	+1.69
Mean High Water of Neap Tide (MHWN)	+0.324	+1.29
Mean Sea Level (MSL)	+0.00	+0.966
Mean Low Water of Neap Tide (MLWN)	-0.296	+0.67
Mean Low Water of Spring Tide (MLWS)	-0.696	+0.27
Lowest Astronomical Tide (LAT)	-0.996	+0.00
Chart Datum (CD)	-0.996	+0.00

TABLE 3.1: Water Levels for Trekkopje Namibia(2010)(Clough Murray & Roberts Marine, 2010)

- Waves

The wave data based on numerically simulated conditions at a point approximately 110 km south west of Wlotzkasbaken and indicated by the Basis of Design report by Clough Murray & Roberts Marine (2010) is as the following:

Parameters	**Significant Wave Height H_s (m)**	**Wave Incidence Angle $\beta(^o)$**	**Peak Wave Period T_p (s)**
Minimum	0.39	170.1	4.90
Maximum	6.34	256.6	19.78
Mean	2.14	204.4	11.46
Median	2.03	203.2	11.17
Standard Deviation	0.83	9.84	2.29

TABLE 3.2: Wave Data for Trekkopje Namibia(2010)Clough Murray & Roberts Marine (2010)

The following data represents the breaking wave characteristics for waves exceeded 10 % of the time.

Wave Direction θ	**Wave Period T(s)**	**Deep Sea Significant Wave Height $H_{o,s}$ (m)**	**Breaking Wave Height H_b (m)**	**Wave Incidence Angle $\theta(^o)$**	**Breaking Depth d_b(m to LAT)**
SSW	13	3.3	3.5	14	4.0
SW	13	3.3	3.9	8	4.5

TABLE 3.3: Breaking Wave Data for Trekkopje Namibia(2010)(Clough Murray & Roberts Marine, 2010)

- Currents

The Benguela current is present in the offshore areas and flows in the direction of north to north-west, parallel to the coastline at an average surface velocity of between 0.1 m/s to 0.3 m/s. The initial nearshore current velocities are to be taken as 0.14 m/s. A net surf zone current, driven by prevailing waves is to have an expected velocity of between 0.3 m/s to 0.5 m/s. It can also be assumed that a wind current in the range of 0.2 m/s to 0.3 m/s would be present. Thus to conclude, a net shoreline longshore current of approximately 0.8 m/s - 1.0 m/s could be expected. All of the currents are given as referenced by the basis of design of Clough Murray & Roberts Marine (2010).

3.1.2 Cofferdam Details

The construction of the sheet pile cofferdam at Trekkopje, Namibia presented several problems. The cofferdam was 39.6 m in length and 11 m wide. As a result of a seabed consisting of mainly hard rock, the construction of the cofferdam was difficult and blasting of the seabed material was required to ensure that the cofferdam and surf zone trench was built to specifications. The cofferdam was inserted to a depth of -1.5 m CD and, with a length of only 39.6 m, the seaward end of the cofferdam was well inside the surf zone and far shallower than the Hallermeier calculated closure depth of -11.84 m (Refer to Appendix A). It can thus be seen why sedimentation was present in and around the structure during the pipeline installation process. A photo of the surf zone trench excavation process and temporary construction jetty is shown in Figure 3.2 and a detailed drawing of the cofferdam structure as drawn up by Clough Murray & Roberts Marine is given in Figure 3.3.

FIGURE 3.2: Trekkopje Cofferdam Photo During Construction (2011)(Image from Clough Murray & Roberts Marine)

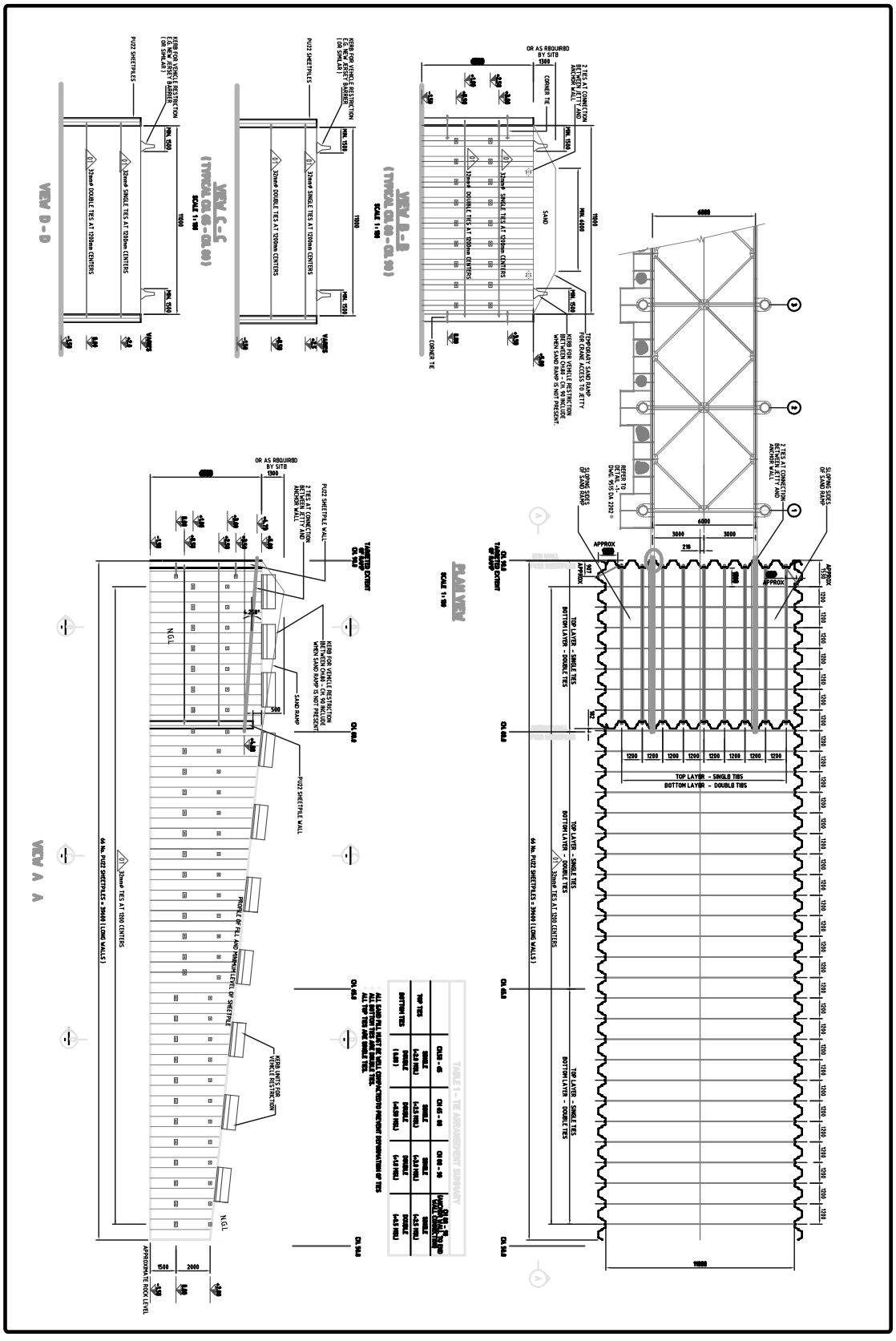

FIGURE 3.3: Trekkopje Cofferdam Details (2010)(Image from Clough Murray & Roberts Marine)

3.2 Desalination plant at Mossgas Mossel Bay (2011)

Clough Murray & Roberts Marine undertook another project at Voorbaai in Mossel Bay (2010). The project included both a 900 mm diameter HDPE intake pipeline, which equalled the biggest HDPE pipeline to be installed in South Africa, and a 630 mm diameter HDPE brine discharge pipeline, both for a desalination plant. The pipeline extends 730 m offshore (water depth approximately -17 m Chart Datum(CD)) adding to a total length of 920 m. CM& M was tasked with the fabrication and installation of both the pipelines including the design and construction of all the temporary works, installation pipe stress and buoyancy checks. Similar to the project at Woltzkasbaken the geotechnical report at Mossel Bay also reported hard rock beneath the sand, but in this case the situation was not as severe. The soil consisted of consolidated sediment (rock) overlain by unconsolidated sediment varying in thickness of approximately 4 m in the beach and fore dune zones, decreasing to less than 1 m thickness 400 m offshore. This thin layer is approximately 400 m wide. The method implemented here for the pipeline installation was a float-and-sink method.

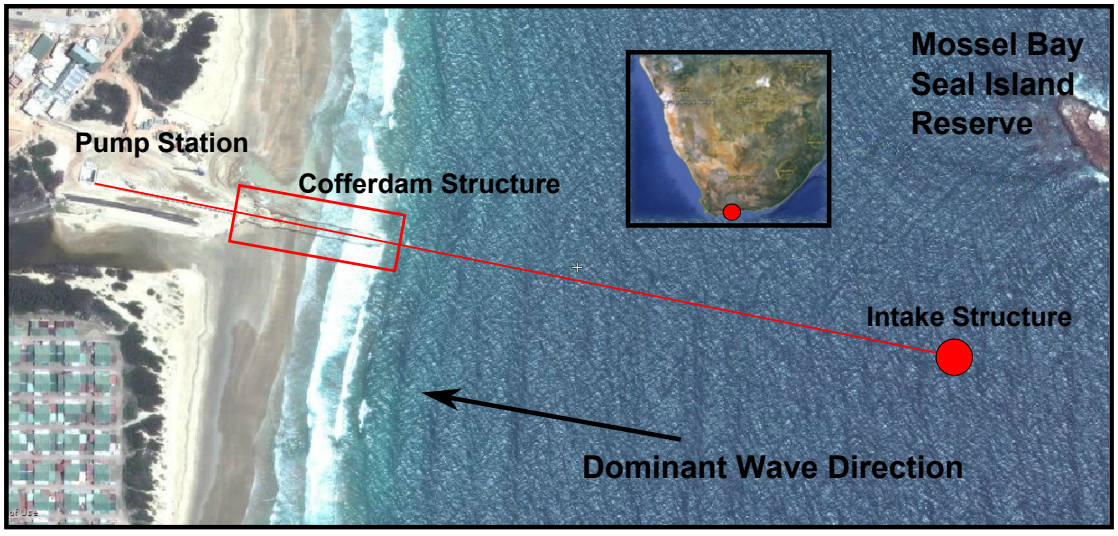

FIGURE 3.4: Mossel Bay Desalination Plant Project RSA (2011)(Image from Google Earth)

3.2.1 Environmental Data at the Mossel Bay Construction Site

- Water Levels

  The following data was used for the Mossel Bay project by Clough Murray & Roberts Marine as specified by the Basis of Design for the Desalination Plant project of 2011 (Clough Murray & Roberts Marine, 2011).

Parameter	**Water Levels (m)**	
	Abbreviation	Relative to Chart Datum
Highest Astronomical Tide	HAT	+2.430
Mean High Water of Spring Tide	MHWS	+2.010
Mean High Water of Neap Tide	MHWN	+1.450
Mean Sea Level	MSL	+1.170
Mean Low Water of Neap Tide	MLWN	+0.880
Mean Low Water of Spring Tide	MLWS	+0.260
Lowest Astronomical Tide	LAT	+0.00
Chart Datum	CD	+0.00

TABLE 3.4: Water Levels for Mossel Bay(2011)(Clough Murray & Roberts Marine, 2011)

- Waves

  The following information is based on data recorded during work done in the Mossel Bay area which belongs to Watermeyer Prestige & Retief (1997) and gives the offshore wave climate for Mossel Bay as indicated by Clough Murray & Roberts Marine (2011).

Return Period	H_s**(m)**
1:1	5.2
1:5	6.11
1:100	7.8

TABLE 3.5: Wave Data for Mossel Bay(2011)(Clough Murray & Roberts Marine, 2011)

- Currents

  The current velocities that were used in the Mossel Bay desalination plant pipeline design are as shown in the following table. The data for the 1 year return period is extracted from studies done by the CSIR (CSIR, 1990).

Return Period	**Surface Current (m/s)**	**Bottom Current (m/s)**
1:1	0.90	0.45
1:10	1.00	0.60
1:100	1.20	0.60

TABLE 3.6: Currents for Mossel Bay(2011)(Clough Murray & Roberts Marine, 2011)

3.2.2 Cofferdam Details

The sheet pile construction at Mossel Bay was done with more ease than that of Trekkopje (Namibia). The cofferdam had a width of 8.4 m and an overall length of 154 m where it stopped at a water depth of -7.0 m CD. This implies that the cofferdam did cross the Hallermeier calcualted closure depth of 6.5 m based on the last 7 year's historical wave data (Refer to Appendix A). However, there is reason to believe that the closure depth was deeper than the calculated value as sedimentation problems were still experienced. A photo during the construction of the cofferdam and the detailed drawing of the cofferdam layout at Mossel Bay 2011 as given by Clough Murray & Roberts Marine can be seen below in Figure 3.5 and Figure 3.6 respectively.

FIGURE 3.5: Mossel Bay Cofferdam Photo During Construction (2011)(Image from Clough Murray & Roberts Marine)

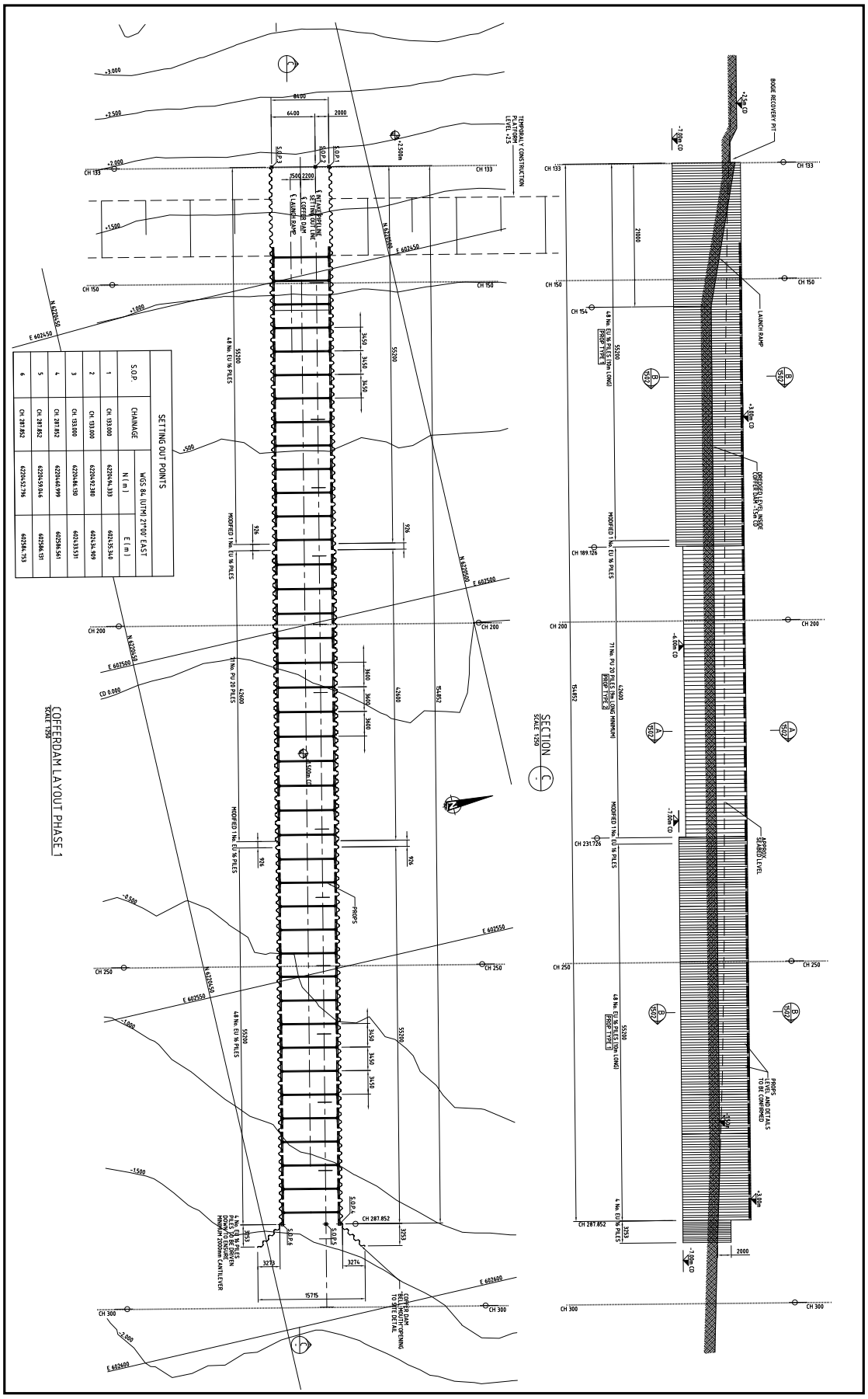

FIGURE 3.6: Mossel Bay Cofferdam Details (2011)(Image from Clough Murray & Roberts Marine)

Chapter 4

Physical Modelling

4.1 Methodology

4.1.1 Introduction

This discussion will outline the procedure which was followed to complete the 3D physical modelling of a temporary cofferdam structure interfering with the natural flow of water and sediment within the surf zone.

To achieve the above mentioned the following will be discussed in the methodology:

I. The goal of the physical model.

II. The scope of testing, including the location and hardware used in the modelling.

III. The environmental data used in the model, considering the environmental data at the prototypes mentioned in Chapter 3.

IV. Key aspects to look for in different processes such as waves, currents and sedimentation.

4.1.2 Goal

The goal of the physical modelling is to replicate the gross aspects of the currents and sediment transport mechanisms exhibited in a real construction project and serve as a visual aid in the understanding of surf zone currents and sediment transport. The values obtained from testing (e.g. sedimentation volumes, wave heights, currents speeds) will be modelled as accurately as possible but no sediment volumes will be taken as viable results when comparing the model to the prototype.

4.1.3 Scope of Testing

The model was built and tested in the hydraulics laboratory of the CSIR (Council for Scientific and Industrial Research) in Stellenbosch. Due to financial and time constraints the model was run on an already built basin used to model a shoreline at Umhlanga Rocks near Durban. A 3D basin with dimensions of 55 m x 32 m x 500 mm was used although the model for this project only covered a 30 m x 30 m area within this basin. Waves were generated with 5 HR Wallingford deep water wave generators adding to a total width of a 20 m wide wave bank. A schematic representation of the information above is given in Figure 4.1.

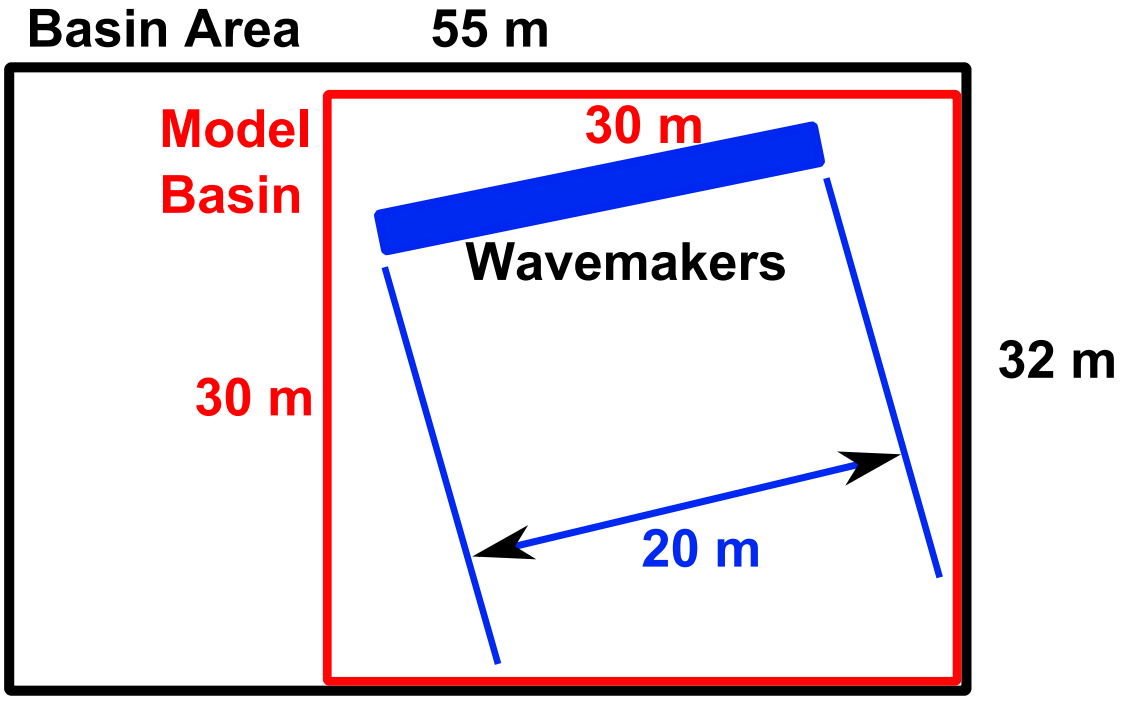

FIGURE 4.1: Physical Model Basin Dimensions

The model had a concrete base with a gradual slope (Refer to the bathymetry Chapter 4.1.4) which was used as the seabed in all but test A12 (refer to Table 4.1), where a part of the basin was filled with fine silica sand to model a movable bed. The model had a scale of 1:50.

A hardboard structure was built and used to model the temporary cofferdam structure within the surf zone. Refer to Figure 4.2 and Figure 4.3 for the cofferdam model and details. Four probes were used, one directional probe in deep water and three probes, one on either side of the mouth of the structure and one in the mouth of the structure, in shallow water to capture the wave data within the basin. This data was used only for monitoring reasons to ensure that the wave field generated in the basin was accurate. The wave probe data was stored and recommended for future studies.

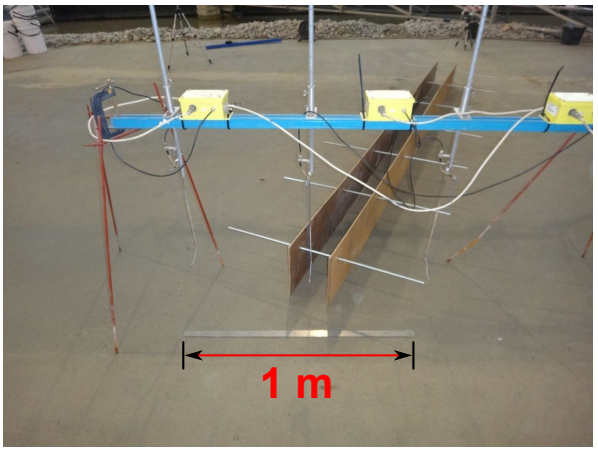

FIGURE 4.2: Hardboard Cofferdam Model

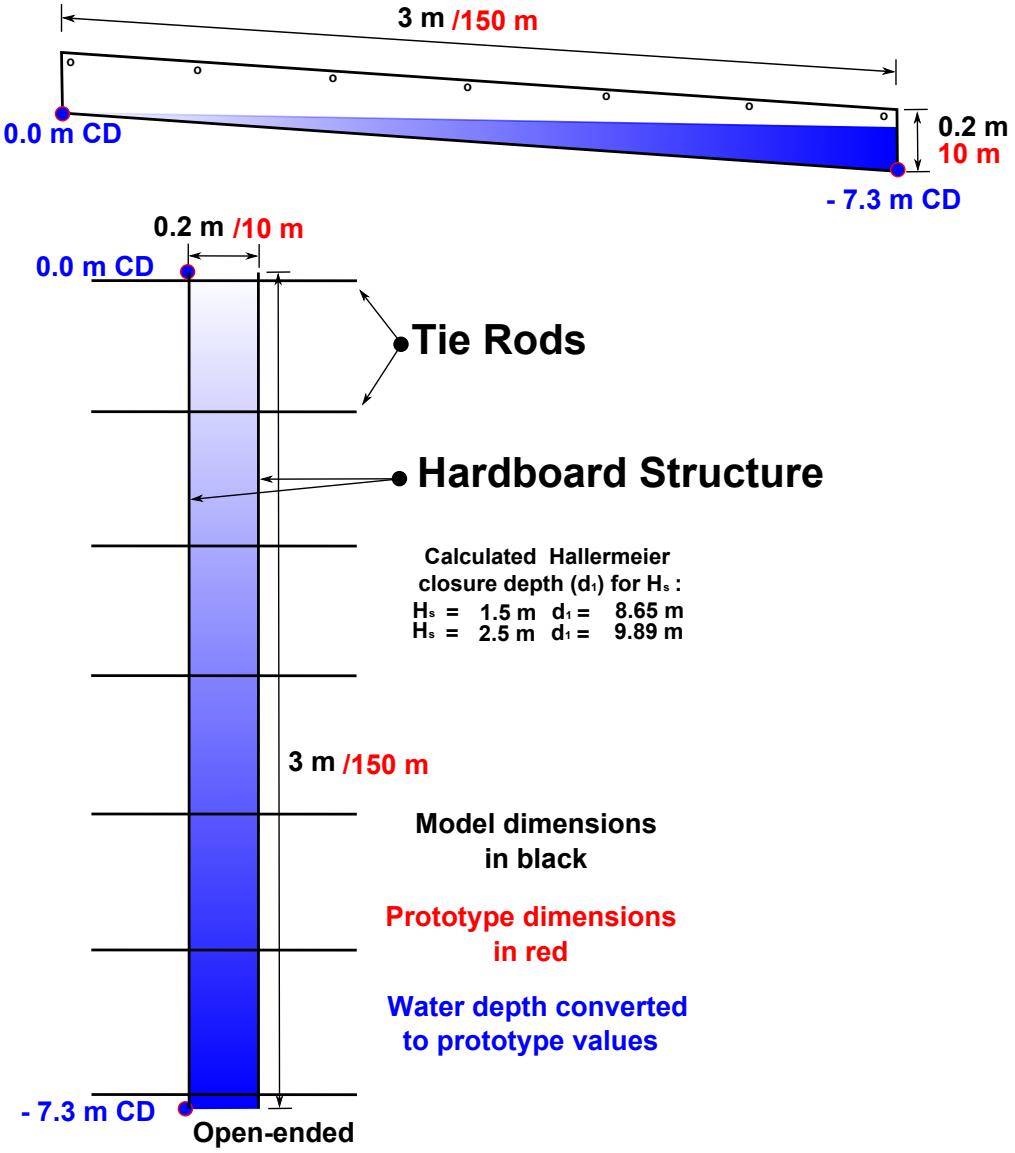

FIGURE 4.3: Detailed Cofferdam Diagram

4.1.4 Environmental Data

The bathymetry of the basin was originally built to replicate a stretch of shoreline at Umhlanga Rocks near Durban for a previous project. The bathymetry had a gradual slope and the basin orientation and contour map can be seen in Figure 4.4.

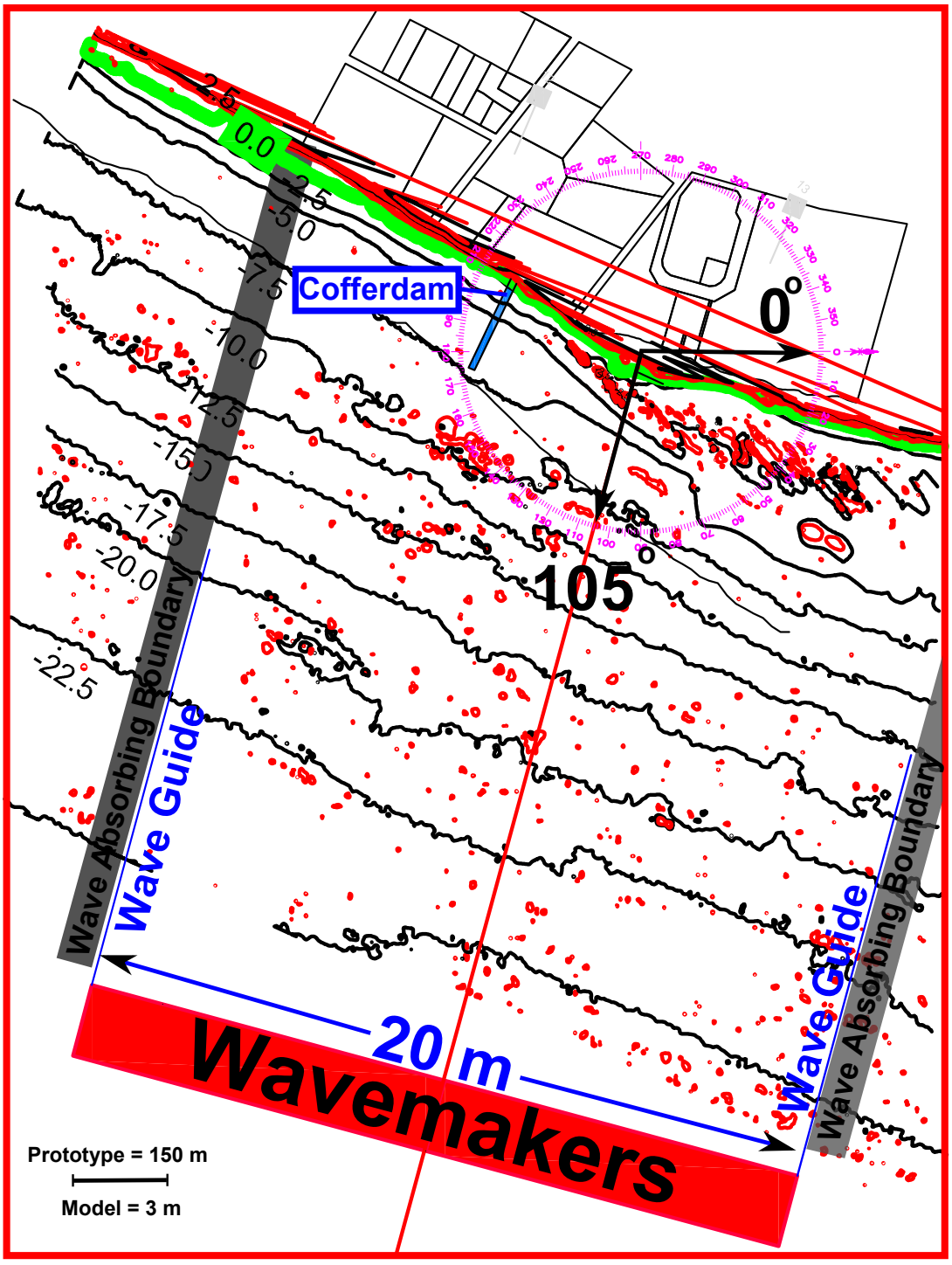

FIGURE 4.4: Physical Model Basin Bathymetry

The environmental data used within the physical model was selected from a combination of research done by the CSIR, prototype data from the projects undertaken by Clough Murray & Roberts Marine and historical data obtained from studies done on the areas of Mossel Bay and Wlotzkasbaken, Trekkopje. After considering the above, a test program was chosen to best represent a wave field that will show the gross aspects of the processes at work at these sites. The test programs are shown in Table 4.1 and Table 4.2 below.

Structure built perpendicular (90^o) to beach, thus at 113.5^o:

Test Number	**Significant Wave Height H_s(m)**	**Peak Wave Period T_p(s)**	**Wave Direction θ(deg)**	**Deep Water Depth d_o(m)**	**Test Water Level (Relative to CD (m))**	**Duration (min)**
A1	2.5	12	105	25	MHWN +1.69	27
A2	1.5	12	105	25	MHWN +1.69	27
A3	2	12	105	25	MHWN +1.69	27
A4	2.5	12	105	25	MHWN +1.69	27
A5	1.5	12	85	25	MHWN +1.69	27
A6	2	12	85	25	MHWN +1.69	27
A7	2.5	12	85	25	MHWN +1.69	27
A8	1.5	12	105	25	MSL +0.97	27
A9	2.5	12	105	25	MSL +0.97	27
A10	1.5	12	85	25	MSL +0.97	27
A11	2.5	12	85	25	MSL +0.97	27
A12	1.5	12	85	25	MHWN +1.69	120

TABLE 4.1: Physical Modelling Test Program A(90^o)

Structure built perpendicular (30^o) to beach, thus at 135^o .

Test Number	**Significant Wave HeightH_s (m)**	**Peak Wave Period T_p(s)**	**Wave Direction θ(deg)**	**Deep Water Depth d_o(m)**	**Test Water Level (Relative to CD (m))**	**Duration (min)**
B1	2.5	12	105	25	MHWN +1.69	27
B2	1.5	12	105	25	MSL +0.97	27
B3	2	12	105	25	MSL +0.97	27
B4	2.5	12	85	25	MSL +0.97	27
B5	1.5	12	105	25	MHWN +1.69	27
B6	2	12	105	25	MHWN +1.69	27
B7	2.5	12	85	25	MHWN +1.69	27

TABLE 4.2: Physical Modelling Test Program B(30^o)

4.1.5 Key Aspects

Observations of the following key aspects, allows one to assess if the model is representing the processes experienced at the prototypes to a level of accuracy which is satisfactory to the modeller. The following observations are based on the theory in the literature review.

I. WAVES

The local wave behaviour at the cofferdam is supposed to be dependent on the sediment build-up. When sediment starts to build-up and move in the direction of the mouth of the structure, the shore-line must shift deeper, away from the initial shoreline. This is expected to push the breaker line back and cause the waves to break at a deeper point relative to the shoreline, although the breaker water depth will be the same at that point as the initial point of breaking. This should cause more cross-shore transport at the mouth of the structure and fill up the structure with sediment at an exceptional rate. Due to the fact that the model bed was not movable in all but one of the tests, the breaker line did not move, but by observing dye introduced in the water, a prediction was made as the flow pattern gave insight into the sediment transport regime.

II. CURRENTS

The currents present during the modelling are expected to be both a longshore current and a cross-shore current. The waves are supposed to induce a longshore current which should then flow up the shoreline until the current makes contact with the structure where the current velocity should decrease in the corner between the shoreline and structure wall, and divert to deep water. Once the current has surpassed the mouth of the structure it should then attempt to re-establish on the opposite side of the structure. A cross-shore current is expected to be present as well and if the modelling is done successfully, some rip currents should be visible along the shoreline. Once sediment is used in the model there may be an undertow visible by observing sediment being transported away from the shoreline.

III. SEDIMENTATION

Once sediment is present within the model it is expected to observe sediment migrating along the shoreline towards the structure as it is being transported by the longshore current. Once the flow of sediment hits the structure, it should fall to the seabed and start to build up against the structure. Some of the finer material may move up along the structure where it should settle at the mouth of the structure. Once the sediment build-up has reached a point where the sediment bank has reached the mouth of the structure and the wave breaking point has been pushed back, sediment is expected to be

deposited inside and on the opposite side of the structure. If the correct wave conditions are to be modelled, some sediment should be transported offshore to settle behind the breaker line and create a sand bar in deeper water. Sand formations, called ripple formations, is also expected to be visible along the seabed in the areas where sediment is mobile.

4.1.6 Physical Modelling Scaling Laws and Limitations

In order to ensure the accurate representation of a prototype within a physical model, certain scaling laws need to be applied. Scaling laws for coastal models, including movable bed models, are well established ((Noda, 1972), (Hughes, 1983)), but a lack of understanding of the errors that occur due to scaling effects, makes the accurate modelling of a prototype a challenging task. For coastal scale models, particularly the ones conducted in the surf zone, the most relevant requirement is to attain similarity of the cross-shore equilibrium bed profiles between the prototype and model (Hughes and Fowler, 1990).

Hughes (1993) defines a *scale ratio*, or just *scale*, as the ratio of a parameter in the prototype to the value of the same parameter in the model, and can be symbolically represented as:

$$N_X = \frac{X_p}{X_m} = \frac{ValueofXinPrototype}{ValueofXinModel} \tag{4.1}$$

where N_X is the prototype-to-model scale ratio of the parameter X, and the subscripts p and m represent prototype and model, respectively.

The model in this study can be defined as an undistorted model, meaning that the vertical and horizontal scale are the same. This implies that:

$$N_L = \frac{L_p}{L_m} \tag{4.2}$$

is applicable to both the water depth and the basin size. By following the mathematical laws and assuming that the gravitational scale (N_g) is equal to 1, ratio's for both velocity N_V and time N_T can be obtained:

$$N_V = \frac{V_p}{V_m} = \frac{(\frac{L}{T})_p}{(\frac{L}{T})_m} = \frac{L_p}{L_m}.\frac{T_p}{T_m} = \frac{N_L}{N_T} \tag{4.3}$$

$$N_T = \frac{T_p}{T_m} = \sqrt{\frac{L_p}{L_m}.\frac{g_p}{g_m}} = \sqrt{N_L} \tag{4.4}$$

Van Rijn et al. (2011) however, states that a scaling problem can be experienced with sediment particle size. If the sediment particle size is too small, the sediment properties become cohesive and will not act appropriately for a movable bed model. Various studies have been done on sediment particle size scaling laws ((Noda, 1972), (Ito and Tsuchiya, 1984)), and many recommendations have been made on which scaling methods to use.

Hughes and Fowler (1990) show that the sediment scaling law should be based on the the fall velocity of suspended sediment particles, and if the fall velocity ratio between prototype and model can be managed, an accurate representation of the sediment transport regimes will be achieved.

4.1.7 Results Interpretation

As stated in the goal of the physical modelling, the results presented in Chapter 4.2 are based on the visual observation of the modeller. Wave probes were used in order to calibrate the wave conditions for each individual run, but the current movement and sediment transport analysis presented in the results and the discussion thereof are based on the visual observations of the modeller before, during and after the specified model tests.

4.2 Results and Discussion

4.2.1 Introduction

The results will be discussed by addressing the outcomes of Test A12 (Refer to Table 4.1 for test details) which was done with a movable bed. The aspects of sediment transport will be identified looking at a series of processes visible during this test. The knowledge of the other tests done with a set bed, will then be used to discuss the effects of an increase in wave height, water level, wave angle and the angle of the structure. The time lapsed images for test A12 can be seen in Appendix D.

4.2.2 Initial Basin Description

The image (Figure 4.5) and two schematics (Figure 4.6 & Figure 4.7) on page 60 and page 61 will be referred to, to show the initial state of the model basin. The intended goal of these figures aims to focus the reader's attention to certain parts of the basin before any sediment has been transported by wave-induced processes. These areas pointed out in this section would prove best to show the surf zone processes when the initial basin state was compared to the basin state after the test was done.

The initial basin photo in Figure 4.5 and the schematic in Figure 4.6 shows sand placed around the structure in a strategic pattern to better show the effects of the sediment transport mechanisms.

Note that the sand fills the entire photo on the bottom right hand side and there is no gap in the sediment layer (Figure 4.5 Point A). This can also be seen by the uniform thickness of the initial sediment layer at profile Z' which represents the cross-shore profile through point A (Figure 4.7). On the southern side of the structure the sediment was deposited in a straight line with the structure mouth, thus there was no sediment deeper than that of the structure mouth (Figure 4.5 Point B). This line can also clearly be seen on the profiles Z', Y' and X' as there is a sudden cut off in sediment. There was also no sediment placed within the structure boundaries (Figure 4.5 Point C) to better show sediment transported into the structure. To clarify this, a close up of the structure mouth, looking from an overhead, shoreline view, has also been provided.

On the northern side of the structure a gap was left open intentionally to try and show the transport of sediment around the structure (Figure 4.5 Point D). This can also be seen by referring to profile W' as the cut-off line for the sediment is much closer to the shoreline than that of the profiles on the southern side of the structure.

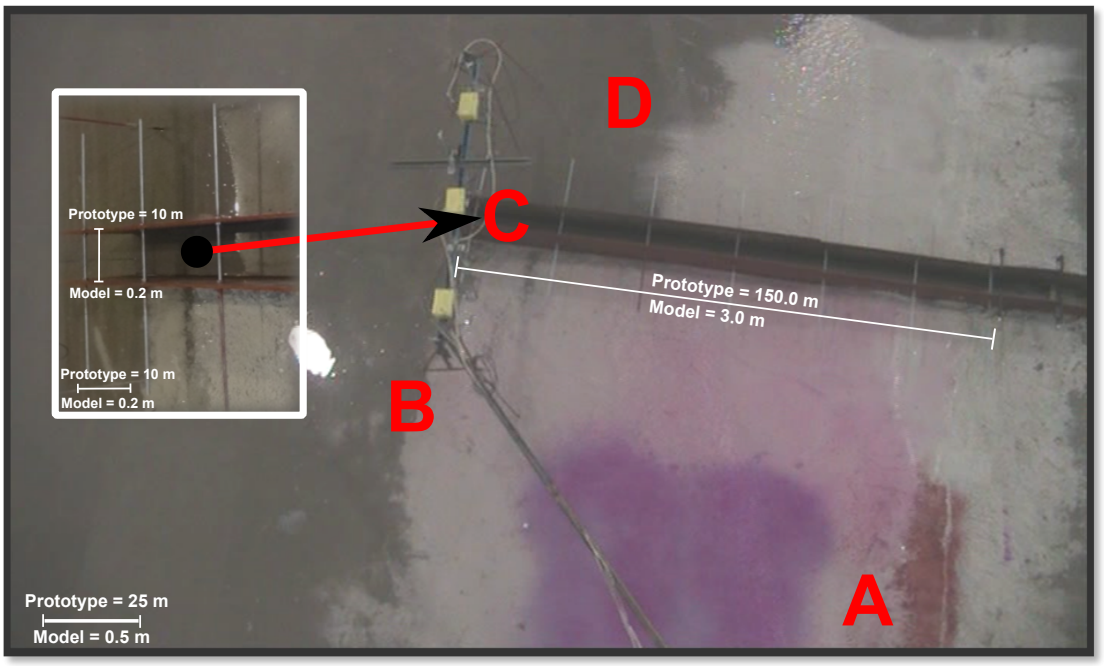

FIGURE 4.5: Initial Physical Model Basin

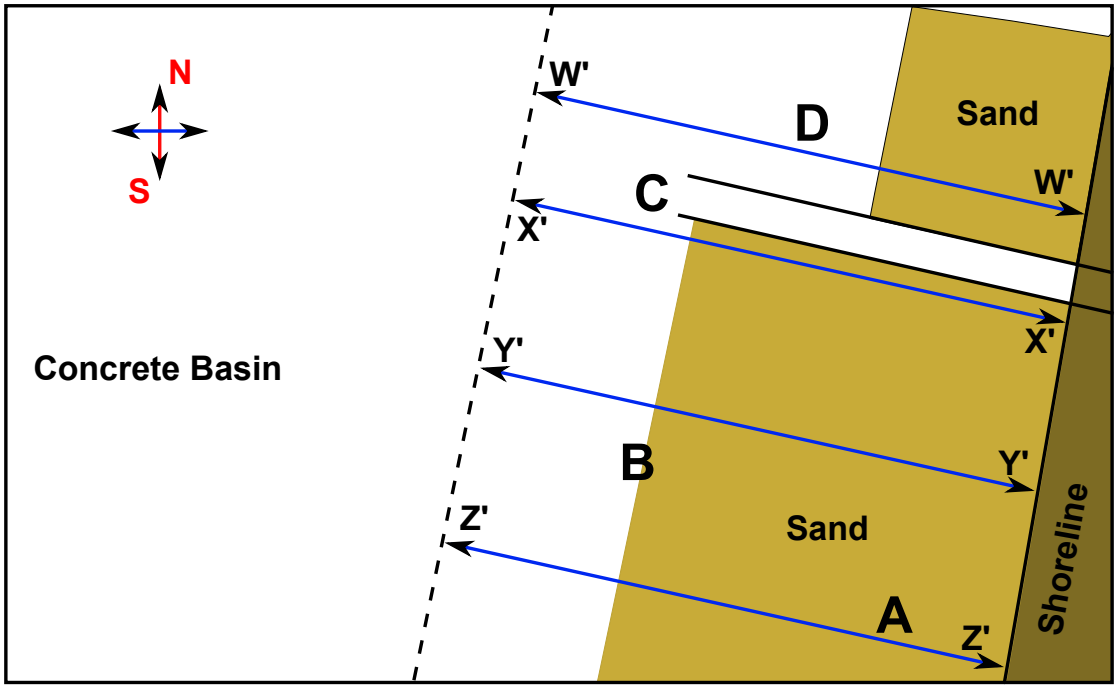

FIGURE 4.6: Initial Physical Model Basin Schematic

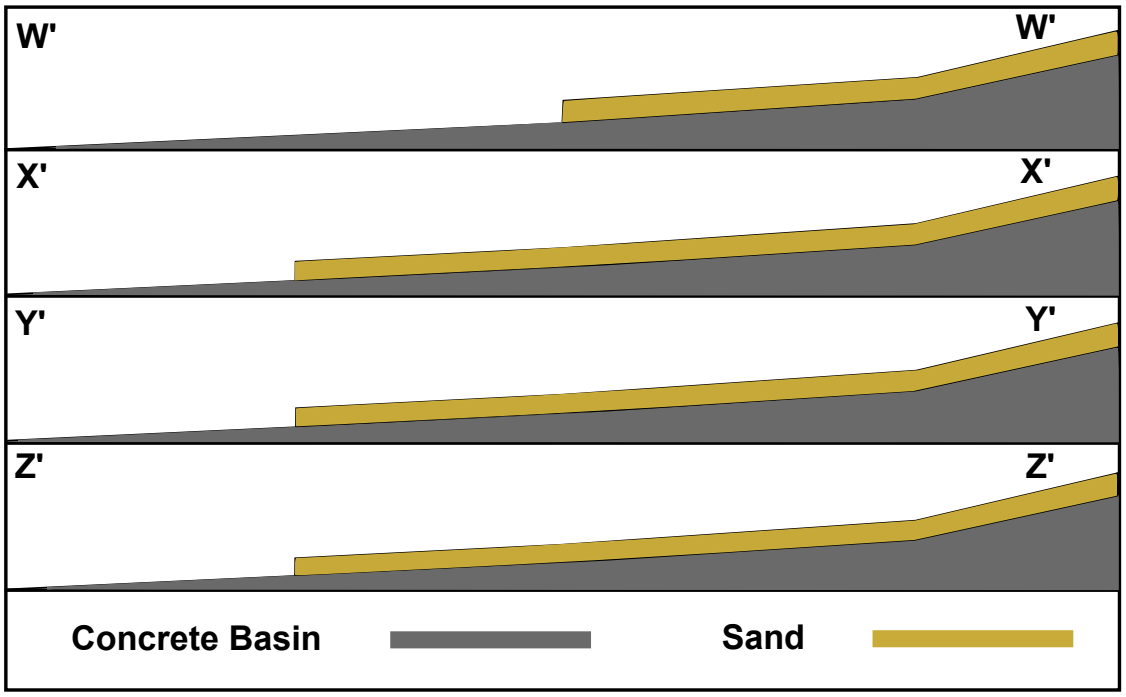

FIGURE 4.7: Initial Physical Model Basin Profile

4.2.3 Final Basin Description

The images (Figure 4.8 & Figure 4.9) and two schematics (Figure 4.10 & Figure 4.11) on page 64 and 65 will be used to identify the gross aspects of the sediment transport processes during the interference of a structure in the surf zone. These figures shows the basin state as it was after the completion of the test. Note that the 120 minute duration of the test in the model is equal to 35 days in the prototype.

By wave agitation and a wave induced longshore current, the sediment is transported from the southern side (upstream of the structure as represented by the gap at Point 1 in Figure 4.9 and Figure 4.10), up along the shoreline after which it settles against the structure. This is where the current velocity decreases, creating a calm spot for sediment to settle (Point 2 in Figure 4.9 and Figure 4.10). This in return creates a sand bar against the southern side of the structure. These processes can also clearly be seen by referring to the sediment profiles in Figure 4.11. In profile Z' a clear gap in the sediment can be seen, to such an extent that the concrete basin floor is visible, and there is no sediment left to cover it. As the profiles move from south to north (Z' to Y' to X'), the build-up of this sand bar against the structure is clearly visible.

As a result of this sand bar at Point 2, the wave breaker line will move seaward from the initial point (indicated by the solid blue line in Figure 4.9), further away from the initial shoreline to a point where it will reach the mouth of the structure (indicated by the

dashed blue line in Figure 4.9). The finer sediment that is still in suspension after the current velocity has decreased, will be carried up the side of the structure and settle at the mouth of the structure. Once the breaker line has moved seaward to a point where waves are breaking within the structure mouth, the waves will push sediment into the structure at an accelerated rate. Thus sediment will be deposited into the structure by the cross-shore transport mechanisms. The result of this can be seen by enlarging the image at Point 4, where one can see sediment inside the structure after the test, where there was no sediment inside the structure before the test.

Another interesting observation is the angle of the ripple formations before hitting the structure, compared to the ripple formation inside the structure. During the test the wave diffraction around the structure was clearly noticeable, along with a wave lag within the structure. The ripple formation before hitting the structure is formed in line with the dominant wave direction as seen in Figure 4.8. Once the wave diffracts around the structure and into the structure, the ripple formation changes orientation to being in line with the shoreline.

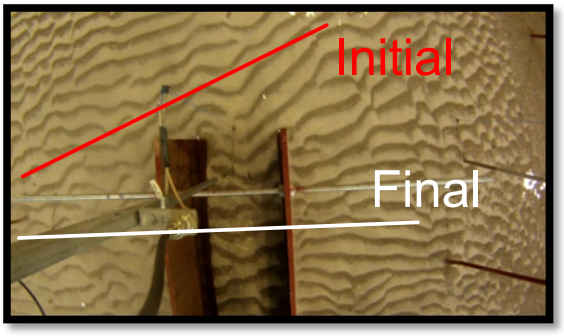

FIGURE 4.8: Ripple Formation

This observation can also be seen as a result of the structure shielding the area from all the wave components directed at the structure, except the small one coming directly into the structure. This can be a valuable observation. If this is the case and the structure is rotated further clockwise, the energy from the wave component directed into the structure will reduce and theoretically the cross-shore transport into the structure should decrease.

As the longshore current will re-establish on the opposite side of the structure (northern side), fine sediment will be transported around the structure, and settle on the northern side of the structure as seen at Point 5. This can also be seen by comparing the initial sediment profile W', with the same profile after the test is done. The sediment layer is thinner and more spread out over the basin floor. As the longshore current re-establishes on the northern side of the structure, erosion should be visible as the sediment the shoreline requires to stay stable on the down-stream side of the structure, is intercepted

by the structure and does not reach this part of the shoreline. Although there are visible signs in the tests done in this study that the longshore currents do start to re-establish on the northern side of the structure, the current is not strong enough to replicate the erosion. As indicated by Point 6, only a little dispersion is visible that spreads out the sand further downstream and evens the sediment layer to create a thinner layer which is spread out wider.

The same ripple formation is visible on the northern side of the structure. The geometry form of this formation can better be seen at Point 7 where the area is enlarged. This ripple formation is a result of localized regions of high flow rate and regions of boundary layer separation caused by irregularities on the substrate surface. Sediment grains will move up the up-stream side of an irregularity or ripple, accumulate on the crest and cascade down the lee side of the ripple into the next trough. Through this process ripples will grow and migrate along the seabed (Bennington, 1990). These small ripples will migrate throughout the basin as long as there is wave energy driving them. At the trough of the ripples the concrete basin is visible throughout most of the basin floor. These results would differ if a thicker sediment layer was introduced, altering the formations and different final positions.

The last phenomenon visible in this test is that of cross-shore transport. The cross-shore transport can exist in a number of different forms for example, the waves transport sediment through turbulent agitation, rip currents carrying sediment back into deeper water or an undertow which moves sediment away from the shoreline. In the case of this model, the sediment had been transported to be deposited just behind the breaker line, as indicated by Point 8, and represents the possible presence of an undertow. However, in over 80% of the tests done, a rip current upstream of the structure was visible. This rip current was more prominent in the tests done with a lower water level (MSL) but was also visible with the test done at MHWN. The sand deposited outside of the breaker line can also be as a result of this rip current. The rip current velocity will decrease the moment it leaves the surf zone and once the velocity decreases the sediment particles will fall down to the seabed. This sediment movement is also clearly visible when comparing the initial sediment profile Z', with that of the basin after the test was completed.

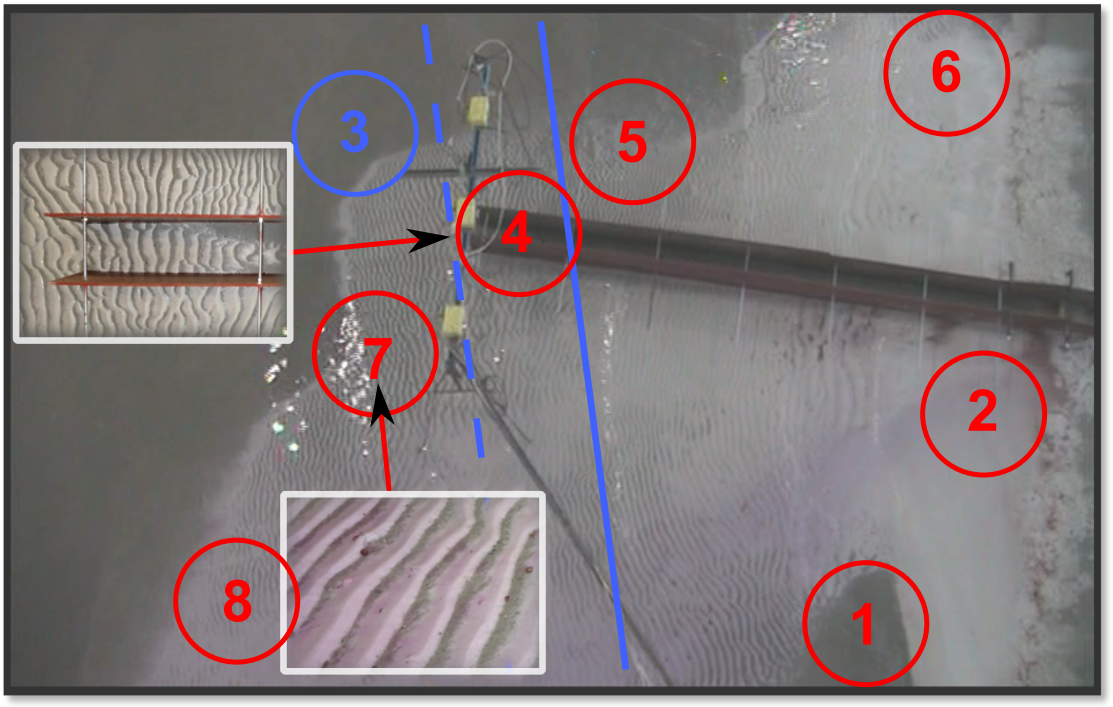

FIGURE 4.9: Final Physical Model Basin

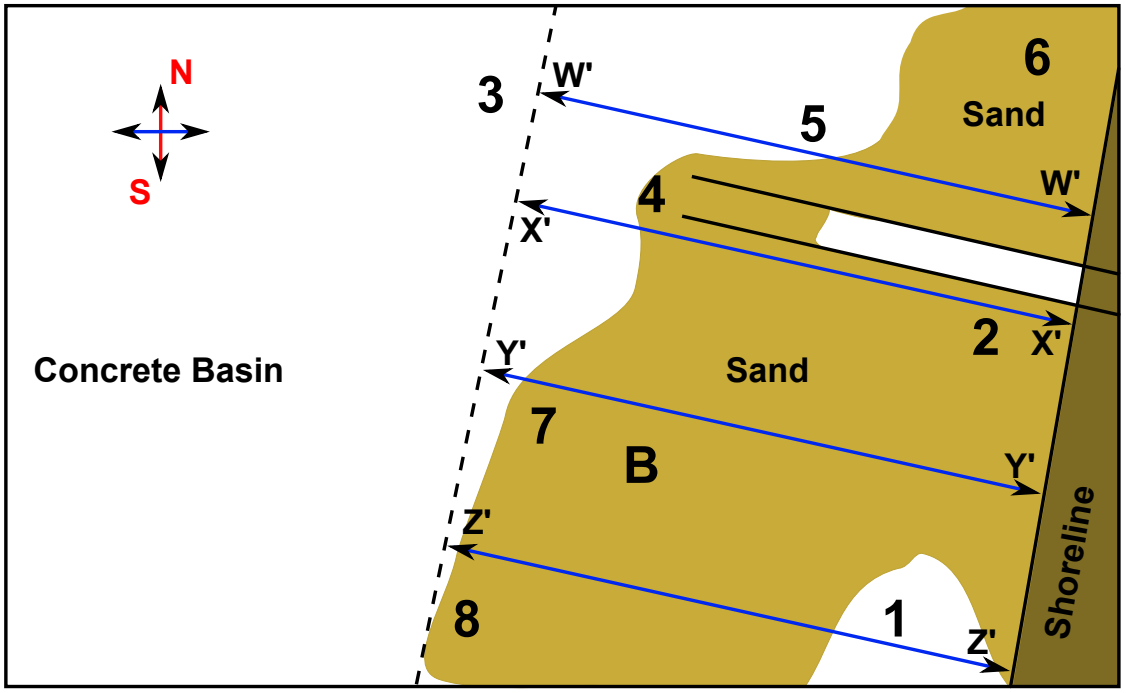

FIGURE 4.10: Final Physical Model Basin Schematic

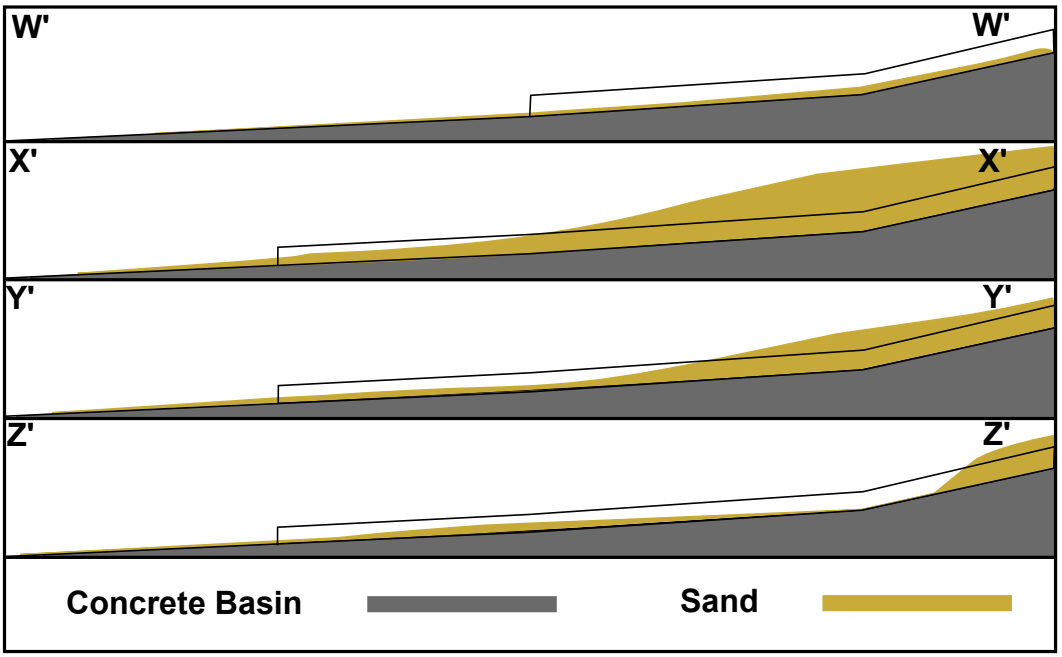

FIGURE 4.11: Final Physical Model Basin Profile

It is important to remember that even with no longshore current, and even outside the breaker line, sediment is moving. Even if it is just side to side or over a very small distance, movement is inevitable. This means that there will never be a situation where no sediment intrusion risk is present during a construction process on a soft seabed. The processes observed in the physical model are, however, of such a nature that they increase the movement of sediment to a point where it becomes problematic. The observations made above can be used to draw up a schematic of the sediment pathways in the test basin. These pathways are a summary of what can be expected when dealing with the situation at hand. Figure 4.12 represents both the longshore transport towards and around the structure, and the cross-shore transport as a result of both the rip currents to deeper water and the waves transporting sediment into the mouth of the structure as observed by the modeller.

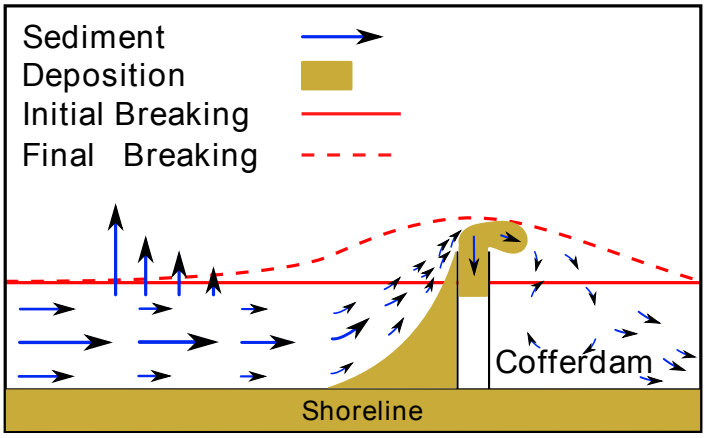

FIGURE 4.12: Sediment Transport Routes

4.2.4 Summary of Observations and Conclusions

After discussing the processes above, the tests with a fixed seabed can now be used to predict what will happen when the wave conditions are changed. By observing dye that was introduced into the water in the all tests conducted with a fixed bed, the currents could be followed and compared with regards to current velocity and direction, for the different wave conditions. The current velocity was obtained by taking the time it took for the dye to pass two consecutive fixed points in the model, which was filmed on video camera. The dye was introduced approximately 0.5 m shallower than the structure mouth, upstream of the structure. The following table shows the longshore current velocity as calculated from the observed dye:

Note: All values have been converted to prototype relevant magnitude.

Test Number	**Significant Wave Height H_s(m)**	**Wave Direction θ(deg)**	**Test Water Level**	**Distance Dye Travelled (m)**	**Time Elapsed (sec)**	**Longshore Current Velocity (m/s)**
A1	2.5	105	MHWN	25	17.2	1.45
A2	1.5	105	MHWN	25	28.9	0.87
A3	2	105	MHWN	25	26.9	0.93
A4	2.5	105	MHWN	25	17.0	1.47
A5	1.5	85	MHWN	25	22.0	1.14
A6	2	85	MHWN	25	17.7	1.41
A7	2.5	85	MHWN	25	10.7	2.34
A8	1.5	105	MSL	25	90.7	0.28
A9	2.5	105	MSL	25	73.5	0.34
A10	1.5	85	MSL	25	41.0	0.61
A11	2.5	85	MSL	25	35.4	0.71

TABLE 4.3: Physical Modelling LSC Velocity Results(90^o)

- An increase in incident angle (β) to the shoreline caused an increase in longshore current velocity. This is evident by observing the dye movement of the tests and comparing the time it took for the dye to travel a certain distance in the individual tests. This larger longshore current velocity indicates an increase in the sediment transport rate. Also note that a decrease in wave angle will thus decrease the longshore current and decrease the sediment transport rate.

- An increase in significant wave height (H_s), caused an increase in longshore current velocity. This is evident by observing the dye movement of the tests and comparing the time it took for the dye to travel a certain distance in the individual tests. This also increases the sediment transport rate.

- Once the mouth of the structure was inside the breaker line or surf zone, the amount of sediment transported into the structure was more than that of the case where the mouth of the structure was outside of the breaker line. Thus sediment build-up within the trench was much less for the time period that the structure mouth was outside the breaker line.

- As the water level decreased from Mean High Water Neap (MHWN) to Mean Sea Level (MSL), the longshore current also retreated at the shoreline. This was evident by observing the dye some distance away from the shoreline travel faster than that of the dye travelling against the shoreline. The longshore current distribution shifted which means that the fastest current was located seaward of the structure mouth, as represented in Figure 4.13. This can be interpreted in the same manner as the previous observation, where the structure mouth was more vulnerable inside the breaker line.

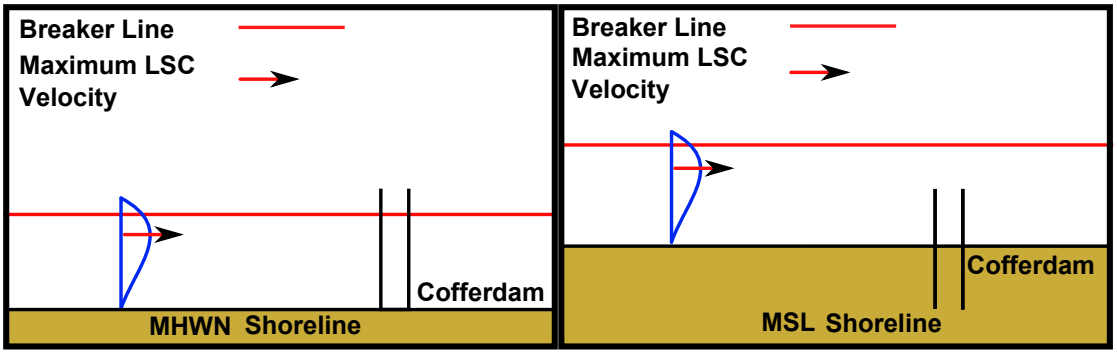

FIGURE 4.13: Longshore Current Velocity Distribution

The last comparison is that of the structure angle change to the shoreline. The currents behaved differently with the change in structure geometry. With a structure perpendicular (90^o) to the shoreline, the current regime was as indicated in Figure 4.14. The current moved up the coast and then drastically decreased the moment it reached the structure or obstruction. The current then slowly moved up the side of the structure until it reached the mouth of the structure. Once the current reached the mouth of the structure the dye dispersed, indicating that the current velocity decreased even further, effectively creating a "dead spot" in front of the mouth of the structure. With the presence of wave breaking at the mouth of the structure, the dye was transported into the structure. With no wave breaking at the mouth, the dye mostly dispersed until it reached the area where the longshore current started to re-establish on the northern side of the structure. This pattern was visible with all wave conditions. Although the process decreased in speed as the current velocity decreased.

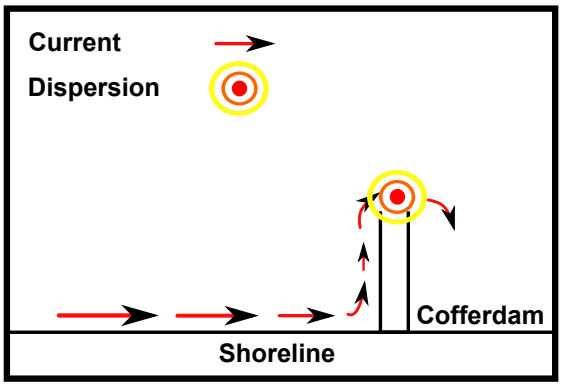

FIGURE 4.14: Current Movement Around a 90^o Structure

If however, the structure is built with a 30^o angle in regards to the shoreline, the current does not follow the same general pattern (Refer to Figure 4.15). Relying on the dye as indication, the current flows from left to right, up the shoreline but when it approaches the structure the longshore current velocity does not decrease as much as that of the perpendicular structure. There is still a decrease in current velocity, but a much less noticeable one. The dye then flows past the structure mouth and only disperses when it reaches deeper waters behind the breaker line. The distance the dye flows past the structure mouth depends on the initial current velocity. With the wave conditions delivering a smaller longshore current velocity this pattern is much less noticeable but still present. In the last mentioned situation, a small amount of dye flowed past the mouth of the structure to show the current re-establishing on the opposite side. In the tests where the wave conditions delivered a larger current velocity, the dye does not re-establish on the opposite side of the structure, but disperses in deeper water as explained. This may be as a result of limited space in the basin for the longshore current to re-establish, or it may be that the dye left the zone where the currents are acting and is now in stagnant water. This query will be addressed in the numerical modelling as the model area will allow the longshore current to re-establish to its full extent.

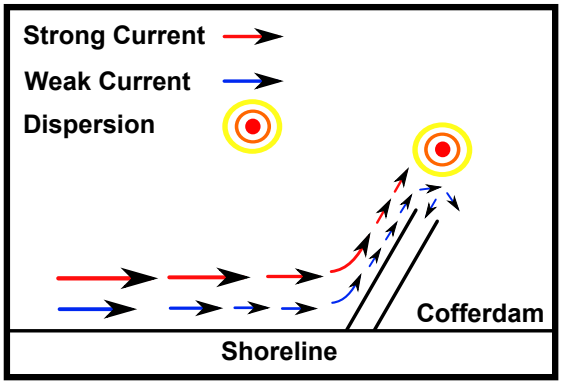

FIGURE 4.15: Current Movement Around a 30^o Structure

4.3 Concluding Remarks

From Chapter 4.2 (Results and Discussion), it is seen that the gross aspects of sediment transport are represented to a satisfactory level for a qualitative test. The processes could be identified and discussed by means of the model results. These observations could be used to answer some aspects of the question that will be further investigated by numerical modelling, "What geometric layout will minimize the sediment build-up inside the cofferdam structure?".

The option to rotate the structure 30^o away from the dominant wave direction was also investigated. Firstly, if the structure is built with a 30^o angle in regard to the shoreline, the current pattern seems to be of such nature that less sediment deposition would be present along the upstream side of the structure. This is positive as this decreases the rate at which the breaker line shifts away from the initial shoreline and will buy the contractor more time before the sediment build-up within the structure would be accelerated. It must also be kept in mind that it is possible that the longshore current did not re-establish. The potential benefit of this outcome will be verified with a more accurate numerical model.

Secondly, if the structure is rotated, the wave component which will be responsible for the main cross-shore transport into the structure mouth would be smaller, which in theory decreases the rate of sediment transport into the structure.

Thirdly, if the current could be decreased before approaching the structure, regardless of the structure angle, the sediment build-up at the structure would theoretically also decrease.

Thus it is proposed that with the knowledge obtained from the physical model results, different geometric layouts must be investigated by means of numerical modelling to confirm the concluding remarks made in this report.

The numerical model will now be discussed.

Chapter 5

Numerical Modelling

5.1 Methodology

5.1.1 Introduction

This discussion will outline the procedure which was followed to complete the numerical modelling to investigate different geometric layouts of an open-ended cofferdam and the effect they have on surf zone sedimentation.

To achieve the above mentioned, the following will be discussed:

I. The goal of the numerical model.

II. The reasoning behind choosing MIKE 21 as the numerical modelling software.

III. The scope of testing.

IV. The environmental data used in the model.

5.1.2 Goal

The goal of the numerical model is to investigate alternative geometric layouts for the open-ended cofferdam structure protecting a surf zone trench in order to minimize sediment build-up within it.

5.1.3 Selection of Numerical Model – MIKE 21

There are a number of numerical models available for modelling coastal areas (Delft3D developed by Deltares, SWASH, MIKE developed by DHI etc.) and the processes therein. MIKE 21[1] was selected instead of the other models because of the combination of accuracy and the productive work rate made possible by the author's familiarity with the user friendly interface. The provision of flexible mesh available in MIKE 21 allows the user to define a smaller mesh size around important areas in the model to generate more accurate, or rather more detailed results in areas of interest. The support available for MIKE 21 was also a compelling reason for its selection.

The author had access to MIKE 21 through the University of Stellenbosch. Stellenbosch University will also be able to provide access to MIKE 21 to future students investigating other possible scenarios on this model. Thus, using MIKE 21 also allows future studies a smooth transition from already generated results, to the modelling of new scenarios.

5.1.4 Scope of Testing

The numerical modelling was completed using the MIKE 21/3 Coupled Model FM (Flexible Mesh) suite within the MIKE 21 model. This specific model integrates the hydrodynamic, spectral wave and sediment transport features all within one model run in order to ensure accurate morphological updates. Due to the site specific characteristics of the problem the model was programmed to replicate a 4000 m long shoreline and the bathymetry was calculated to resemble a simple Dean profile without any irregularities within the area of importance (See Chapter 5.1.5). The environmental data was chosen to represent a stable problem from which the change in geometric layout of the surf zone trench and cofferdam structure alike could best be analysed. Once a qualitative validation of the model was done based on the knowledge of longshore currents and surf zone wave behaviour (Refer to the Literature in Chapter 2), different structures were tested in the model. This was done to see what effect the same wave field, current speeds and other environmental data will have on the sediment behaviour in and around the surf zone trench, subject to different geometrical layouts of the cofferdam structure. The model was set to run for 19 days but in order to save computational time, a speedup factor was implemented on the sediment transport model. This allows the user to speed up the sediment transport rate by a certain factor in order to speed up the modelling. A factor of 6 was used in this study. The scenarios tested for this study will be compared with each other to see what the effect of the change in geometric layout of the cofferdam

[1]For a brief summary of each of the MIKE models, refer to Appendix E. The description of each of the models were summarized from the user manuals provided by DHI with the license of the MIKE suite.

will be. All of the numerical modelling runs were completed using a constant initial water depth and no tidal variance was applied .

Due to the fact that a surf zone cofferdam is a site specific structure, and the design specifications of it rely on parameters which will differ between different locations, a universal manner needs to be found to express the structure's design specifications, in this case its length. The structures in the numerical tests will for the above reasons not be interpreted by using their exact length dimension (L), but rather as a function of their length ratio R_L between structure length (L), and surf zone width (W_s). A R_L = 1 W_s, will mean that the structure length is equal to that of the surf zone width. The wave heights used in the model were low compared to annual storm wave heights and therefore the structure lengths often exceeded the surf zone width in the model. The structure width will be denoted as (w). The proposed run list of scenarios is listed in the Table 5.1, Table 5.2 and Table 5.3 on the following pages:

ID	**Description**
SCN01	A structure with a R_L = 1W_s and a width of 0.2W_s. The structure is orientated perpendicular to the shoreline. The trench is dredged out to a depth of the mouth of the structure which is 4.5 m deep. This layout can be related to Test A10 of the physical modelling done in Chapter 4. With the exception of the bathymetry, the other environmental data including the wave height, wave period, wave direction and position of the structure mouth compared with the surf zone width, are similar. This also correlates with the Trekkopje case study as the mouth of the structure is on the edge of the initial breaker line and the breakerline will move past the structure mouth within the early stages of the model run.
Simplified Layout	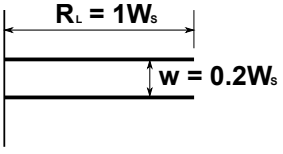

TABLE 5.1: Numerical Modelling Run List (1)

ID	Description
SCN02	A structure with a $R_L = 2W_s$ and a width of $0.2W_s$. The structure is orientated perpendicular to the shoreline. The trench is dredged out to a depth of the mouth of the structure which is 7.25 m deep. This layout can be related to Test A5 of the physical modelling done in Chapter 4. With the exception of the bathymetry, the other environmental data are similar.
Simplified Layout	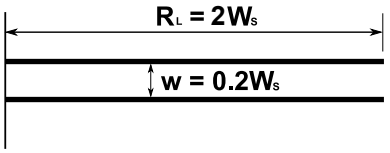
SCN03	A structure with a $R_L = 3W_s$ and a width of $0.2W_s$. The structure is orientated perpendicular to the shoreline. The trench is dredged out to a depth of the mouth of the structure which is 9.5 m deep.
Simplified Layout	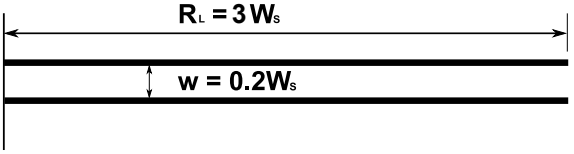
SCN04	A structure with a $R_L = 2W_s$ and a width of $0.2W_s$. The northern side of the structure is extended to the north east with a 45 ^{o} arm. The arm has a R_L of $0.6W_s$. The trench is dredged out to a depth of the mouth of the structure which is 7.25 m deep.
Simplified Layout	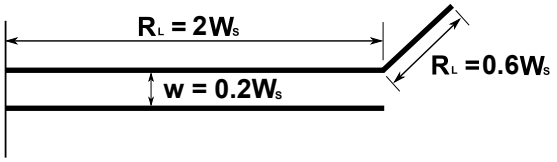
SCN05	A structure that reaches a horizontal $R_L = 2W_s$ in from the shoreline and has a width of $0.2W_s$. The entire structure is orientated 22^o to the north-east. The trench is dredged out to a depth of the mouth of the structure which is 7.25 m deep.
Simplified Layout	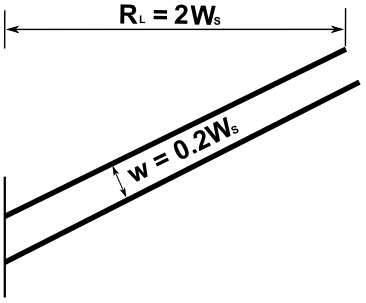

TABLE 5.2: Numerical Modelling Run List (2-5)

ID	Description
SCN06	A structure that reaches a horizontal $R_L = 2W_s$ in from the shoreline and a width of $0.2W_s$. The entire structure is orientated 22^o to the south east. The trench is dredged out to a depth of the mouth of the structure which is 7.25 m deep. This layout can be related to Test B7 of the physical modelling done in Chapter 4. With the exception of the bathymetry and the wave height, the other environmental data including the wave period, wave direction and position of the structure mouth compared with the surf zone width are similar.
Simplified Layout	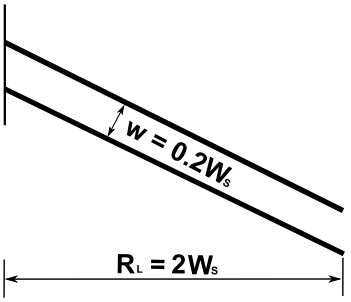
SCN07	A structure with a $R_L = 2W_s$ and a width of $0.2W_s$ which is orientated perpendicular to the surf zone. The end of the structure is sealed with a flat sheet. It is assumed that the gate sealing the cofferdam mouth, does not let any sediment into the surf zone trench.
Simplified Layout	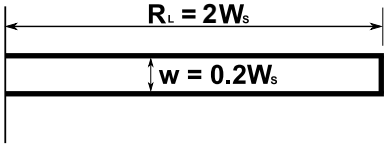
SCN08	A structure with a $R_L = 2W_s$ and a width of $0.2W_s$ which is orientated perpendicular to the surf zone. Two wings are extended to each side of the cofferdam at a normal angle to that of the cofferdam wall. The wings have a $R_L = 0.4W_s$. This structure is similar to that of the structure used by Tideway Offshore Construction at Bluestream on the Turkish Coast (Refer to Chapter 2.6.2.1).
Simplified Layout	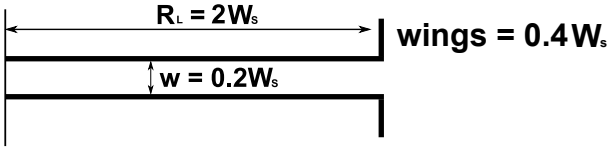

TABLE 5.3: Numerical Modelling Run List (6-8)

The structure lengths were chosen in accordance with the surf zone width of the numerical model. SCN01 as defined above correlates well with the case study of Trekkopje, Namibia. From here the structure length and orientation will be altered to investigate what effect the altered geometric layout of the different scenarios will have on the sediment accumulations in and around the structures.

5.1.5 Environmental Data

- Bathymetry

The bathymetry of a test, as conducted in this study, differed from site to site depending on the location of the project, the characteristics of the geological survey that is present in that particular area. Due to the unique characteristics of the seabed at each location of the existing projects, a general bathymetry was chosen for the numerical model.

A gradual sloping bathymetry was created to isolate the problem in order to only concentrate on the physical shape of the surf zone trench and cofferdam structure, and not irregularities in the seabed.

The bathymetry was determined by using the Dean formula to create a bathymetry profile as shown in Figure 5.1. The Dean formula is as follows (Dean, 1977):

$$h = A.y^{\frac{2}{3}} \tag{5.1}$$

where h is the water depth, A is the sediment scale parameter and y is the cross-shore distance from the shoreline. The sediment scale parameter used in the calculation is the D_{50} grain size of the sediment found at the specific area. For this case the D_{50} value is 0.275 mm.

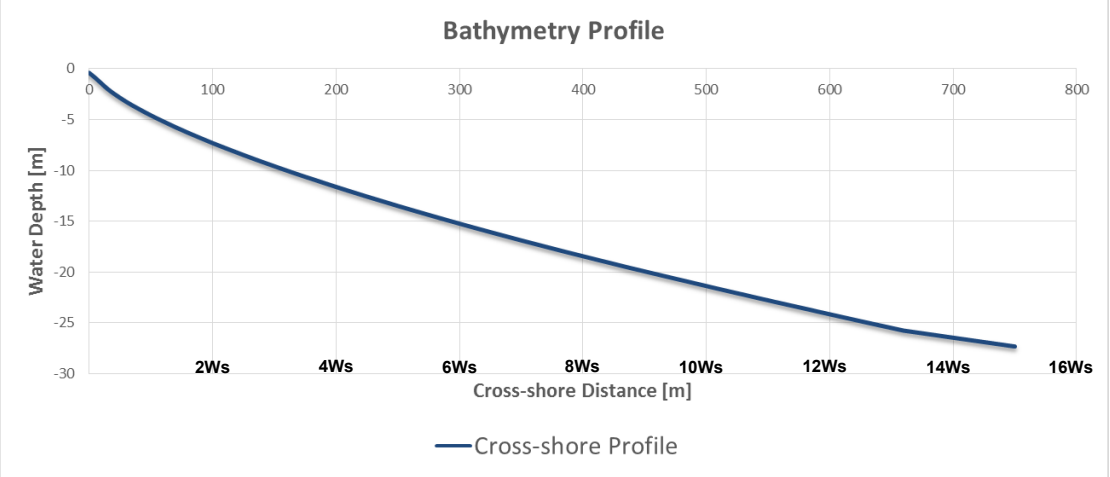

FIGURE 5.1: Numerical Model Cross-shore Profile

The model area consists of a 4000 m long shoreline and has a total cross-shore distance of 750 m. This was chosen to allow the longshore current to develop and stabilize before getting to the area of interest around the surf zone structure. For each individual test the entire trench was set to the depth of the mouth of the structure (Refer to Appendix G for graphical presentation). This varies from test to test as the length, and thus the water depth at the mouth of the structure, differs between the tests. The mesh element size allocation will be discussed later on in this chapter. The total bathymetry plan view is as shown in Figure 5.2. The shoreline runs from north to south. Thus the structure was orientated in a west to east direction.

The bathymetry files were compared after each test in terms of bed level changes to see what effect the structure orientation had on the sediment build-up in the area of concern. Comparisons were made with regards to bed level change vs time, current movement patterns and wave patterns.

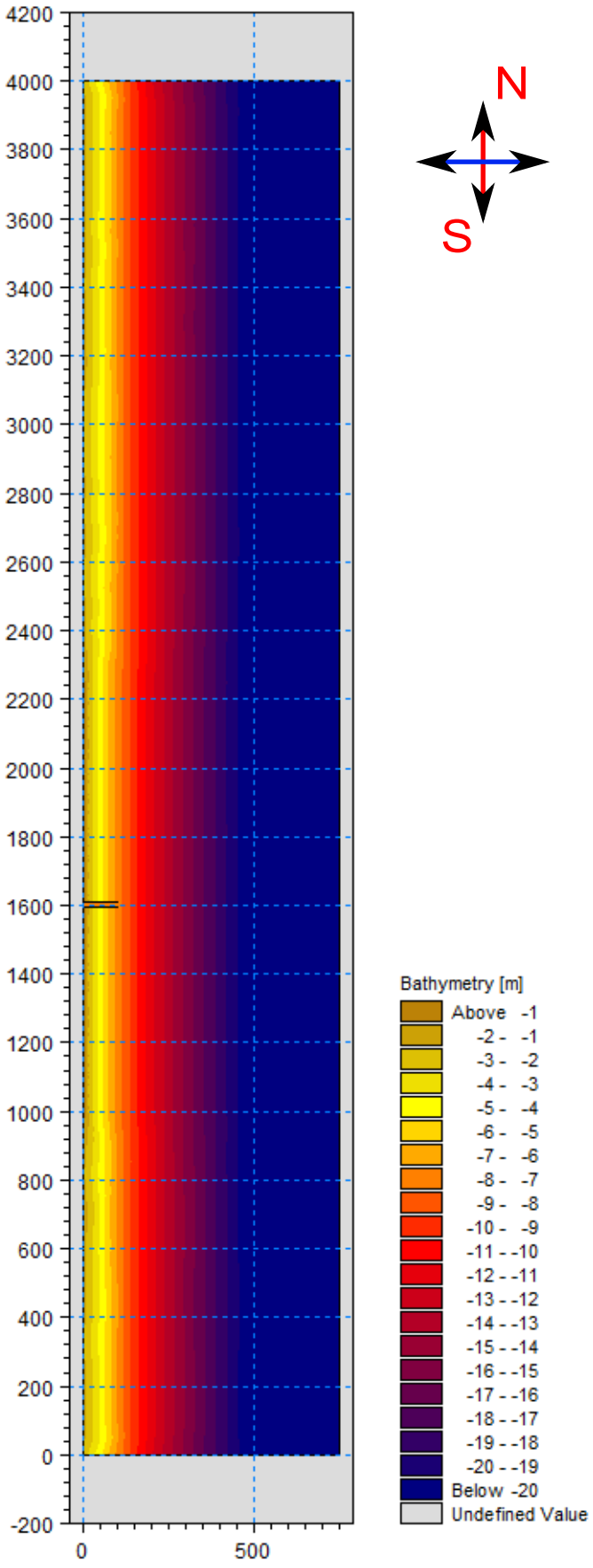

FIGURE 5.2: Numerical Model Bathymetry Plan View

- Waves

The wave condition used for the numerical tests was determined by combining knowledge of historical data and calibrated data from the physical modelling. A wave condition was chosen to get a balance between effective run time per test and the level of accuracy of the results. One single constant wave condition was implemented at the eastern boundary of the model and the wave climate was updated throughout the model according to the morphological progression of the model. The reason for choosing one single wave condition was due to gains in computational time and due to the fact that the wave condition is not the main factor of interest in this study. The effect the wave height and direction has on the sediment transport is different and unique for each location and the general effects they have on the longshore current, have already been illustrated in the physical model.

The wave climate is summarized in Table 5.4.

Significant Wave Height H_S(m)	**Wave Period T(s)**	**Wave Direction θ(degrees) relative to True North**	**Directional Spreading (degrees)**
1.5	12	60	5

TABLE 5.4: Numerical Modelling Wave Climate

- Currents

The currents in the model were generated by means of two mechanisms. The first current was generated over the entire model area and represents currents due to major oceanic currents and surface currents due to wind action on the surface of the water level. This current had an approximate velocity of 0.25 m/s and flowed from north to south. The second mechanism was that of wave generated currents within the surf zone. The wave generated currents are the important currents which are responsible for the longshore sediment transport. A maximum longshore current of approximately 1.0 m/s was generated in the surf zone by the imposed oblique wave condition.

- Sediment Properties

The sediment properties used within the model were defined using a sediment table generated with a toolbox within the MIKE Zero interface. This sediment table defines the lower and upper limits of the sediment properties as well as the transport capabilities of the sediment in the model. These transport capabilities include sediment movement and

settlement properties. As the model integrates between specified values it is very important to generate a sediment table with values applicable to the specific wave condition. The D_{50} sediment grain size is 0.275 mm. This value was optimized through a series of numerical runs. An initial value of 0.35 mm was chosen as this value was used for past studies regarding sediment transport modelling of the coast of Namibia (Kaergaard and Fredsoe, 2012). Finally through some experimentation to calibrate the numerical model and to get it to represent the sediment transport processes more accurately, the final value of 0.275 mm was selected. This value is still a valid grain size for the coasts of both Mossel Bay and Namibia.

- Model Mesh Allocation

An unstructured triangular mesh with concentrated zoning was specified in the model to ensure detailed results in areas of importance. Three element area sizes were specified. This was done in order to generate detailed results around the structure but to ensure that computational time was kept as short as possible. Figure 5.3 on the following page illustrates the three element area sizes. In deep water a large and coarse grid size is specified as this was not the area of importance for this study (A). The calculations were still done with the same formula but over a larger area. The second area size was allocated along the shoreline (B). As the longshore current was important and it needed to develop with a certain level of accuracy, a finer grid was implemented along the shoreline for a more detailed output. The last grading was that of the area around the surf zone structure (C). This was the area of importance for this study as the behaviour of the currents, waves and most important, the sediment in this region constitutes the objective of this study. MIKE 21 recorded 6697 nodes and 13117 elements within the modelling domain.

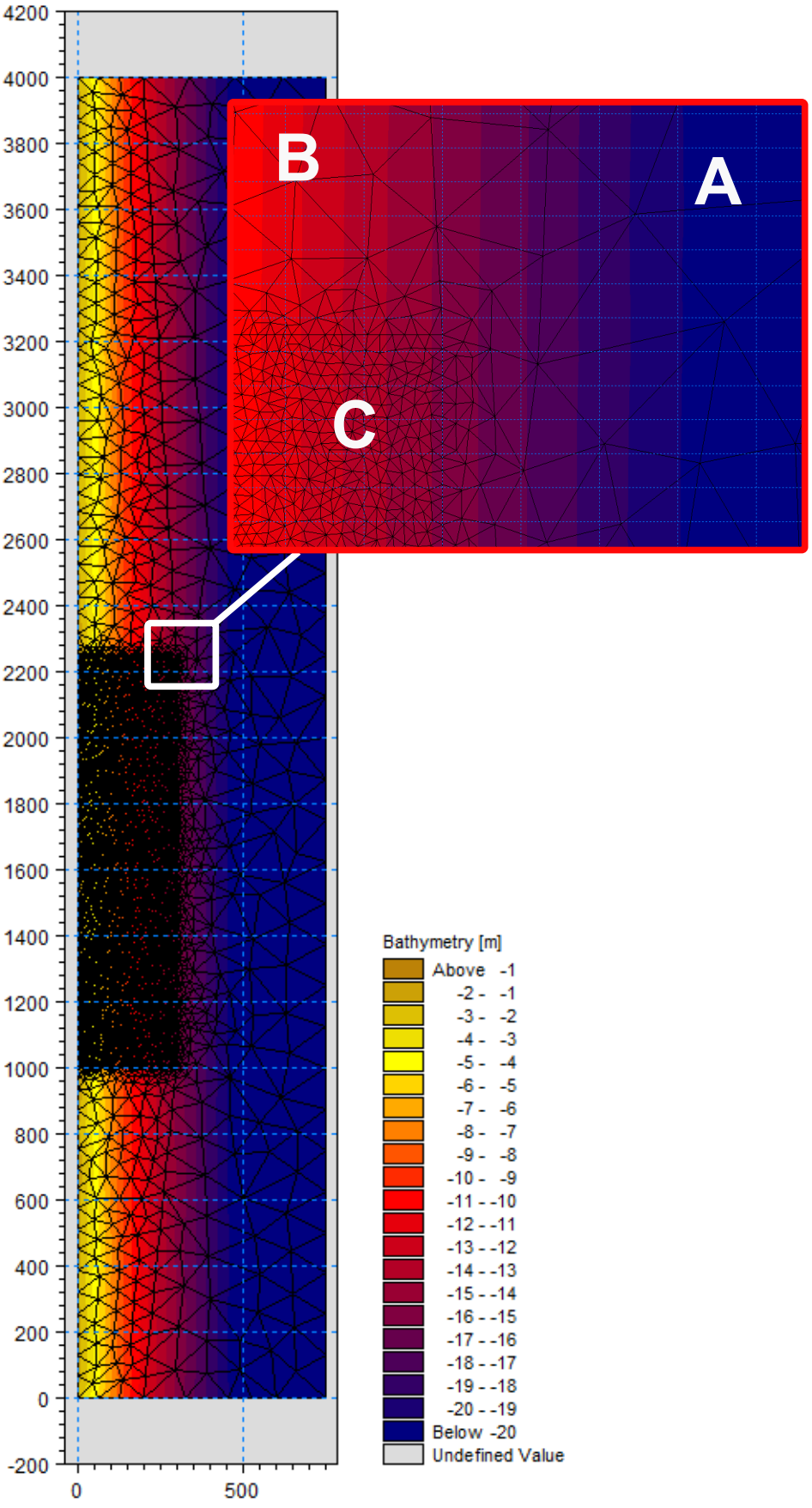

FIGURE 5.3: Numerical Model Mesh Allocation

5.2 Validation

A qualitative validation of the numerical model was done using the knowledge of surf zone processes obtained from literature and the physical modelling done at the CSIR. Three main aspects will be inspected:

- Wave transformation
- Longshore current properties
- Sediment movement patterns

5.2.1 Wave Transformation

In order to do a qualitative validation of the numerical model, signature features of the surf zone were inspected to show that the main processes were modelled correctly. According to the definition of the surf zone from the literature study in Chapter 2, the first point of wave alteration will occur when the wave propagates into the shoal zone. At this point the wave energy will begin to interact with the seabed and the wave height will increase due to shoaling.

When considering the Spectral Wave output file, it is clearly visible that in deeper waters the input wave height is maintained at 1.5 m. As an indication of waves passing into the shoal zone there shall be an increase in wave height as a result of shoaling. This point in the model is approximately 250 m ($R_L = 5W_s$) east of the shoreline at an average depth of 14 m. This can be seen at point A in Figure 5.4. It must be kept in mind that some sediment, even though it is a very small amount, will start to move back and forth at this point. The wave height will thus increase until the point of breaking is reached where the maximum wave height shall be recorded. An average increase in wave height from 1.5 m to 1.9 m (27%) is experienced in the model as a result of shoaling. This is indicated at point B. Note that the breaker line is a straight line along the shoreline, which it should be as the bathymetry is a gradual sloping one along the shoreline.

Once the waves pass the breaker line the wave height should decrease significantly until it fades away as it approaches the western boundary of the model. This is also visible as depicted at point C. As the waves approach the shoreline at an angle of 30^o, an interesting observation can be made around the cofferdam structure.

On the northern side of the structure a wave height is recorded in excess of 2 m. This increased wave height is a result of a bunch up of energy. The structure reflected the waves coming in from the north east. This can be seen by observing the wave direction

vectors against the northern side of the structure in the enlarged window of Figure 5.4. The reflected waves interacted with the waves coming in just above the reflection point and this interaction resulted in an increase in wave height. As the energy of these waves were reflected, the area where the energy should have been was shielded and created a calm or "dead" spot on the southern side of the structure as well as inside the trench. Thus, on the southern side of the structure the wave height was decreased to a wave height smaller than 1 m. The diffraction is clearly visible when comparing the wave direction vectors at point D with those of the waves just north of the structure. The northern waves were not affected by the structure and only experience refraction as a result of the bathymetry but not diffraction caused by an obstacle in their way.

Inside the structure the wave height was smaller as this area was shielded even more by the narrow corridor. A wave height of approximately 0.6 m was experienced deep into the structure. The same colour scale applies to the zoomed image than that of the larger image.

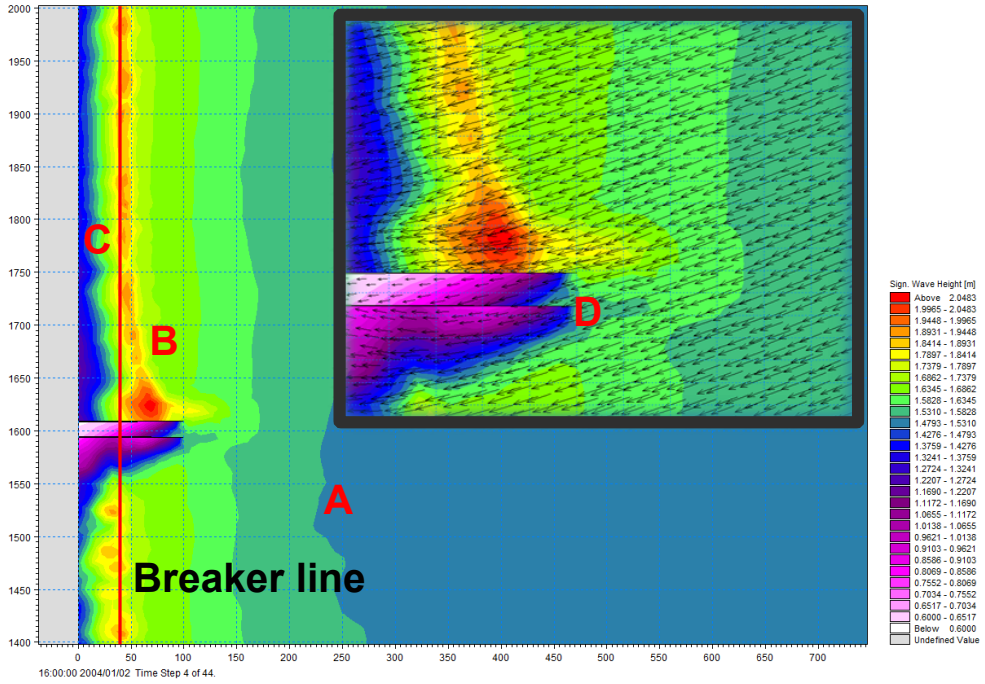

FIGURE 5.4: Wave Validation

5.2.2 Longshore Current Properties

Along with the wave analyses a similar analyses can be made considering the current movements in the model. As a result of oceanic currents there shall be a small current visible over the entire area of the model, even in the deep waters as seen in Figure 5.5. Referring to the Trekkopjes case study in Chapter 3, the oceanic currents vary between

0.1 m/s and 0.3 m/s, depending on the circumstances. An average current velocity of 0.26 m/s was generated in the offshore area of this model. This value correlates well with that of the Trekkopje case study, although the area of interest was in the surf zone.

In order to validate the current movement, a stronger current should exist in the surf zone. This current should start to increase just outside of the breaker line and increase from thereon. The initial breaker line was between 40 m and 50 m ($R_L = 1W_s$) away from the shoreline and the longshore current started to increase in velocity at a cross-shore distance of 55 m ($R_L > 1W_s$). This is a good indication that the currents experienced in the surf zone of the model are wave induced currents. The current ran from north to south at a speed of approximately 0.9 m/s which has a good correlation with the current speed of the case studies at both Trekkopjes and Mossel Bay.

The current deviation in regards with the structure appears to be accurate. As a result of the deviation, as seen at point A in Figure 5.5, a near stagnant area was created in the corner between the shoreline and the cofferdam structure. Keep in mind that it was a near stagnant area in terms of the current, yet there was still wave action in this area. The current increased in velocity as it moved along the structure side as it was forced to move around it. It then attempts to re-establish on the southern side of the structure which it eventually did on the downstream shoreline. This re-established longshore current can be seen in the lower zoomed window of Figure 5.5. Take note that the image showing the re-established longshore current was taken at the same time step than that of the other two impressions, just further down south in the model. The next aspect which should be visible is the longshore current distribution in the surf zone.

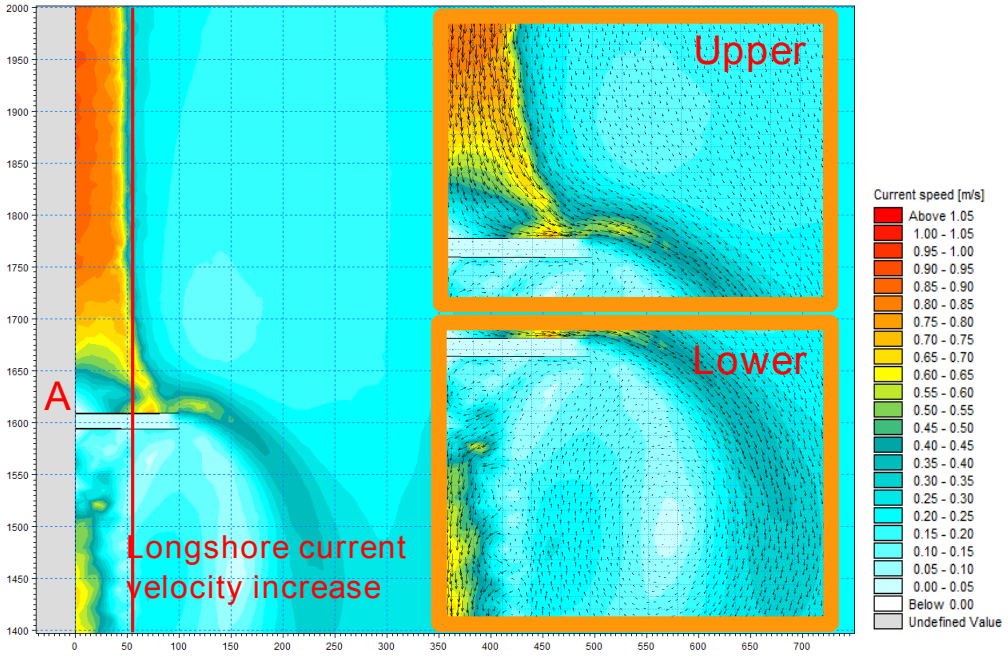

FIGURE 5.5: Current Validation

The current is also a good match compared to that of a past study done on the numerical modelling of nearshore currents and sediment transport around a groyne structure. Figure 5.6 shows the current movements around a surf zone groyne modelling by Walker et al. (1991).

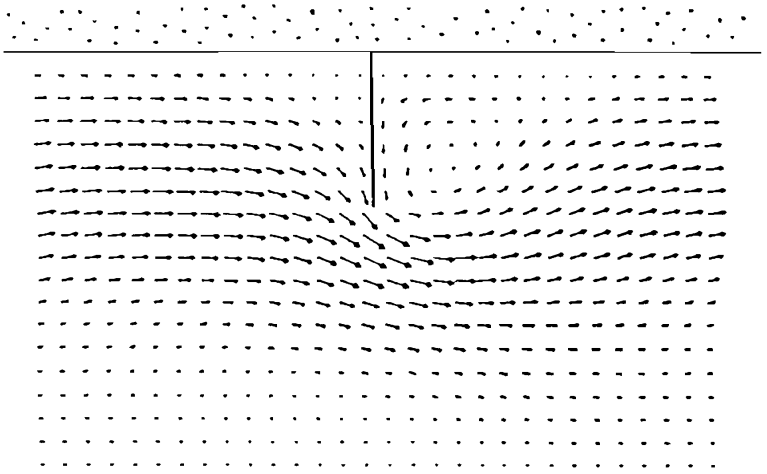

FIGURE 5.6: Nearshore Current Movement of past study by (Walker et al., 1991)

The longshore current within the model did not correlate with that of the literature. The reason for the lack of this distribution was due to changes in the bathymetry. The Dean profile (Dean, 1977) used for the bathymetry ended at the 0 m elevation contour against the western boundary of the model. As the test started, and the sediment started to move, the Dean profile changed by forming an irregular formation in the surf zone. The graph in Figure 5.7, visually illustrates the change in bathymetry over the entire bed profile of the model area. The Dean profile created an irregular form in the surf zone due to the currents, signifying that the bathymetry became deeper along the western boundary of the model. The graph, along with the image of the bed level change shown in Figure 5.7 and Figure 5.8, proves that this irregularity was confined to the surf zone and the bathymetry returned to its natural form as the cross-shore distance increased.

The bed level change output compares the difference of the bed level at a specific time step to that of the initial bed level. If the figure shows cold colours (blue to purple), it indicates erosion. If the figure shows warm colours (yellow to red) it indicates deposition of sediment. Figure 5.8 depicts that the sediment was eroded against the model boundary and deposited just outside the surf zone. This created a drop in bathymetry before the bed level returned to the initial form of the Dean profile.

Even though the longshore distribution could not be calibrated to fit the theoretical distribution form, the total sediment movement patterns (discussed next) were modelled to a satisfactory level of accuracy when compared to that seen in theory and in real life.

FIGURE 5.7: Changed Bathymetry Profile

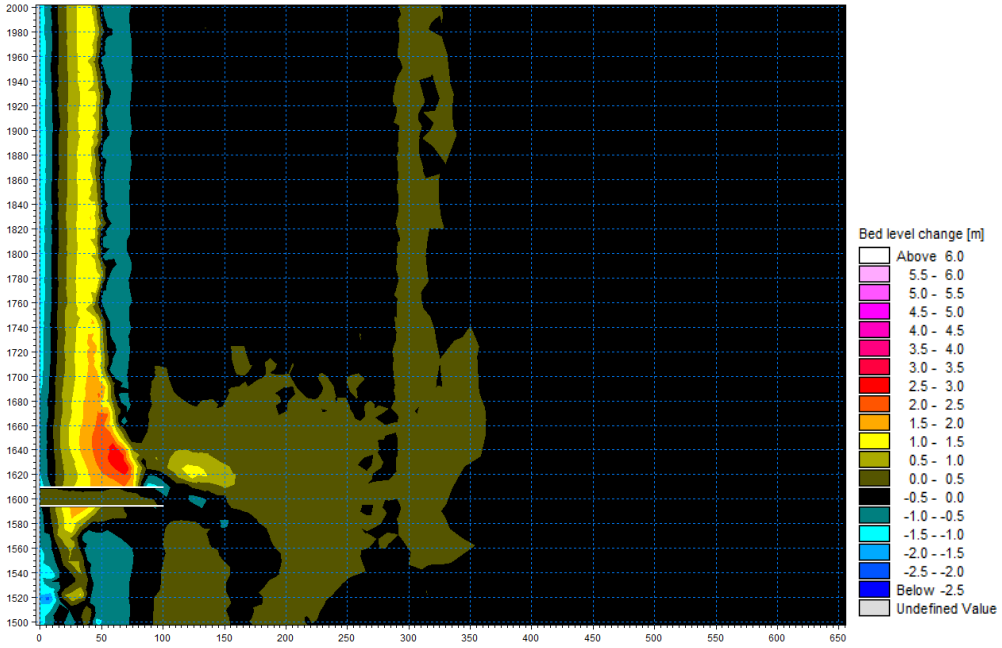

FIGURE 5.8: Bed Level Change

5.2.3 Sediment Movement Patterns

The longshore current revealed an increased current velocity within the surf zone restricting the significant sediment movement to the area of importance for this study, the surf zone.

Now that the main wave and current processes are visible, attention shifted to the movement of sediment. The movement of sediment should have correlated with the current velocity and pattern, and should have increased due to current speed and turbulence created by wave breaking.

Observing the sediment output file given in Figure 5.9, the observation can be made that the sediment movement was confined, as would be expected, mainly to the surf zone. Note that the length of the vector arrows indicates the magnitude of the sediment transport within that specific element (Figure 5.9). This observation proved that the sediment movement correlated with the current movement. As the sediment built up, the wave breaker line retreated further seaward, away from the initial shoreline. This affected the longshore current which in return caused further sediment build-up. This cycle continued until the effect of the obstruction on the longshore current was reduced by a new shoreline configuration.

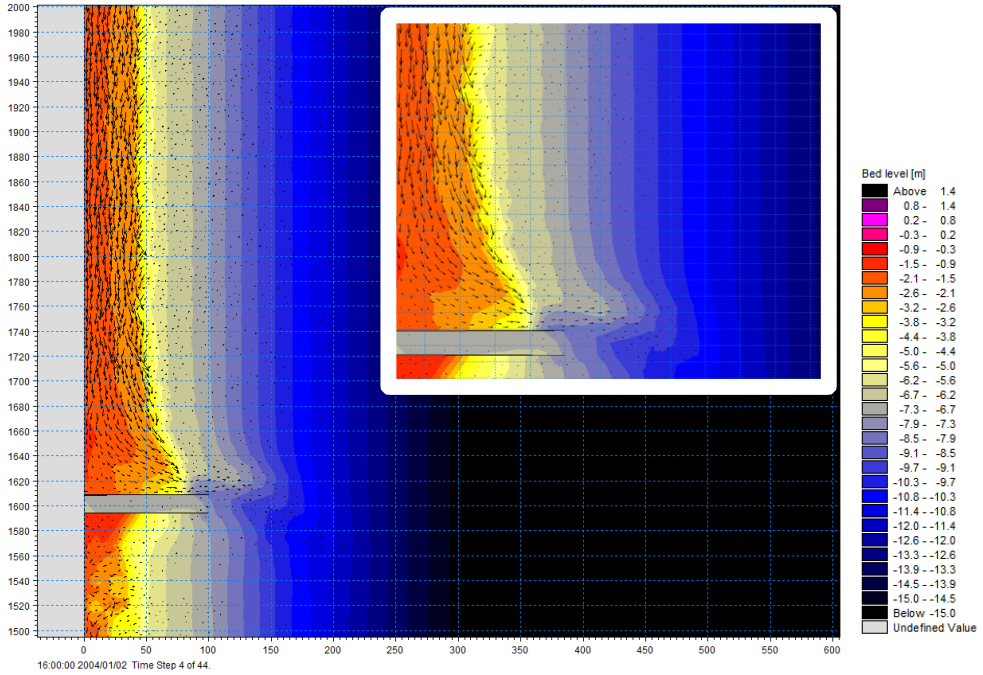

FIGURE 5.9: Sediment Validation

Time lapsed images of Scenario 02, the model run used for the validation can be seen in Appendix F.

The model has now been validated and it is ready to be used to investigate the effect of a geometric layout change of the cofferdam structure. The 8 scenarios modelled will be discussed in the next section.

5.3 Results and Discussion

5.3.1 Introduction

The results of this study will be discussed by using the following method:

- Due to the nature of the study a failure point will be defined.
- Next the failure points of each individual test will be identified.
- The tests will then be ranked from most effective to the least effective structure.
- There will then be a discussion, declaring the reasoning for the structure's success or failure.

5.3.2 Definition of Failure

The final interpretation of the 8 scenarios required additional analyses. Analysing the results in terms of different aspects can invoke different opinions as to which of the scenarios were most effective. The reason for this is that the structures all have different characteristics. Comparing these structures ultimately constitutes the aim of this study, the analyzing of different characteristics and identifying the best one. The problem with structures with different geometric characteristics is that it is hard to find common ground on which to compare the different scenarios. To clarify this problem, one parameter or point of failure needs to be identified by which all the structures can be judged. This relates to the objective of the study. The objective implies that the investigation of the geometric layout of the cofferdam structures will deliver the most effective structure in terms of sediment build-up at the mouth of the structure and inside the surf zone trench. This forms the criteria by which the structures will be judged. **The structure which retains its natural bed level within the surf zone trench and at the mouth of the structure the best, or for the longest period, is thus the most effective structure layout**. This will be the primary criteria by which the structures will be judged. Later discussions will then contemplate other aspects that may invoke alternative opinions.

Sediment build-up at the mouth of the structure or within the surf zone trench is inevitable, suggesting that at some point in time the sediment will reach the structure mouth and then be forced into the trench by the prevailing wave condition. This implies that along with sediment deposition, a second parameter comes into play for deciding if the structure is effective or not. This parameter is time. If the build-up of sediment is

inevitable as stated above, the structure which buys the contractor the most time before needing attention in terms of maintenance or upkeep (i.e. sediment removal from the trench), is therefore the most effective.

Due to the various layouts tested, a third parameter was also identified that constitutes an important role in the interpretation of the results. That parameter is the location of the data points. As a result of the layout difference, there is no one coordinate in the model by which the structures can be compared. An applicable point for one scenario may have absolutely no relevance to another. Points thus needed to be identified for each scenario, which monitored the same effect on that individual structure, as that of another point for another structure. The monitoring points for each structure can also be defined by means of a line. This line is parallel with the pathway in which the pipeline needs to be installed. Once the pipeline pathway has been compromised, the structure has failed and is no longer effective. The northern boundary of this pathway will thus serve as the failure line by which the effectiveness of each structure will be judged. Keep in mind that the structure is under attack from a unidirectional wave condition from the north east side. This failure line for Scenario 02 is graphically represented in Figure 5.10.

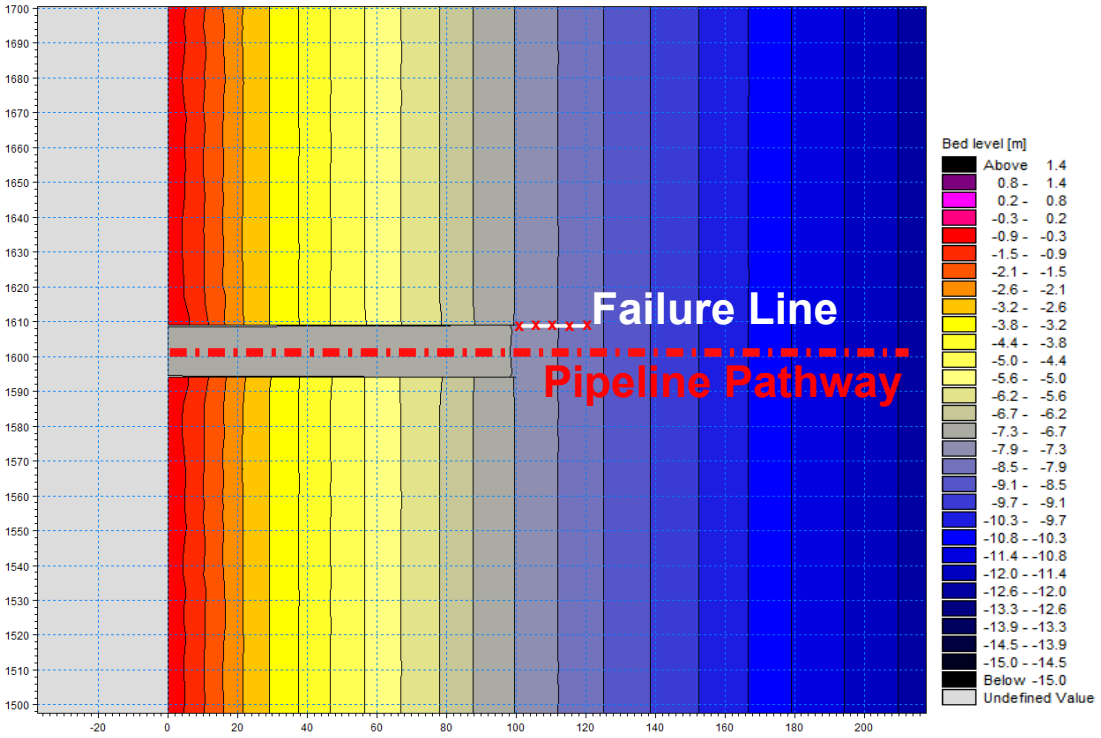

FIGURE 5.10: Failure Line Representation

The failure line for each structure will start at the seaward extent of the cofferdam's northern wall, and will continue on into deeper waters for a distance of 20 m. Once the sediment crosses this line, sediment will start to build-up in front of the mouth of

the structure and be washed into the trench by the waves breaking at the mouth of the structure. Why is this defined as a line and not a single point? This is because different structures will have different sediment movement patterns. Some will have sediment creeping around the structure corner into the trench while others will have a sediment bank coming from a wider zone around the mouth of the structure and then move in from deeper water. Either way, if the sediment transport crosses the failure line in significant volumes, the pipeline pathway will have been compromised.

In order to represent the failure line on a graph, 5 data points will be identified along this line. The weakest data point, the one that indicates failure first, will be used as the failing point for that specific structure. Once the failing point of each structure has been identified, these points will be analysed in terms of bed level change, and analysed using a graph which will indicate the bed level change vs the time. If the bed level change has a sudden jump in magnitude, it will serve as an indication of sediment starting to move pass the failure line.

5.3.3 Identification of the Individual Scenarios' Failure Points.

Five points have been placed on the failure line for each structure. The points were located at intervals of approximately 5 m, starting 0.5 m from the cofferdam's northern edge. A graphical representation of the failure point layout in Scenario 02 is given in Figure 5.11 below. Table 5.5 indicates the coordinates of the five points for each structure and a graphical representation of the points for each structure can be seen in Appendix G.

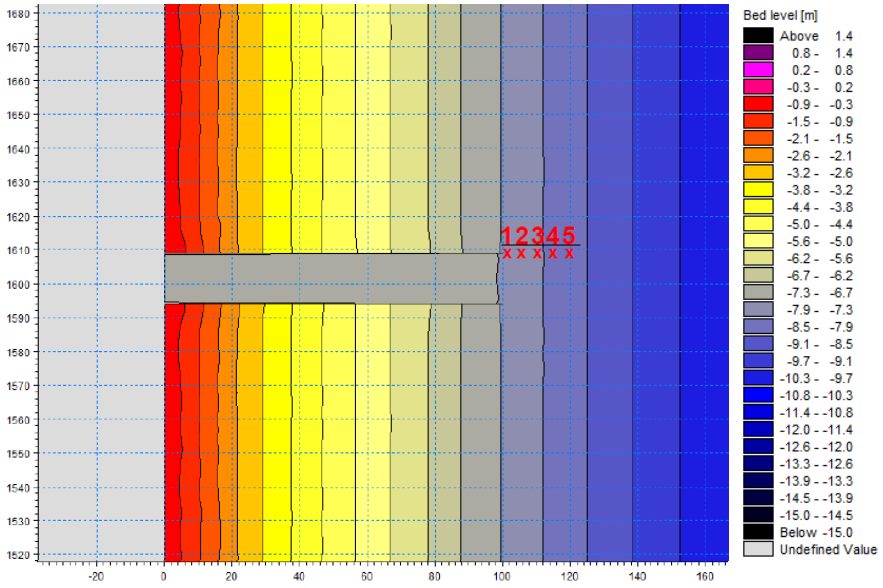

FIGURE 5.11: 5 Failure Points of Scenario 02

ID	Coordinates				
	Point 1	**Point 2**	**Point 3**	**Point 4**	**Point 5**
Scn01	(50.5,1609)	(55,1609)	(60,1609)	(65,1609)	(70,1609)
Scn02	(100.5,1609)	(105,1609)	(110,1609)	(115,1609)	(120,1609)
Scn03	(150.5,1609)	(155,1609)	(160,1609)	(165,1609)	(170,1609)
Scn04	(100.5,1609)	(105,1609)	(110,1609)	(115,1609)	(120,1609)
Scn05	(100.5,1649)	(105,1651)	(110,1653)	(115,1655)	(120,1657)
Scn06	(100.5,1569)	(105,1567)	(110,1565)	(115,1563)	(120,1561)
Scn07	(100.5,1609)	(105,1609)	(110,1609)	(115,1609)	(120,1609)
Scn08	(100.5,1609)	(105,1609)	(110,1609)	(115,1609)	(120,1609)

TABLE 5.5: 5 Failure Points Coordinates

In order to identify the weakest point or failure point of each structure, the bed level changes at each scenario's 5 points were compared. The point that showed indications of a major increase in bed level change first, was taken as the failure point. The graphs of the bed level change with respect to time for each scenario can be seen in Appendix H. Table 5.6 shows the failure point of each scenario. Keep in mind, R_L is the ratio of structure length (L) to surf zone width (W_s).

ID	Description	Failure Point Number	Coordinates
Scn01	Straight $R_L = 1W_s$	1	(50.5,1609)
Scn02	Straight $R_L = 2W_s$	1	(100.5,1609)
Scn03	Straight $R_L = 3W_s$	3	(160,1609)
Scn04	Straight $R_L = 2W_s$ with 45^o Arm	1	(100.5,1609)
Scn05	Angled North $R_L = 2W_s$	2	(105,1651)
Scn06	Angled South $R_L = 2W_s$	2	(105,1567)
Scn07	Closed Mouth $R_L = 2W_s$	2	(105,1609)
Scn08	Straight $R_L = 2W_s$ with two wings	2	(105,1609)

TABLE 5.6: Individual Failure Point Coordinates

5.3.4 Ranking of Structures

The failure point of each scenario has been identified. These 8 points were compared with each other, in order to determine which structure was the most effective. The rankings were determined by means of percentage. Time step 1 (**day 0**) will serve as the start of the model run and can be denoted as the 0% mark, whereas time step 44 (**day 19**) served as the final point in time and can be denoted as the 100% mark. Thus the structure with the highest percentage was the most effective one. The rankings are given both in Table 5.7 as a listed result, and in Figure 5.12 as a graphical presentation.

ID	Description	Failure Percentage	Ranking
Scn03	Straight $R_L = 3W_s$	86.4%	1
Scn04	$R_L = 2W_s$ 45^o Arm	79.5%	2
Scn08	$R_L = 2W_s$ with two wings	62.1%	3
Scn02	Straight $R_L = 2W_s$	36.0%	4
Scn07	Closed Mouth $R_L = 2W_s$	34.1%	5
Scn05	Angled North $R_L = 2W_s$	25.0%	6
Scn06	Angled South $R_L = 2W_s$	23.0%	7
Scn01	Straight $R_L = 1W_s$	6.8%	8

TABLE 5.7: Structure Ranking based on percentage of time before significant sediment intrusion

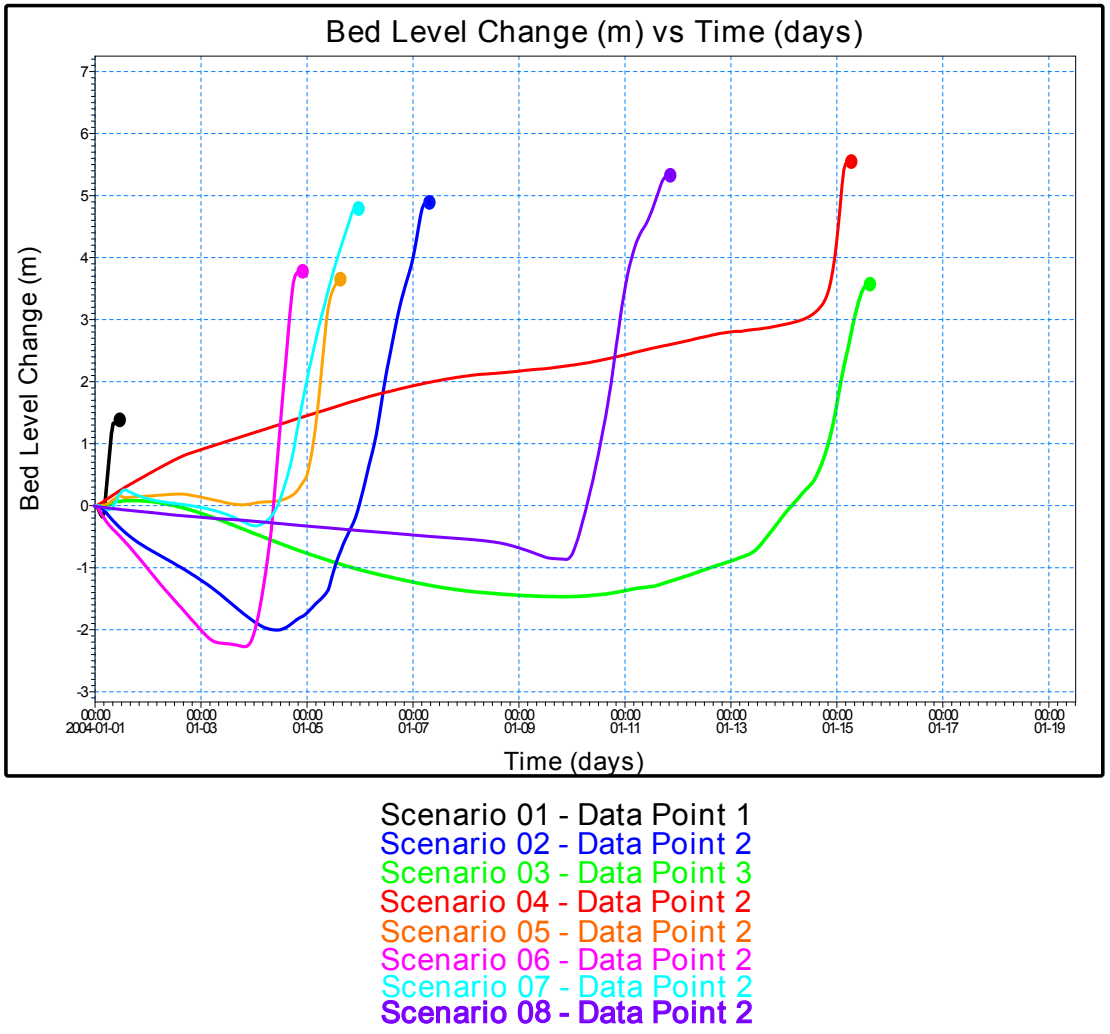

FIGURE 5.12: Bed Level Change vs Time

5.3.5 Discussion of Layouts

The ranking procedure implemented in the previous chapter focusses on the intrusion of sediment into the surf zone trench. It gives the reader a general idea of which structure is deemed to be the most effective by comparing it with the time it takes for that intrusion of sediment to become a project-delaying problem. It does however not discuss topics such as structural integrity, practical implementation, and the financial aspects of changing designs. These topics can prove to be a valuable turning point in deciding whether or not to choose a certain design. For example, it is of no use to select a structure based on its ability to maintain the initial bed level of the pipeline pathway, but the extra cost of the new longer structure is more than that of the maintenance cost of the alternative shorter structure. This chapter will discuss issues such as this and point out the changes in the geometric layout which seemed to be most effective. It is possible that a combination of two or more scenarios can prove to deliver the best results.

In Chapter 5.3.2 it is stated that the eventual filling up of the surf zone trench with sediment is inevitable on long time scales. Proof of this statement is evident when observing the results of Scenario 01, 02 and 03. These structures all have the same general layout, a straight structure perpendicular to the beach, with an increase in R_L of $1W_s$ (within this specific numerical model its an 50 m increase) with each consecutive scenario. As a reminder W_s = surf zone width. These scenarios represent the default shape of a cofferdam structure, with the length depending on the contractor's design.

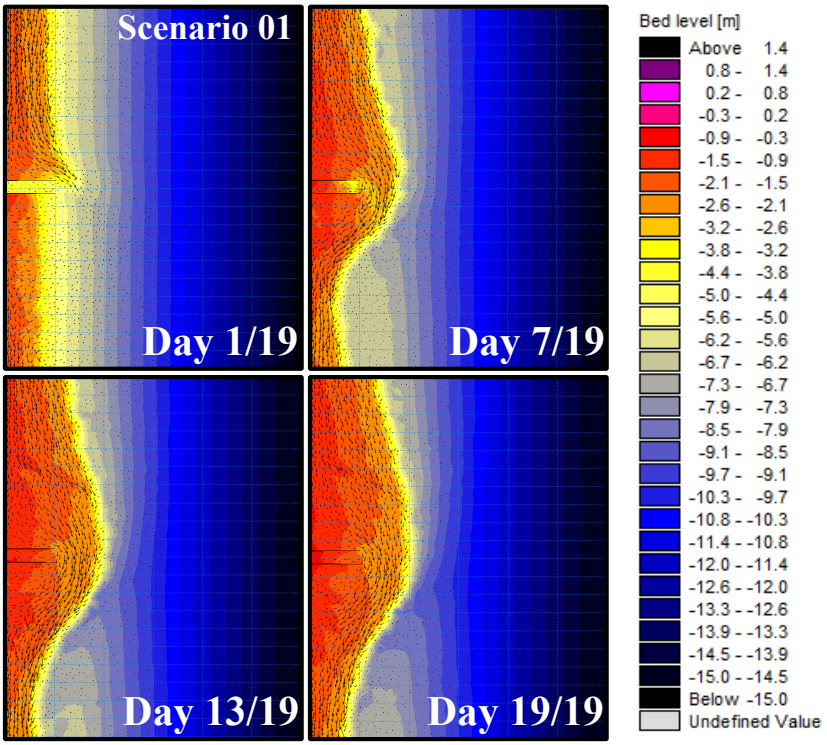

FIGURE 5.13: Scenario 01 Sediment Movement

Looking at Scenario 01 (Straight structure with a $R_L = 1W_s$), although not exactly the same but a structure which creates similar circumstances and problems as the one built at Trekkopjes, Namibia, the sedimentation problem experienced with a short cofferdam structure can clearly be seen (Refer to Figure 5.13). At the initial stages of the run the structure mouth was located just outside the wave breaker line. As the structure blocked the longshore current, sediment settled in the area where the longshore current velocity decreased. The sediment build-up in these calm areas caused the wave breaker line to retreat away from the initial shoreline. As this process continued, the longshore current, the point of depth induced wave breaking and a very active sediment movement zone, soon reached the mouth of the cofferdam. Once this point was reached, the power of the breaking waves washed the sediment into the trench. The pipeline installation technique will require the trench to be dredged to a level profile and will only make the cross-shore sediment movement worse. The initial bed slope restricted sediment movement in the cross-shore direction to a certain extent, whereas the level profile did not. However once the sediment build-up reached the mouth of the cofferdam not all of the sediment entered the mouth. It continued to follow the longshore current as it re-established on the southern side of the cofferdam. The sediment processes continue to build this shape until it created a new shoreline leaving the cofferdam structure buried in the surf zone.

In Figure 5.14, the cross-shore profile of the pipeline pathway is shown at three different time steps: the initial profile, the profile at the defined failure point and the final profile. Here it can be seen that if no maintenance is done in order the keep the sediment at bay, the structure will be buried almost completely at the end of the test and the trench will have to be dredged again.

FIGURE 5.14: Scenario 01 Cross-shore Profile

The same three time step images of the bed level of Scenario 02 (Straight structure with a $R_L = 2W_s$) are illustrated in Figure 5.16a on the following page. When compared to the images of Scenario 01, the same process was evident. The only difference was that the sediment took more time to reach the cofferdam mouth. This leads us to believe that if the length of the structure is increased, the contractor will have more time before the surf zone trench gets compromised with sedimentation. There was however a significant increase in the volume of sediment that reached the structure if it was allowed to develop to that point. This was due to the initial water depth to which the active surf zone was forced. Keep in mind that the surf zone will retreat seawards if the sediment is blocked by the structure. The farther away the surf zone retreated from its initial position, the deeper the water became, in effect creating more space (volume) for the sediment to fill up. This increase in volume can be observed in both the vertical jump between structures of different lengths on Figure 5.12, and also in Figure 5.15 showing the cross-shore profiles of Scenario 02 at the respective time steps.

FIGURE 5.15: Scenario 02 Cross-shore Profile

Another process was visible in Scenario 02 (See Figure 5.16b). Before the sediment made its way around the structure, erosion was visible on the southern side of the structure. As the sediment flowing from the north was blocked by the structure, the sediment that was meant to keep the shoreline in its natural position was kept away from this area. However, there was still wave energy and a longshore current which continued to move sediment down the shoreline. As no sediment was being brought in from the north, sediment was being taken from the shoreline creating a depression in the bed level downstream. The bed level change for Scenario 02 is given in Figure5.16b. In these images erosion of the surf zone seabed is clearly visible at the downstream side of the structure.

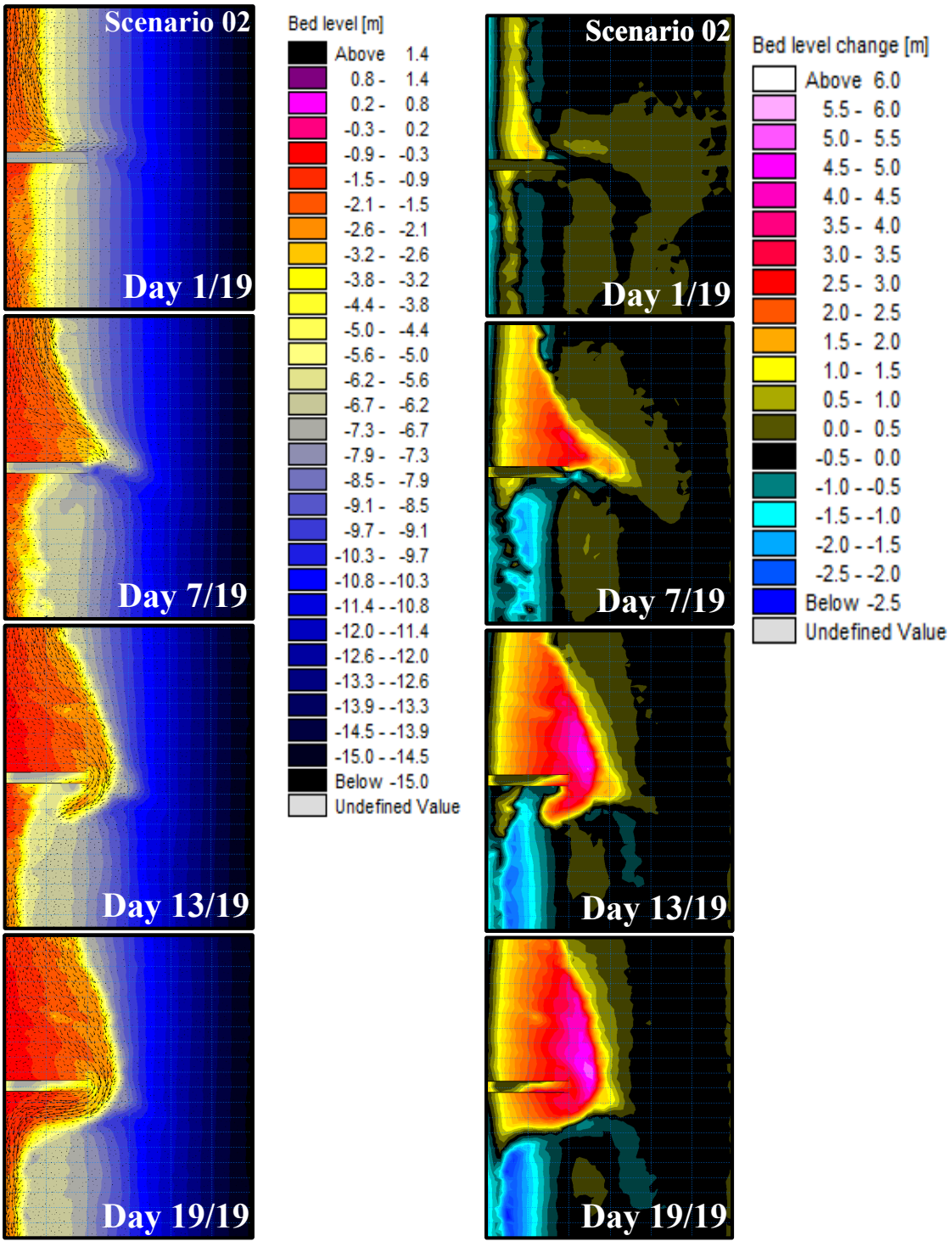

(A) Bed Level (B) Bed Level Change

FIGURE 5.16: Scenario 02 Bed Levels and Sediment Movement

The same general behaviour of currents, waves and sediment could be observed when Scenario 03 (Straight structure with a $R_L = 3W_s$) was considered (See Figure 5.17). As expected, and confirming the statement made earlier, the increase in length of the cofferdam in Scenario 03 only bought more time before the sediment reached the mouth of the structure. Also, referring to Figure 5.12 and Figure 5.18, the statement made about the longer the structure, and delay of failure becomes, the bigger the volume of sediment becomes that enter the pipeline pathway was confirmed. This increase of volume is referring to the volume of sediment at the mouth of the structure and not the entire trench. In these images the sediment volume inside the trench also seemed to decrease with an increase in structure length. If the test run time was increased, the sediment build-up inside the trench of the longer structures would eventually fill up to match the bathymetry on the outside of the structure.

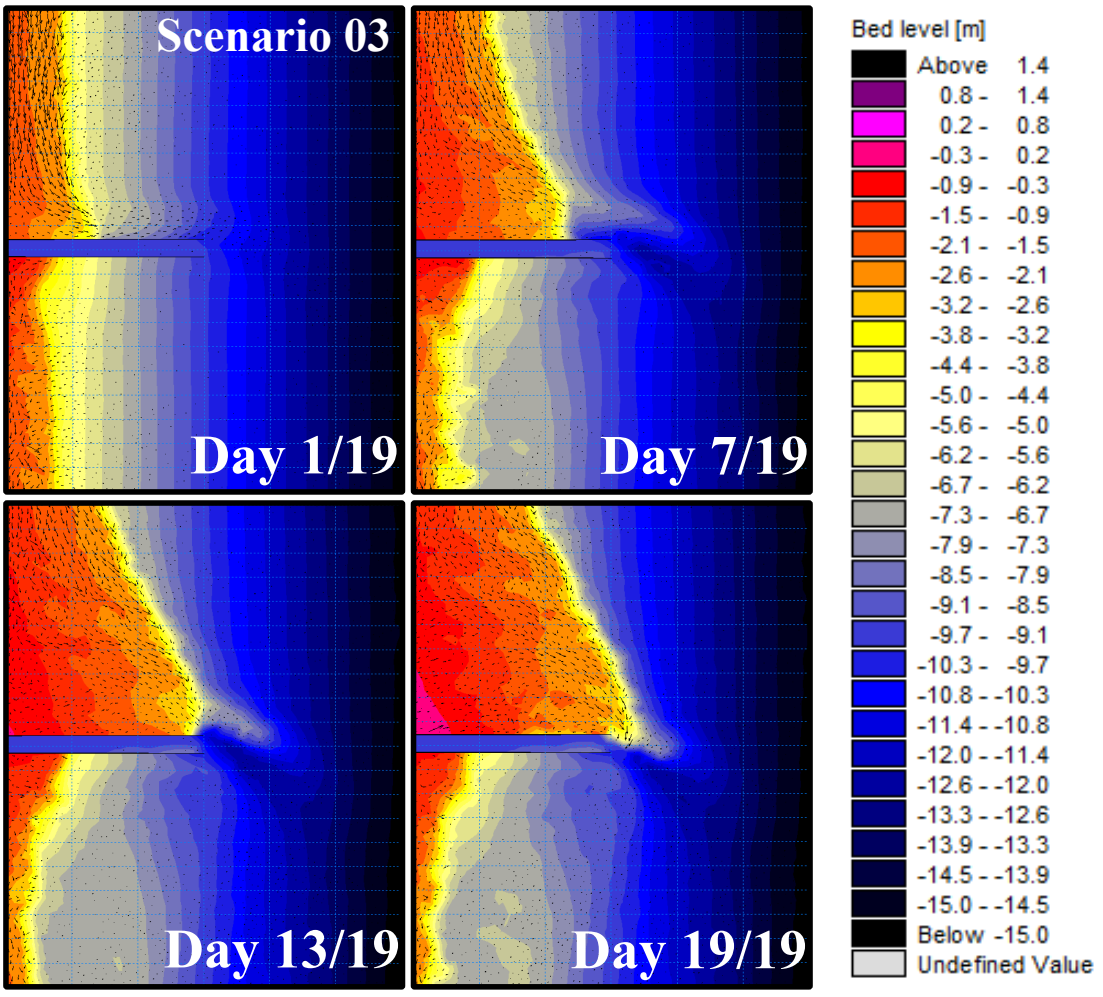

FIGURE 5.17: Scenario 03 Bed Levels and Sediment Movement

FIGURE 5.18: Scenario 03 Cross-shore Profile

As the length of the structure was increased, another area of concern was revealed. In order to prevent excess stresses in the pipeline, free span areas in the pipeline must also be prevented. As the sand bar formed from the northern side of the structure, a depression became visible in front of the cofferdam mouth in deeper water. A small indication of this impression is visible in Scenario 02, but the length of the structure is amplifying its effect (See Figure 5.17). The depression is caused by the prolonged exposure to an accelerated current velocity in this area. As the structure diverts the longshore current away from the shoreline, the current gets concentrated around the tip of the structure where it goes around the structure. This concentration causes an increase in current velocity. Until the northern shoreline sediment bank reaches the tip of the structure, the sediment which is in the area around the tip of the structure will migrate downstream due to the accelerated current and create a depression in this area. Thus if the structure gets longer, the time which the area around the structure tip is exposed to an increased longshore current velocity, without sediment fill-in gets longer. Thus the depression will get deeper.

Concluding the sediment movement of Scenario 03, these images once again show that a longer structure, with the mouth built outside of the breaker line, can buy the contractor more time before sediment build-up in the trench or at the mouth of the structure becomes a problem. It does however show that if a structure is too long it can cause the erosion of sediment which creates a depression in front of the structure mouth.

Another aspect to take into consideration is the construction time of the cofferdam itself. In order to get the equipment safely over the water, a jetty needs to be constructed. This jetty is built using pylons and does not affect the longshore transport. After the jetty is built, the sheet piling must be installed from a designated point. If this point is the shoreline, the installation of the cofferdam must be faster than the rate of the sediment

build-up against the structure. If this cannot be achieved then the sandbar will just move along with construction, and once the cofferdam is completed, the sediment will already be at the edge of the structure ready to be washed into the trench. Not only does the construction time pose a problem, but it needs to be remembered that a longer structure requires more material and in effect will be more expensive. At this point a financial analyses must be done to determine if the additional cost of the longer structure is less than that of the maintenance cost to upkeep a shorter structure. If not, the structure would prove ineffective.

When considering the images of Scenario 04 (Straight structure with a $R_L = 2W_s$ and a 45^o extended arm) at the same time steps, and comparing them with the same images seen on the previous page, a better solution may have been found.

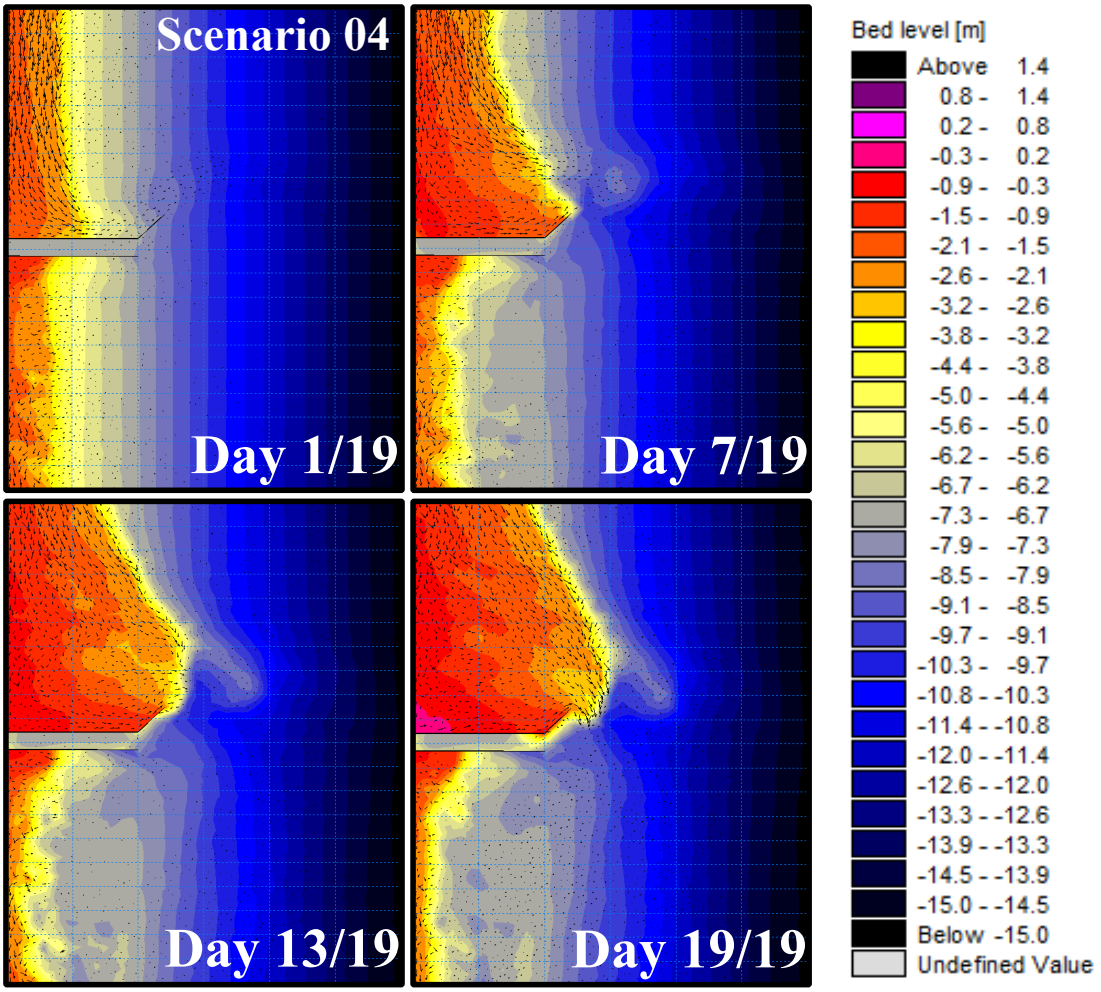

FIGURE 5.19: Scenario 04 Bed Levels and Sediment Movement

In this Scenario 04 a medium length structure ($R_L = 2W_s$), retained the sediment almost just as well as the longer structure in Scenario 03 ($R_L = 3W_s$). The only structural difference was a 45^o arm extended from the northern cofferdam wall. It also seemed to keep the pipeline pathway flatter and more level than that of the structure in Scenario 03. The depression in front of the structure shifted to the north and as illustrated in Figure 5.20, it appears to be more level. However, the structural integrity and practical implementation of the design in Scenario 04 was a cause for concern. When building a cofferdam, a bracing system is implemented to reinforce the sheet pile walls. This is done to make sure the cofferdam can endure the harsh environment it is constructed in. A huge amount of force is imposed on the cofferdam walls in the form of soil loads and wave forces. The bracing system uses the opposite wall of the cofferdam to ensure structural integrity as the forces imposed on the structure works in on it from the outside-in. When constructing the extended arm, as was done in Scenario 04, the wave forces would be immense. The structure had a bigger surface area facing the incoming wave direction, and there was no wall against which it could be braced to carry the weight of the sediment. A detailed investigation will have to be done in order to ensure that the structural integrity of the cofferdam is not compromised.

FIGURE 5.20: Scenario 04 Cross-shore Profile

As a result of the good outcome of Scenario 04 (Horizontal $R_L = 2W_s$), an option was investigated where the whole structure is rotated to the north. In this way an angle is obtained like the one in Scenario 04, and the basic construction design is used, meaning that the conventional bracing system can be implemented. The results however, are disappointing. Consulting Figure 5.21 and Figure 5.22, it is clearly visible that Scenario 05 did not retain the sediment nearly as long as Scenario 04. The sediment build-up within the trench is also more than that of Scenario 04. The question is why isn't this structure so effective?

FIGURE 5.21: Scenario 05 Cross-shore Profile

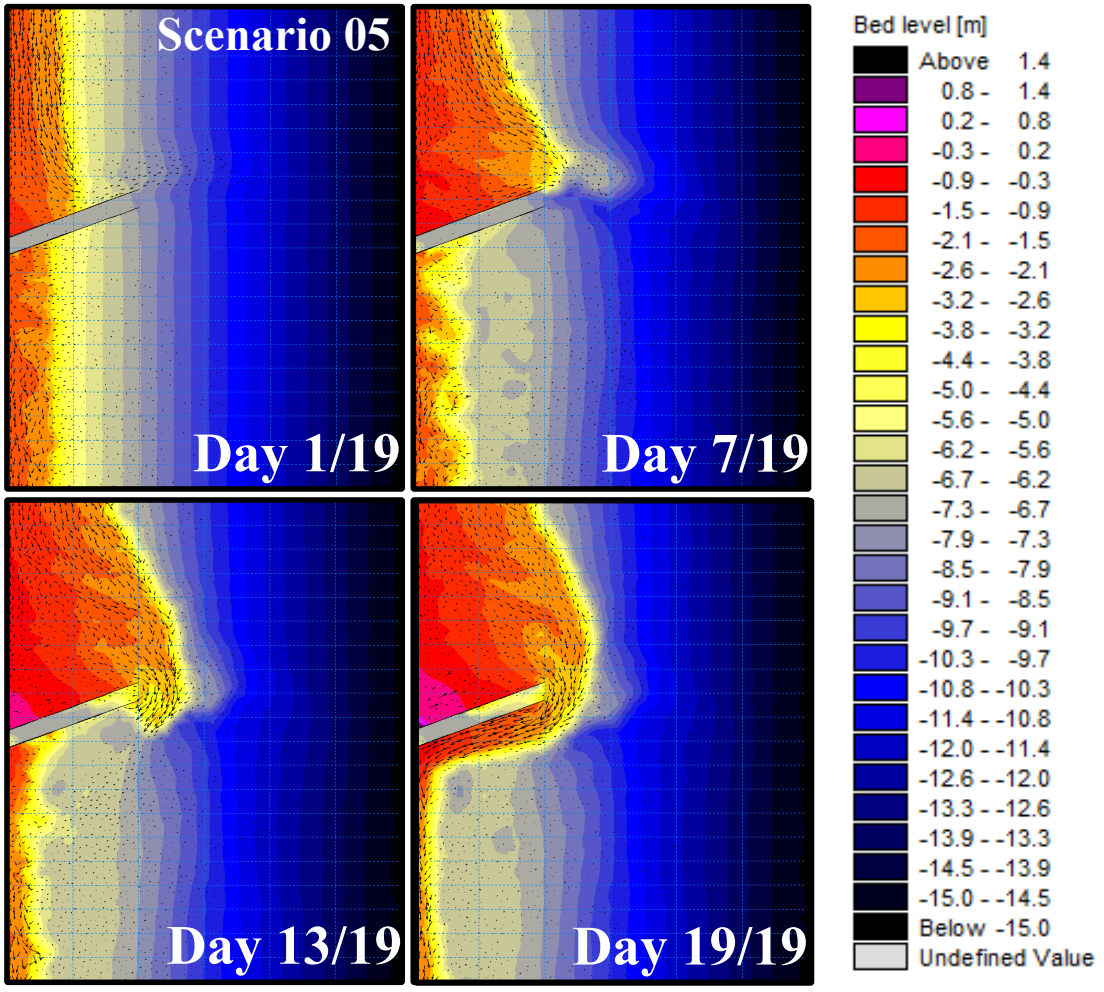

FIGURE 5.22: Scenario 05 Bed Levels and Sediment Movement

Three time lapsed images of the current movement of each the two scenarios are provided in Figure 5.23. When the two scenarios were compared, it was observed that the current in Scenario 05 came down from the north, then created a calm spot when it hit the

structure. In this calm spot sediment started to settle. Later on the current spread out and started to flow around the structure with a moderate deviation. In Scenario 04, the current came down from the north, hit the structure and created a calm spot, similar to as in Scenario 05. The calm spot was a bit smaller which meant the rate of sediment deposition slowed down. The current was then directed west and flowed over the 45^o arm. The arm acted as a ramp which almost turned the current back to the north. Subsequently (second time step 7/19 days) this process created an eddy or spiral, which delayed the sediment from moving around the structure edge. Eventually the sediment build-up became too great and the surf zone was level to the edge of the structure. At this stage the same process took shape as seen with all the other structures.

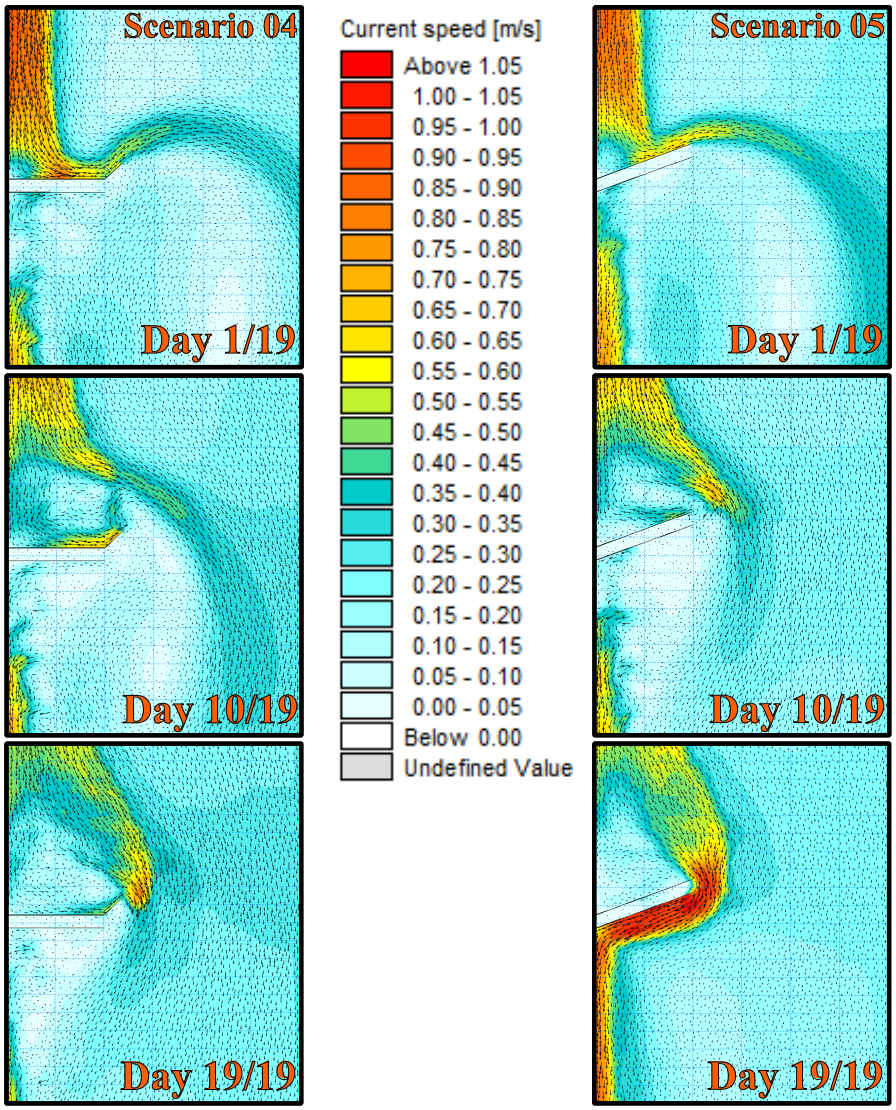

FIGURE 5.23: Scenario 04 vs Scenario 05 Currents

In contrast to Scenarios 04 and 05, a structure angled to the south, as seen in Scenario 06 (Horizontal $R_L = 2W_s$), was tested. This structure did not yield any more success than any of the other scenarios, but did clarify some of the questions asked during the

physical modelling. Firstly, in Chapter 4.2, it was stated that there are doubts that the longshore current re-established on the southern side of the structure as it was believed that the modelling basin was too small. Secondly, it was stated that the structure tested in the physical model which had a similar layout that the one in Scenario 06 may have had a positive outcome. The dye movement in the model basin led to believe that the current will carry the sediment past the mouth of the structure and deposit it in deeper waters. The numerical model however showed that the longshore current does re-establish on the southern side of the structure, and that the sediment is not carried out to deeper waters, but settles in the same pattern as the other scenarios. These processes are shown in Figure 5.24a and Figure 5.24b below.

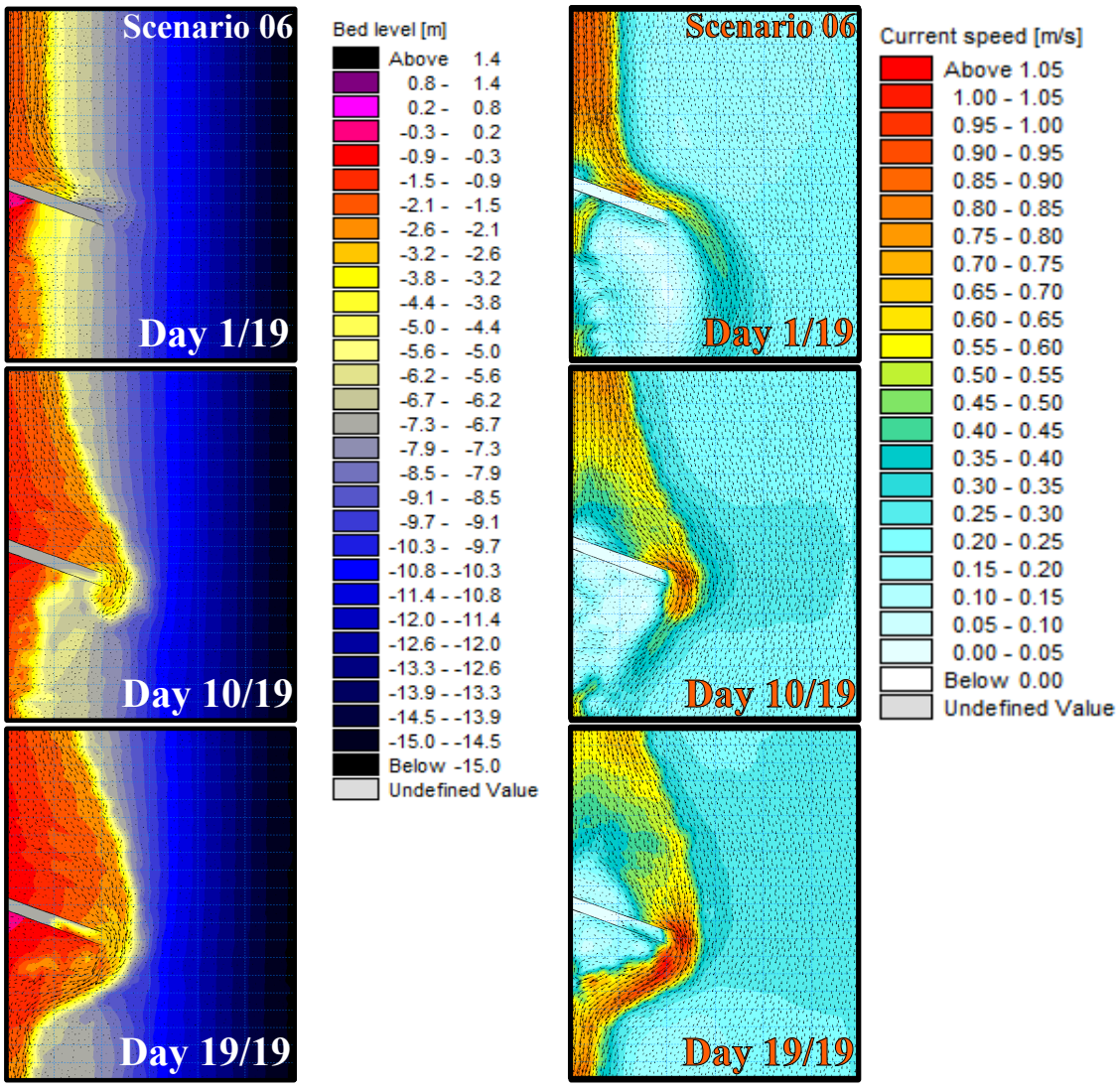

(A) Scenario 06 Sediment Movement (B) Scenario 06 Current Movement

FIGURE 5.24: Scenario 06 Sediment and Current Movement

Scenario07 tested in the numerical modelling had a straight structure closed off at the mouth with a $R_L = 2W$.

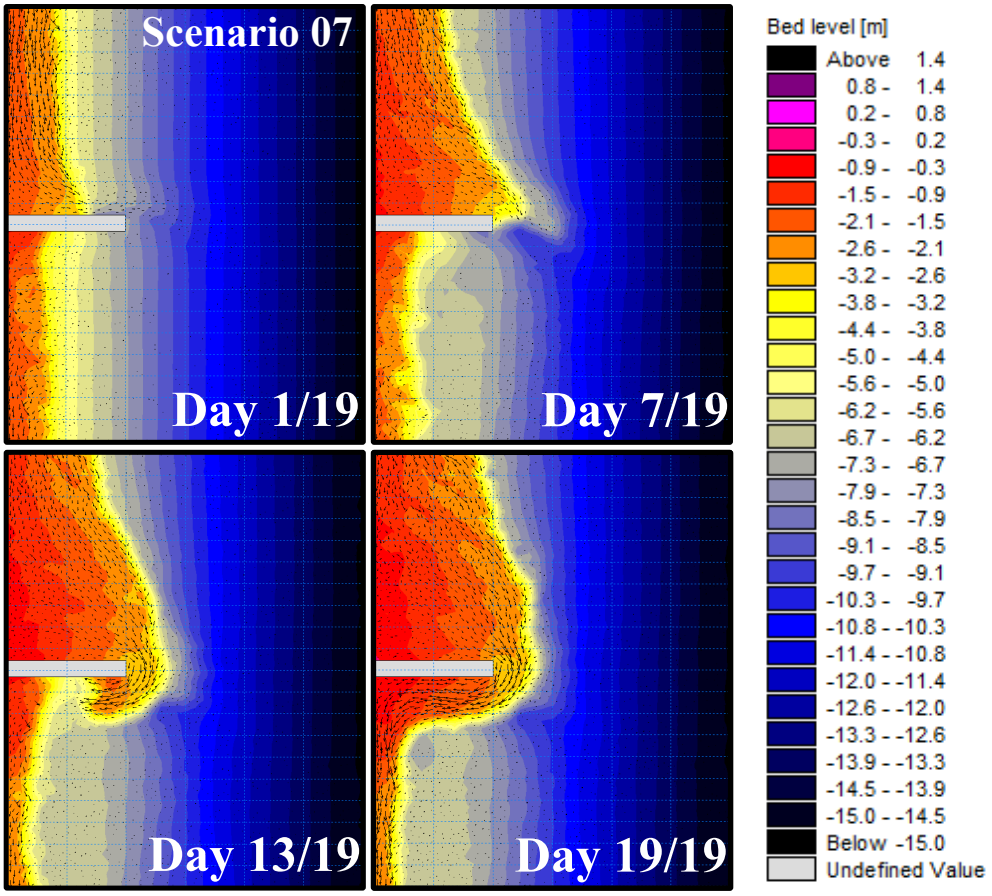

FIGURE 5.25: Scenario 07 Sediment Movement

This layout had much the same behaviour as that of Scenario 02 (Straight structure with a $R_L = 2W_s$). The only difference was that Scenario 07 was closed off at the end of the structure. The sediment movement was of the same nature up until it reached the end of the structure. Where Scenario 02 was open and allowed sediment to enter the trench, this structure forced the sediment to pass the structure mouth. The final formation of sediment was reached a bit earlier as less sediment was washed into the trench. The assumption can be made that there will be no sediment within the surf zone trench, which is true. No sediment can go into the structure if it is sealed off. But the pipeline does not only extend until the end of the structure, it still needs to be installed out to deeper waters. Once the mouth of the structure is opened to install the pipeline, a mass of sediment is in the way. Two main problems will arise at this moment. If the sediment has formed a sandbar around the structure, waves will break against the sealed off mouth of the structures, hitting it with intense forces. The gate of the structure would have to be designed to withhold these forces which may result in a more expensive structure. Assuming that the first problem is overcome and the gate

survives the onslaught from the waves, the moment the gate is removed from the mouth, waves will wash sediment, hoarding in front of the structure straight into the trench. If the plan is to dredge this area in front of the mouth, it must be kept in mind that this is a very active area in the surf zone and dredging will not be easy, if possible at all.

From personal discussions with pipeline experts from Clough Murray & Roberts Marine based in Cape Town, it came to my understanding that this method has been implemented. The main problem with this, however, was not the sediment at the mouth, but the forces the waves imposed on the closing gate. The gate was installed and the waves just ripped it apart over time. They are still considering using this method again, this time using a stronger gate. Some interesting techniques came forth in the discussion by which this structure could be made successful. The most appealing is to use a sacrificial sleeve. The sleeve will be installed from within the cofferdam travelling underneath the sediment out to a point where the sediment is no longer a problem. The pipeline will then be pulled from the shoreline, through the sacrificial sleeve and out the end point of the design. This option seems to carry promising possibilities.

There are however, other issues that need to be investigated when considering this option. Firstly it has been mentioned that the sediment build-up in front of a surf zone trench is a very unique situation. Each site will have different challenges and other characteristics. If this sacrificial sleeve method is to be successful, the sediment build-up at the mouth must be investigated. The weight of the sediment will impose a very large force on the sleeve and it must be able to withstand the weight. Secondly the width of the sandbar must be determined. If the sleeve is not long enough, it will be closed off by the sediment. It is possible to blow open the sleeve if the amount of sediment in the sleeve is small enough, otherwise the sleeve will be of no use. It must also be noted that this option, if implemented, can only be implemented for the on-bottom tow method described in Chapter 2.5.

The last numerical test was that of Scenario 08. A straight structure (normal to the shoreline) with a $R_L = 2W_s$ and wings extended to both the north and the south of the structure. The wings are perpendicular to the cofferdam walls and extend the same normal horizontal distance ($R_L = 0.4W_s$) than that of the 45^o arm in Scenario 04.

The structure does however fail at an earlier stage than that of Scenario 04. If Figure 5.26 is consulted, a similar sediment movement pattern to that of Scenario 04 is evident. The sediment movement, thus also the longshore current, is deflected back in the north eastern direction. The sediment also builds up in the semi-enclosed area on the northern side of the structure. As the wings are extended at right angles to the cofferdam walls, the area where sediment can collect is smaller than that of Scenario 04 where the arm is extended at a 45^o angle. Thus sediment will fill up the area in a shorter time period

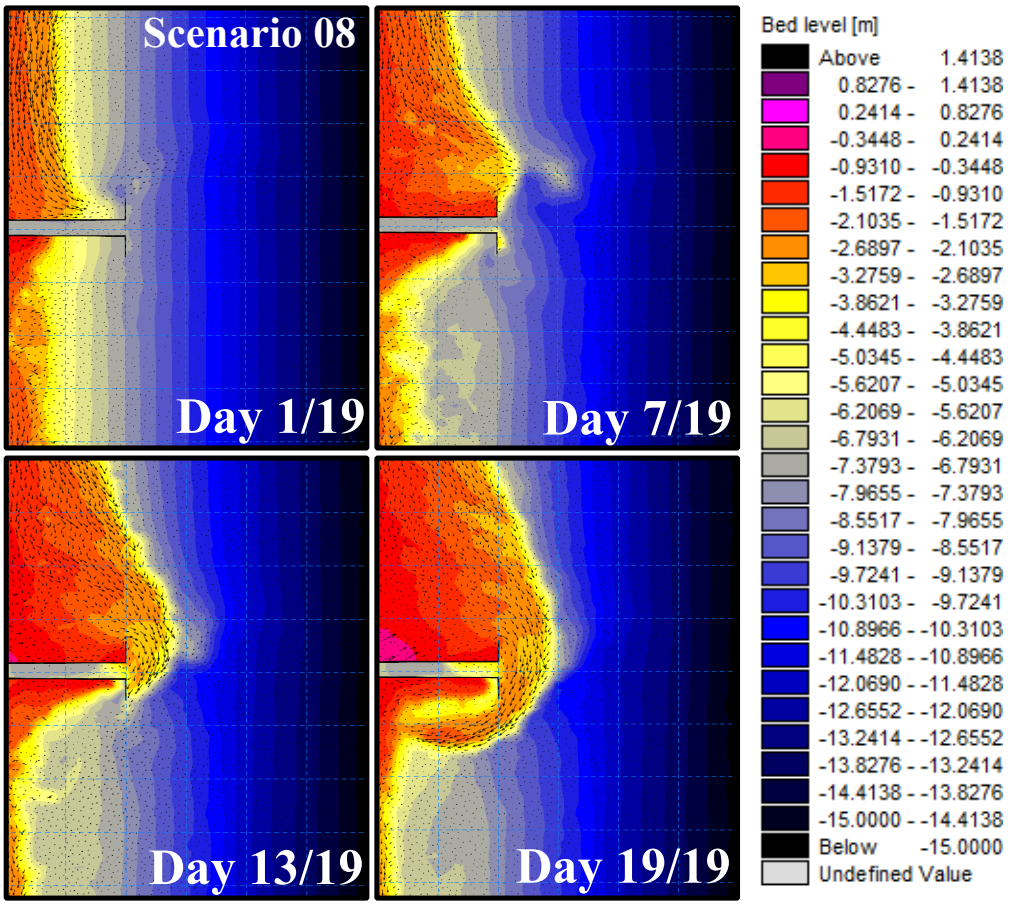

FIGURE 5.26: Scenario 08 Sediment Movement

and start to move around the tip of the wing and towards the mouth of the cofferdam structure. Although Scenario 04 was more effective, Scenario 08 has proven to be more effective than the other structures (Scenario 02, 05, 06 and 07) with the same structure length to surf zone width ratio ($R_L = 2W_s$). Also the same concern as in Scenario 04 and 07 comes to mind, regarding the structural integrity of the extended wings. Tideway Offshore Construction (2011) has proven this structure possible but it is recommended that care must be taken during the design process.

5.4 Sensitivity Study of the Most Effective Structure (Scenario 04)

5.4.1 Introduction

It has been identified that for the specific wave condition applied in the numerical model, Scenario 04 ($R_L = 2W_s$) has proven to be the most effective structure. With a smaller R_L than Scenario 03 ($R_L = 3W_s$), the structure maintained a clear pipeline pathway for a similar time period by just adding a 45^o arm to the upstream side of the structure.

In the literature review in Chapter 2 on page 17, it is stated that longshore sediment transport can occur in both directions at the same location at different time intervals. It is, however, also stated that this change in sediment transport direction is often seasonal, when the weather patterns change. Taking into account that cofferdams are temporary structure, seldom in the water for periods of longer than 4 months, it is a relatively safe assumption to make that a unidirectional wave condition will be present at any location where the longshore sediment transport rate is large enough to cause sedimentation problems in a temporary surf zone cofferdam. The assumption is made that if the wave direction does shift slightly at a location, it will not shift dramatically within the relatively short construction period. This implies that if the waves do come from both the north and the south of a structure built perpendicular to the shoreline, the incidence angle would be so small in regards with the shoreline, that longshore sediment transport build-up against the temporary structure would prove to be a minor problem.

With that said, Scenario 04 is the only scenario where the structure is neither symmetrical, nor tested from both sides such as Scenario 05 and 06 combined. For this reason a sensitivity study was done on Scenario 04 to see what effect a wave direction shift will have on the effectiveness of the structure. The effect of a wave angle shift is already shown in the physical modelling in Chapter 4, and will now be confirmed.

5.4.2 Scope of Sensitivity Study

The same structure of Scenario 04 will be exposed to 4 different wave conditions. The first wave condition is the same as the wave condition done in the numerical study of this study, thereafter 3 more tests were conducted, shifting the wave angle with each consecutive test. Investigating the effect the wave condition have on longshore sediment transport is not the goal of this study, but it does effect the outcome of this study. As the effects of the change in wave height and water level have also been shown in the physical modelling of this study, these parameters will be kept the same for the sensitivity study. The 4 wave conditions and structure forms used in the sensitivity study are shown below in Table 5.8 and Figure 5.27.

ID	Significant Wave Height H_S(m)	Wave Period T(s)	Wave Direction θ(degrees) relative to True North	Wave Direction β(degrees) relative to Shoreline (Incidence Angle)
A	1.5	12	60	30
B	1.5	12	80	10
C	1.5	12	100	-10
D	1.5	12	120	-30

TABLE 5.8: Sensitivity Study Input Data

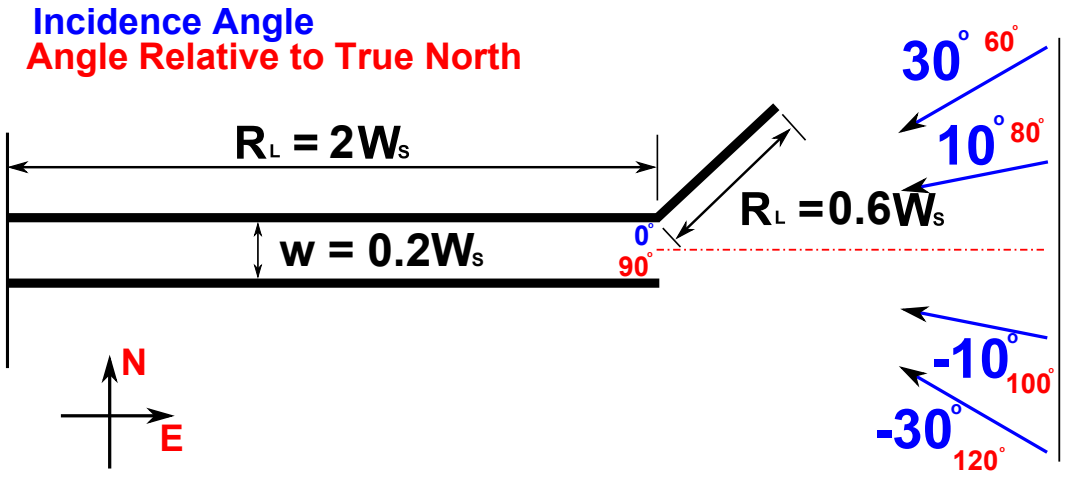

FIGURE 5.27: Sensitivity Study Layout

5.4.3 Discussion of Sensitivity Study

All 4 of the tests conducted during the sensitivity study will be discussed by referring to Figure 5.28. A full page is used in order to show the results of all 4 tests adjacent to each other to give a clear indication what the difference is between the tests at each of the given time steps. The wave direction of each test is given in the first window of each column and is also represented by the white arrow in each window.

In the numerical modelling of this study, this structure was tested using an incidence angle (β) of 30^o and is represented in column **A** of Figure 5.28. With an incidence angle this large, the sediment transport processes will be coming from the north and will be quite large considering both transport rate and volume. The structure was designed with a sediment transport field with these characteristics in mind. It is thus visible that the sediment builds up on the northern side on the structure and erodes on the southern side of the structure. In the last window of column **A**, it is evident that the sediment has made its way around the structure tip and started to obstruct the path of the pipeline. The sediment accretion on the northern side of the structure has progressed to a point where a positive bed level is shown in the corner between the shoreline and the northern wall of the structure indicating dry land (represented by the color PINK). Erosion on the southern side has progressed to the point that the deeper, level profile has almost reached the shoreline.

In column **B** a wave incidence angle (β) of 10^o was implemented. This wave angle is closer to a normal angle to the shoreline and according to the findings in the physical modelling in Chapter 4, the longshore current velocity and in effect the longshore sediment transport rate should decrease. When comparing column **B** to **A**, this is also evident in the numerical test. The same accretion is seen on the northern side of the structure as well as the same erosion on the southern side of the structure. All of these processes just develops at a slower rate and at the end of the test the sediment bank has barely reached the mouth of the structure or the pipeline pathway. There is also no positive bed level value indicating dry land in the corner between the shoreline and the northern wall of the cofferdam structure. This confirms the findings of the physical modelling and confirms that if the incidence angle is smaller, and the structure is built with the correct orientation in regards with incoming wave condition, the sedimentation problems experienced with a temporary cofferdam will be smaller.

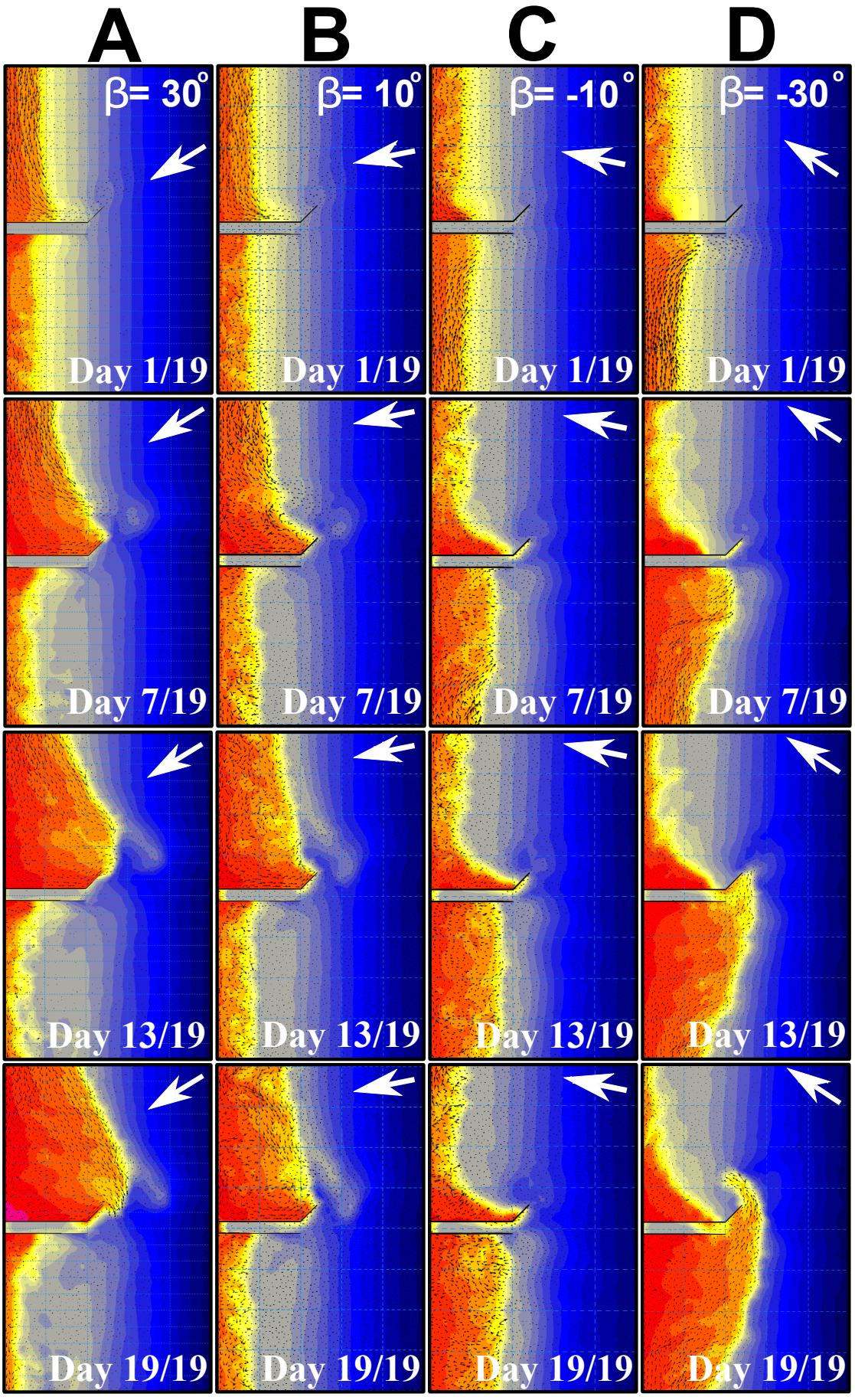

FIGURE 5.28: Sensitivity Study Results

If a wave incidence angle (β) of -10^o is applied to the model, the longshore current and sediment transport processes should change direction from south going to north going in the model. If column **C** is consulted, it is clear that this is indeed the case. Although at a slow rate, sediment accretion is now visible on the southern side of the cofferdam and erosion is visible on the northern side of the structure. In this case the southern wall of the cofferdam will act like a normal straight structure without any alternative geometric differences. It also shows that there is no significant sediment deposition at the mouth of the structure in comparison with a situation with a larger incidence angle, as seen in column **D**. There are however some differences in the sediment patterns. The 45^o arm is now extended in such a manner that the face of the structure is not close to parallel to the incoming waves but rather close to normal to them. Meaning that waves will hit the structure face from the front. This will cause a large force on this structure and may prove to be a problem. Also the extended arm will act as a shield and protect the upstream side from wave interference and as a result will cause an enhancement of the accretion close to the structure on the northern side. The starting point of the typical erosion process of the downstream side will then shift up the shoreline and will be seen a bit more to the north.

If column **D** is observed, where a wave incidence angle of -30^o is applied, the same processes will be seen as in column **C**. Only, as in the case of columns **A** and **B**, the longhsore current and in effect the longshore transport rate will be increased causing a larger sedimentation build-up. The sediment accretion on the southern side of the structure has developed to a point where sediment has passed the tip of the structure and obstructed the pipeline pathway at the mouth of the structure. It is clear that in this case, the arm extended to the north east of the structure has a negative effect as it only help to trap the sediment in front of the structure instead of letting it move past the mouth of the structure. This will also enhance the erosion effect on the northern side of the structure. A large accretion is shown against the northern side of the structure and is due to wave diffraction driving sediment into the corner between the shoreline and the northern wall of the structure. This is also visible with the other case but on a smaller scale leading us to the conclusion that the extended arm on the downstream side of the structures slightly enhanced this effect. However, the erosion process a bit further up the shoreline to the north, is once again fully formed and shows a large amount of erosion, similar to the southern shoreline in column **A**.

5.4.4 Conclusions and Recommendation of Sensitivity Study

By changing the wave incidence angle of the incoming wave condition, the effect of the non-symmetrical structure layout of Scenario 04 in the numerical modelling could be analysed with reference to the sediment movement around the structure. It is clear that if a unidirectional wave condition is present at a certain location, the structure is most effective with the 45^o extended arm being built to extend to the outside of the structure, from the upstream wall of the cofferdam as the case in column **A** in Figure 5.28. If the arm is extended on the downstream side of the structure, as the case in column **D** in Figure 5.28, it will have a negative effect in regards with sediment build-up in and at the mouth of the cofferdam structure as it will block the sediment in this area from moving past the structure mouth and to the downstream shoreline.

If the wave condition at a certain location is not unidirectional but is able to shift in such a manner as to cause sediment transport from both the north and the south, the sediment transport rate will be smaller. However, should this be the case, it is recommended that an assessment be conducted to investigate the outcome if the structure is altered to form a Y shape with two extended arms, one to the north and one to the south.

5.5 Concluding Remark

In Chapter 5.2 it is shown that the numerical model yields results emulating observations of an active surf zone interrupted by a structure in the surf zone.

Using the numerical model, different structure layouts were investigated, ranked and discussed. The author's opinion of the structures, performance were given by defining a failure point (Chapter 5.3.2) and giving the structures a ranking according to their effectiveness in regards with maintaining the initial cross-shore profile of the pipeline pathway (See Chapter 5.3.4).

A conclusion was reached that Scenario 04, a structure perpendicular to the shoreline with a length to surf zone width ratio (R_L) of $2W_s$ and an arm extended at 45^o in the upstream direction of the structure, was the most effective. The arm extended a normal horizontal distance of $0.4W_s$. Even so, there are concerns about the constructability and structural integrity of the structure layout.

It is also proven that an increase in structure length will increase the amount of time before the sediment build-up will start to intrude the pipeline pathway. There is, however, reason to believe that a second limit is applicable as an increase in structure length revealed a more prominent erosion process at the mouth of the structure before the sediment from the upstream shoreline reaches the mouth of the structure. It must also be kept in mind that if the cofferdam construction rate is not faster than that of the sediment build-up on the northern side of the structure, a longer structure will prove to be ineffective.

The numerical model also answered the questions raised with the physical model in this study. In Chapter 5.3 it is stated that a structure built with an angle in the downstream direction, as is the case in Scenario 06, may have a positive effect as the current will carry the sediment out to deeper waters. It is also stated that this may be because the longshore current does not re-establish on the northern side of the structure due to a limit in the physical size of the basin used for the physical model. It is proven in the numerical model that the longshore current will fully re-establish in a situation where there is enough space to do so and if this is the case, the structure in Scenario 06 will also prove to be ineffective.

Alternative methods of implementing the cofferdam structures for the installation of a submarine pipeline are also briefly discussed and some opinions of experts are documented.

Chapter 6

Study Conclusion

By combing the observations from both the physical modelling and numerical modelling the following conclusions were made.

The most effective structure for the cofferdam is a structure with a length to surf zone width ratio(R_L) of $2W_s$, built perpendicular to the shoreline with an extended arm built out at a 45^o angle from the upstream edge of the cofferdam structure. There is, however, concern considering the constructibility of this design as the extended arm will be exposed to large forces from the incoming wave climate. From the physical modelling the change in sediment behaviour can be seen considering the change in wave condition.

A second conclusion regarding the length of the structure was made. If the contractor is able to build the cofferdam faster than the rate of sediment build-up against the structure, an increase in length will buy the contractor more time before the sediment will compromise the pipeline pathway. Keep in mind that a depression in the bathymetry in front of the structure mouth became more prominent as the length of the structure increased.

Chapter 7

Recommendations

In order to best utilize the findings of this study in future cofferdam shore crossing projects, the following recommendations are made.

A thorough investigation must be done on the structural integrity and constructability of a straight cofferdam structure perpendicular to the shoreline with a length to surf zone width ratio (R_L) of $2W_s$ and a 45^o arm extending from the upstream side of the cofferdam wall. This investigation should include an accurate time line study and a comparison between the above mentioned structure and a default cofferdam structure (straight with a determined length). Also included should be a financial analyses to ensure that the structural changes and installation do not become more expensive than the maintenance costs of a default cofferdam structure.

In order to improve the findings of this study, and improve the results of future studies regarding the same topic, the following recommendations are made.

A pipeline construction project similar to the ones described in this study should be identified at an early stage of the project to enable monitoring of a full scale case. The construction of the surf zone trench and protecting cofferdam must then be monitored in terms of incoming wave climate, current speed and direction, bathymetry changes and sediment characteristics. It is important to measure rate of bed level change around the structure and take note of the construction speed of the cofferdam. With the data mentioned above, a study should be undertaken including a quantitative large scale physical model and detailed numerical model.

It is also recommended that alternative methods of sediment control, such as bypass pump systems and upstream groins, be investigated.

References

Anıl Arı Güner, H., Yüksel, Y. and Cevik, E. (2011), *Determination of Longshore Sediment Transport and Modelling of Shoreline Change*, ISBN 978-953-307-189-3, InTech, Yildiz Technical University, Turkey.

Basco, D. and Pope, J. (2004), 'Groin functional design guidance from the coastal engineering manual', *Journal of Coastal Research* **SI 33**, 121–130.

Bennington, J. (1990), Hofstra University Lecture. Long Island, New York.

Bijker, E. (1967), Some considerations about scales for coastal models with movable bed, Technical report, Delft Hydraulics Laboratory, Delft, The Netherlands.

Bijker, E. (1971), 'Longshore transport computations', *Journal of Waterways, Harbors and Coastal Engineering Division 97* **4**, 687–703.

Birkemeier, W. (1985), 'Field Data on Seaward Limit of Profile Change', *Journal of Waterway, Port, Coastal, and Ocean Engineering* **111**(3), 598–602.

Bosboom, J. and Stive, M. (2012), *Coastal Dynamics /0.3.*, VSSD, Delft in Netherlands.

Boskalis Dredging and Marine Experts (2012), 'Balgzand - Bacton Pipeline (BBL)'. Boskalis Prject Sheet.

Bowditch, N. (2002), *The American Practical Navigator: an Epitome of Navigation*, Vol. 9, National Imagery and Mapping Agency.

Bruun, P. (1962), 'Sea-level rise as a cause of shore erosion', *Journal of the Waterways, Harbours and Coastal Division* **88**, 177–130.

Capobianco, M., Larson, M. and Nicholls, R. (1997), Depth of closure: A contribution to the reconcilliation of theory, practice and evidence, *in* 'Proc. Coastal Dynamics '97', ASCE, New York, pp. 506–515.

Chadwick, A. (1989), 'Field measurements and numerical model verification of coastal shingle transport', *Advances in Water Modelling and Measurement* pp. 381–402. BHRA, Cranfield, Bedford.

Chadwick, A., Morfett, J. and Borthwick, M. (2004), *Hydraulics in Civil and Environmental Engineering 4th edition*, Spon Press, Abingdon.

Clough Murray & Roberts Marine (2010), Basis of Design for Trekkopje Desalination Works, Technical report, Cape Town.

Clough Murray & Roberts Marine (2011), Design Basis for Mossel Bay Offshore Pipeline, Technical report, Cape Town.

Coastal Environmental Services (2001), The draft subsequent environmental impact report for the port of Ngqura, Eia report, 6140, Grahamstown, South Africa.

Cowper, N. S. and Thomas, A. (2014), 'The Nerang Sand Bypass System, November, 2014', pumpindustry, The Australian Pump Magazine.
URL: *http://www.pumpindustry.com.au/*

CSIR (1990), Environmental data for the design and operation of the Mossel Bay SPM, Technical report, Stellenbosch.

Dean, R. (1977), Equilibrium beach profiles: U.S. Atlantic and Gulf coasts, Ocean Engineering Report 12, Newark.

Dean, R. and Dalrymple, R. (2002), *Coastal Processes with Engineering Applications*, Cambridge University Press, The Pitt Building, Trumpington Street, Cambridge, United Kingdom.

Dean, R. and Maurmeyer, E. (1983), *Models for beach profile response*, CRC Press, Boca Raton, FL.

Dixon, A., Heath, K. and Theron, F. (2014), 'Personal correspondence'. Clough Murray & Roberts Marine, Cape Town.

Doria, A. and Guza, R. (2013), 'Estimating Changes in Near-shore Bathymetry with Subaerial Survey', *American Meteorological Society* **30**, 2225–2232. La Jolla, California.

Fernandez, M. (1981), Tow Techniques for Marine Pipeline Installation, Master's thesis, Delft University of Technology, Delft. Prepared for ETCE, Energy Technology Conference & Exhibition.

Fredsoe, J. and Deigaard, R. (1992), *Mechanics of Coastal Sediment Transport*, Vol. 3, World Scientific Publishing Co. Pte. Ltd, London.

Frijlink, H. (1952), 'Discussion des formulas de debit solide de kalinske, einstein et meyer-peter et mueller compte tenue des mesures recentes de transport dans les rivieres neerlandaises', *Journal Hydraulique Societe Hydraulique de France* **2**, 98–148.

Gerwick, B. (2007), *Construction of Marine and Offshore Structures*, Vol. 3rd Edition, Taylor and Francis Group.

Grant, G., Man, J., Hill, C., Johnson, S., Campbell, K., Mohseni, O., Wallick, J., Lewis, S., O'Connor, J., Major, J. and B.K., B. (2008), Experimental and field observations of breach dynamics accompanying erosion of Marmot cofferdam, Sandy River, Oregon, University of Minnesota, pp. 1–10.

Hallermeier, R. (1981), 'A Profile Zonation For Seasonal Sand Beaches from Wave Climate', *ELSEVIER* **4**, 254–277. Amsterdam.

Hamilton, D. and Ebersole, B. (2000), 'Establishing uniform longshore currents in a large-scale sediment transport facility', *Coastal Enginnering* **42**, 199–218.

Harris, T. (1978), Review of Coastal Currents in Southern African Waters, SANSP Report 30, National Scientific Programmes Unit: CSIR. pp 109.

Holthuijsen, L. H. (2007), *Waves in Oceanic and Coastal Waters*, Cambridge University Press, New York.

Holthuisjen, L., Booij, N. and Herbers, T. (1989), 'A prediction model for stationary, short crested waves in shallow water with ambient currents', *Coastal Engineering* **13**, 23–54.

Hughes, S. (1983), 'Movable-bed modeling law for coastal dune erosion', *Journal of Waterways, Port, Coastal and Ocean Engineering* **109**, 167–179.

Hughes, S. (1993), *Physical Models and Laboratory Techniques in Coastal Engineering*, Vol. 7, World Scientific Publications, USA.

Hughes, S. and Fowler, J. (1990), Validation of movable bed modeling guidance, Proc. 22nd ICCE, Delft, pp. 1–10.

Hugo, P. (2013), The impact of climate change effects on the planform of headland-bay beach on the southern coast of South Africa, Master's thesis, University of Stellenbosch.

ISCHEBECK (2014), 'Piling procedures: PILE DRIVING', Website, 28 June 2014. **URL:** *http://www.ischebeck.es/en.home/tablestacado/golpeo-es.html*

Ito, M. and Tsuchiya, Y. (1984), Scale-model relationship of beach profile, Proc. 19th ICCE, Houston, USA, pp. 1386–1402.

Jonsson, I. (1966), Wave boundary layers and friction factors, Proceedings of the 10th Coastal Engineering Conference, ASCE, pp. 127–148.

Kaergaard, K. and Fredsoe, J. (2012), 'Numerical modelling of shoreline undulations part 2: Varying wave climate and comparison with observations', *Coastal Engineering* **75**, 77–90.

Kamphuis, J. (1991), 'Alongshore Sediment Transport Rate', *Journal of Waterway, Port, Coastal and Ocean Engineering* **117**(6), 624–640.

Kana, T., White, T. and McKee, P. (2001), 'Management and engineering guidelines from groin rehabilitation', *Journal of Coastal Research* **SI**(33), 57–82,.

Komarek, J. (2014), City of lake Oswego/City of Tigard Water Supply Partnership Summary of Oversight Committee Meeting, Technical Report 40, City of Lake Oswego and City of Tigard. Tigard Public Library.

Komen, G., Caveleri, L., Doneland, M., Hasselman, K., Hasselman, S. and Janssen, P. (1996), 'Dynamics and modelling of ocean waves', *Quarterly Journal of the Royal Meteorological Society* **122**(530), 564–565. Part B.

Kuriyama, Y. and Sakamoto, H. (2014), 'Cross-hore distribution of long-term average longshore sediment transport rate on a sandy beach exposed to waves with various directionalities.', *Coastal Enginnering* **86**, 27–35.

Longuet-Higgens, M. (1970), 'Longshore Currents Generated by Oblique Incident Sea Waves', *Journal of Geophysical Research* **75**(33), 6778–6789. Oregon State University.

Longuet-Higgens, M. and Stewart, R. (1964), 'Radiation in water waves; a physical discussion, with apllications', *Journal of Dea-Sea Research* **11**, 529–562. Pergamon Press Ltd.

Mather, A. and Strech, D. (2012), 'A perspective on Sea Level Rise and Coastal Storm Surge from Southern and Eastern Africa: A case study near Durban', *Water, ISSN 2073-4441* **4**(1), 237–259. This article belongs to the Special Issue Flood Risk Management.

Nairn, R. and Dibajnia, M. (2004), 'Design and construction of a large headland system, Keta sea defence project, West Africa', *Journal of Coastal Research* **SI**(33), 294–314.

Nemati, K. (2007), 'Temporary Structure : Cofferdams', University of Washington. Department of Construction Management, Lesson 4.

Nicholls, R., Birkemeier, W. and Hallermeier, R. (1996), Application of depth of closure concept, *in* 'Proc. 25', ASCE, Orlando, pp. 3874–3887.

Noda, E. (1972), 'Equilibrium beach profile scale-model relationship', *Journal of Waterways, Harbors and Coastal Engineering Division* **98**(4), 511–528.

NSW Government (2014), 'Tweed Sand Bypassing, 8 November 2014'.
URL: *http://www.tweedsandbypass.nsw.gov.au/operations/general-information/construction-overview*

PetroMin Pipeliner (2012), 'Pipelay Vessels and Techniques', Published on website.
URL: *http://www.pm-pipeliner.safan.com/mag/ppl0112/t50.pdf*

PILEBUCK (2014), 'Types of sheet pile', Website, 27 June 2014.
URL: *http://www.pilebuckinternational.com/specs-2/*

Poolebay Coastal Management (2014), 'New Rock Groynes, Branksome Beach Winter 2008/09'. 6 Noverber 2014.
URL: *http://www.poolebay.net/rock-groynes.html*

Reniers, A. and Battjes, J. (1996), 'A laboratory study of longshore currents over barred and non-barred beaches', *Coastal Enginnering* **30**, 1–22.

Ribas, F., Falques, A., Van den Berg, N. and Caballeria, M. (2013), 'Modelling shoreline sand waves on the coasts of Namibia and Angola', *International Journal of Sediment Research* **28**, 1–11. Catalonia.

Sandhurst Equipment Rental (2014), 'Vibratory Pile Drivers', Website, 25 June 2014.
URL: *http://www.sandhurst-rent.com*

Schoonees, J. (2012), 'Coastal Sediment Transport: Lecture Notes'. University of Stellenbosch, South Africa.

Schoonees, J. and Theron, A. (1996), 'Improvement of the most accurate longshore transport formulae', *Coastal Engineering* pp. 3652 – 3665. Research Engineers, CSIR, P.O. Box 320, Stellenbosch,7599, South Africa.

Schoonees, J. and Theron, A. (2002), 'Development of an accurate longshore sediment transport model', *Journal of the South African Institute of Civil Engineering* **44**, 12–17.

Swart, D. and Fleming, C. (1980), Longshore water and sediment movement, ASCE, Sydney, pp. 1275–1294.

ThyssenKrupp (2014), 'Interlock designs'. 27 August 2014.
URL: *http://tk-steelcom.com.au/products/piling-sections/sheet-pile-interlock-sealant/*

Tideway Offshore Construction (2011), Shore approach feasibility study report, Technical Report 2, 4880 GB Breda, The Netherlands.

U.S. Army Corps of Engineers (2002), 'Coastal engineering manual'. Engineering Manual 1110-2-1100, Washington, D.C.

Van der Meer, J. (1990), *Static and dynamic stability of loose materials in: Coastal protection*, Balkema. Rotterdam, Ed. Pilarczyk K.W.

Van Rijn, L. (1998), *Principles of Coastal Morphology*, Aqua Publications, www.aquapublications.nl, The Netherlands.

Van Rijn, L. (2013), Design of hard structures against erosion, Aqua Publications, www.aquapublication.nl , The Netherlands.

Van Rijn, L., Tonnon, P., Sanchez-Arcilla, A., Caceres, I. and Grune, J. (2011), 'Scaling laws for beach and dune erosion processes', *ELSEVIER: Coastal Engineering* **58**, 623–636.

Vercruysse, W. and Fitzsimons, M. (2006), 'Landfall and shore approach of the new langeled pipeline at Easington, UK', *Terra et Aqua* (102), 12–18.

Vlasblom, W. (2003), 'Lecture notes on dredging equipment and technology'. 27 August 2014, Central Dredging Association (CEDA).
URL: *http://www.dredging.org/documents/ceda/downloads/vlasblom1-introduction-to-dredging-equipment.pdf*

Walker, D., Dong, P. and Anastasiou, K. (1991), 'Sediment transport near groynes in the nearshore zone', *Journal of Coastal Research* (7), 1003–1011.

Wang, H., Wang, A., Bi, N., Zeng, X. and Xiao, H. (2014), 'Seasonal distribution of suspended sediment in the Bohai Sea, China', *ELSEVIER: Continental Shelf Research* . Qingdao.

Wright, L., Boon, J., Kim, S. and List, J. (1991), 'Modes of Cross-shore Sediment Transport on the Shoreface of the Middle Atlantic Bight', *ELSEVIER: Marine Geology* **96**(1-2), 19–51.

Young, I. (1999), *Wind Generated Ocean Waves*, Vol. 2 of *Ocean Engineering Series*, ELSEVIER.

Appendix A

Closure Depth Values and Calculations for Mossel Bay and Trekkopje

A.1 Mossel Bay (2011) Closure Depth

The wave data as follows were obtained from the CSIR (Stellenbosch) as recorded by their Waverider buoy off the Coast of Mossel Bay. The data was collected on behalf of the Transnet National Port Authority (TNPA).

A.1.1 Input Parameters

Significant Wave Height H_S(m)	**Wave Period T_e(s) = T_s (Hallermeier, 1981)**	**Standard Deviation σ**	**Gravitational acceleration g**
1.24	13	0.5	9.81

TABLE A.1: Closure Depth Calculation Input Parameters for Mossel Bay

A.1.2 Formulae

$$H_e = \bar{H}_s + 5.6\sigma \tag{A.1}$$

$$d_1 = 1.75H_e - 57.9(\frac{H_e^2}{gT_e^2}) \tag{A.2}$$

A.1.3 Answer

Closure depth = **6.5 m**

A.2 Trekkopje, Namibia (2010) Closure Depth

The wave data as follows were obtained from Clough Murray & Roberts Marine (2010).

A.2.1 Input Parameters

Significant Wave Height H_S(m)	**Wave Period T_e(s) = T_s (Hallermeier, 1981)**	**Standard Deviation σ**	**Gravitational acceleration g**
3.3	13	0.85	9.81

TABLE A.2: Closure Depth Calculation Input Parameters for Trekkopje, Namibia

A.2.2 Formulae

$$H_e = \bar{H}_s + 5.6\sigma \tag{A.3}$$

$$d_1 = 1.75H_e - 57.9(\frac{H_e^2}{gT_e^2}) \tag{A.4}$$

A.2.3 Answer

Closure depth = **11.84 m**

Appendix B

Bijker's Formula Mathematical Derivation

$$q_b = \frac{Ad_{50}V\sqrt{g}}{C}\exp\left(\frac{-0.27\triangle d_{50}\rho g}{\overline{\mu\tau_{cw}}}\right) \tag{B.1}$$

where q_b is the bed load transport, A is an empirical coefficient (1.0 for non-breaking waves and 5.0 for breaking waves), d_{50} is the sediment particle diameter, V is the mean current velocity, C is the Chezy coefficient ($= 18\log(12h/k_s)$), where k_s is the bottom roughness, $\triangle$ is the relevant apparent density of the bed material ($= (\rho_s - \rho)/\rho$), ρ is the mass density of the water, ρ_s is the mass density of the bed material, g is the gravitational acceleration, μ is the ripple factor and τ_{cw} is the time averaged bed shear stress due to currents and waves.

The ripple factor which indicates the influence of the of the form of the bottom roughness can be expressed as:

$$\mu = \left(\frac{C}{C_{90}}\right)^{1.5} \tag{B.2}$$

where C_{90} is the Chezy coefficient based on the sediment particle size exceeded 10% of the time, d_{90}.

The combined shear stress at the bed induced by both waves and the current ($\tau_{b,cw}$) is:

$$\tau_{b,cw} = \tau_{b,c}[1 + \frac{1}{2}(\xi\frac{U_0}{V})^2] \tag{B.3}$$

where $\tau_{b,c}$ is the bed shear stress due to currents only, U_0 is the maximum wave orbital velocity near the bed and the Bijker coefficient ξ can be expressed as:

$$\xi = C\sqrt{\frac{f_w}{2g}} \tag{B.4}$$

in which f_w is the Jonsson wave friction factor (Jonsson, 1966).

Bijker continued on to assume that the bottom transport is present in the near-bed layer with a thickness equal to that of the bottom roughness k_s, and the bed load transport concentration (C_b) could be calculated as:

$$C_b = \frac{q_b}{6.34 k_s u_*} \tag{B.5}$$

with the shear stress velocity u_* as

$$u_* = \sqrt{\frac{\tau_{b,c}}{\rho}} \tag{B.6}$$

Then to make provision for suspended load transport (q_s), Bijker coupled the bed load transport formula to that of Einstein's suspended load transport formula:

$$q_s = 1.83 Q q_b \tag{B.7}$$

where Q is a function of the water depth d, the bed roughness k_s, and the two Einstein Integrals I_1 and I_2. All of which can be expressed by the following equations.

$$Q = [I_1 ln(\frac{33d}{k_S}) + I_2] \tag{B.8}$$

(Values of which can be found in Table B.1.

with

$$I_1 = R\int_A^1 \{\frac{1-\xi}{\xi}\}^b) d\xi \tag{B.9}$$

$$I_2 = R\int_A^1 \{\frac{1-\xi}{\xi}\}^b ln(\xi) d\xi \tag{B.10}$$

where ξ is the dimensionless height (z/d), A is the dimensionless roughness (k_s/d),

$$R = \frac{0.216A^{(b-1)}}{(1-A)^b} \tag{B.11}$$

$$b = \frac{w}{\kappa u_*} \tag{B.12}$$

where κ is the von Karman's constant.

When both the transport modes have been calculated a simple equation exists to calculate the total bed load transport (q_t):

$$q_t = q_b + q_s = q_b(1 + 1.83Q) \tag{B.13}$$

k_s/h	b =0.00		b =0.20		b =0.40		b =0.60		b =0.80	
	Q	q_s/q_b	Q	q_s/q_b	Q	q_s/q_b	Q	q_s/q_b	Q	q_s/q_b
0.00001	303000	554000	32800	60000	3880	7100	527	964	88	161
0.00002	144000	263000	17900	32700	2430	4440	377	689	71.6	131
0.00005	53600	98000	7980	14600	1300	2370	239	438	53.6	98
0.0001	25300	46300	4320	7900	803	1470	169	310	42.7	78.2
0.0002	11900	21800	2330	4260	496	907	119	218	33.9	62
0.0005	4360	7980	1020	1870	260	475	74.3	136	24.6	45
0.001	2030	3720	545	998	158	290	51.2	93.7	19.1	34.9
0.002	940	1720	289	529	95.6	175	35.1	64.2	14.6	26.7
0.005	336	615	123	226	48.5	88.7	20.8	38.1	10.0	18.3
0.01	153	280	63.9	117	28.6	52.3	13.8	25.2	7.3	13.4
0.02	68.9	126	32.8	60.0	16.5	30.2	8.9	16.3	5.2	9.5
0.05	23.2	42.4	13.1	24.0	7.7	14.1	4.8	8.7	3.1	5.7
0.1	9.8	18.0	6.3	11.5	4.1	7.5	2.8	5.1	2.0	3.6
0.2	3.9	7.1	2.8	5.1	2.0	3.7	1.5	2.8	1.2	2.1
0.5	0.8	1.5	0.7	1.3	0.6	1.1	0.5	0.9	0.4	0.7
1	0	0	0	0	0	0	0	0	0	0
k_s/h	b =1.00		b =1.50		b =2.00		b =3.00		b =4.00	
	Q	q_s/q_b	Q	q_s/q_b	Q	q_s/q_b	Q	q_s/q_b	Q	q_s/q_b
0.00001	20.0	36.6	2.33	4.26	0.973	1.78	0.432	0.790	0.276	0.505
0.00002	17.9	32.8	2.31	4.23	0.973	1.78	0.432	0.790	0.276	0.505
0.00005	14.4	28.2	2.28	4.17	0.967	1.77	0.432	0.790	0.276	0.505
0.0001	13.6	24.9	2.25	4.11	0.967	1.77	0.432	0.790	0.276	0.505
0.0002	11.9	21.8	2.21	4.04	0.967	1.77	0.431	0.789	0.275	0.504
0.0005	9.8	17.9	2.13	3.90	0.962	1.76	0.431	0.789	0.275	0.504
0.001	8.4	15.3	2.05	3.76	0.951	1.74	0.430	0.787	0.275	0.504
0.002	7.0	12.8	1.96	3.58	0.940	1.72	0.428	0.784	0.274	0.502
0.005	5.4	9.8	1.78	3.26	0.907	1.66	0.424	0.776	0.273	0.499
0.01	4.3	7.8	1.62	2.96	0.869	1.59	0.417	0.763	0.270	0.494
0.02	3.3	6.0	1.42	2.59	0.809	1.48	0.404	0.740	0.264	0.483
0.05	2.2	4.0	1.10	2.02	0.694	1.27	0.374	0.684	0.249	0.456
0.1	1.5	2.7	0.84	1.53	0.568	1.04	0.339	0.620	0.236	0.432
0.2	0.9	1.6	0.55	1.01	0.414	0.76	0.317	0.580		
0.5	0.3	0.6	0.17	0.32						
1	0	0	0	0						

FIGURE B.1: Einstein integral factor Q values (Anıl Arı Güner et al., 2011)

Appendix C

Photos of Case Studies

C.1 Trekkopje Trench Excavation

C.2 Trekkopje Temporary Works

C.3 Trekkopje Launch-way

Appendix D

Physical Model Time Stepped Images

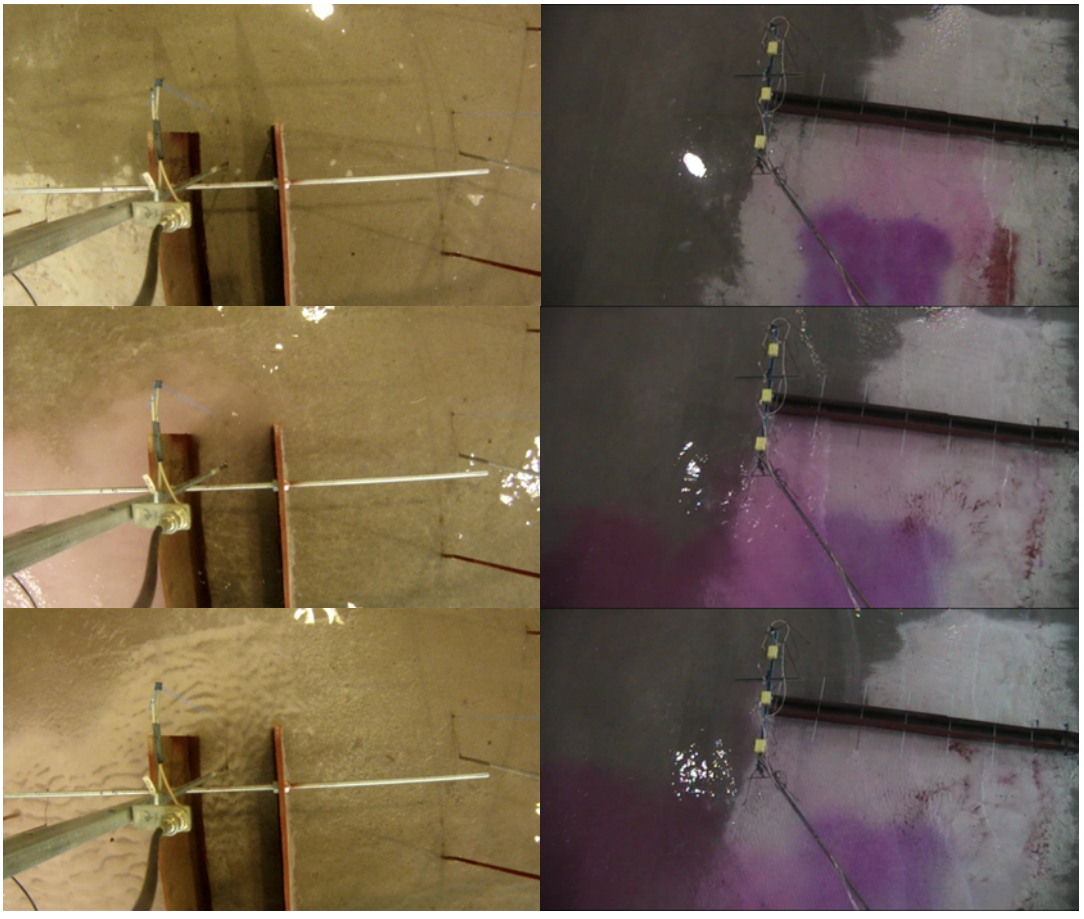

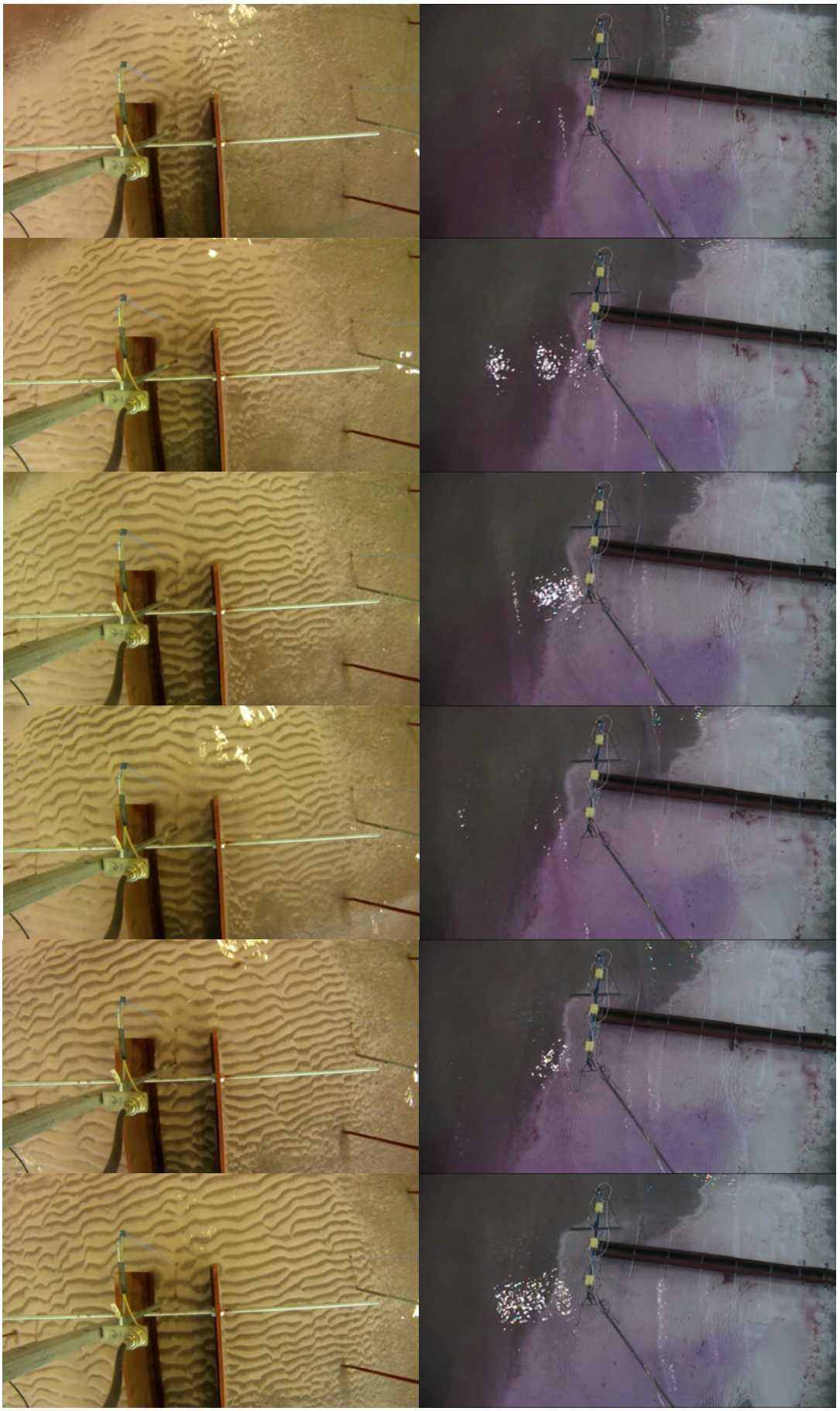

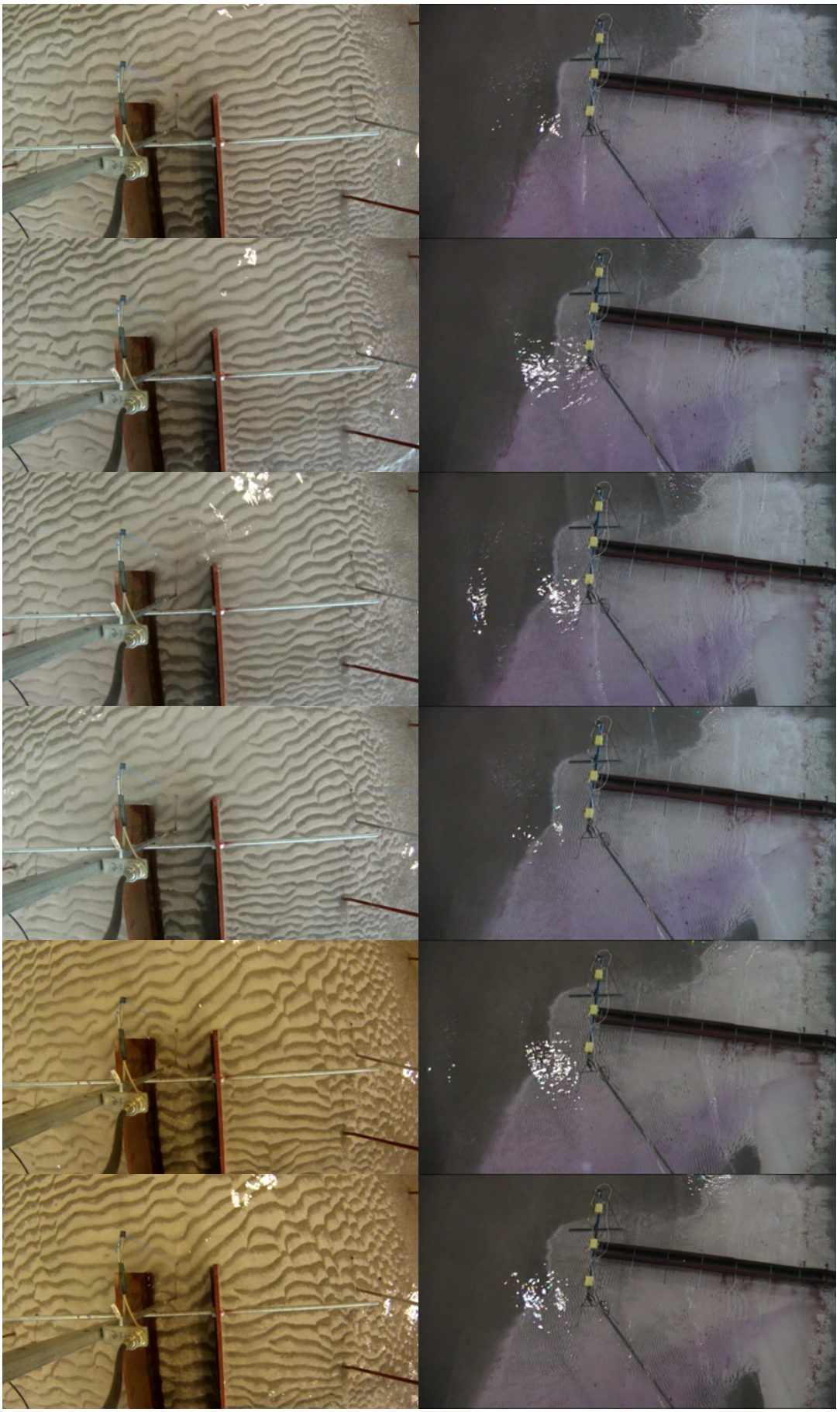

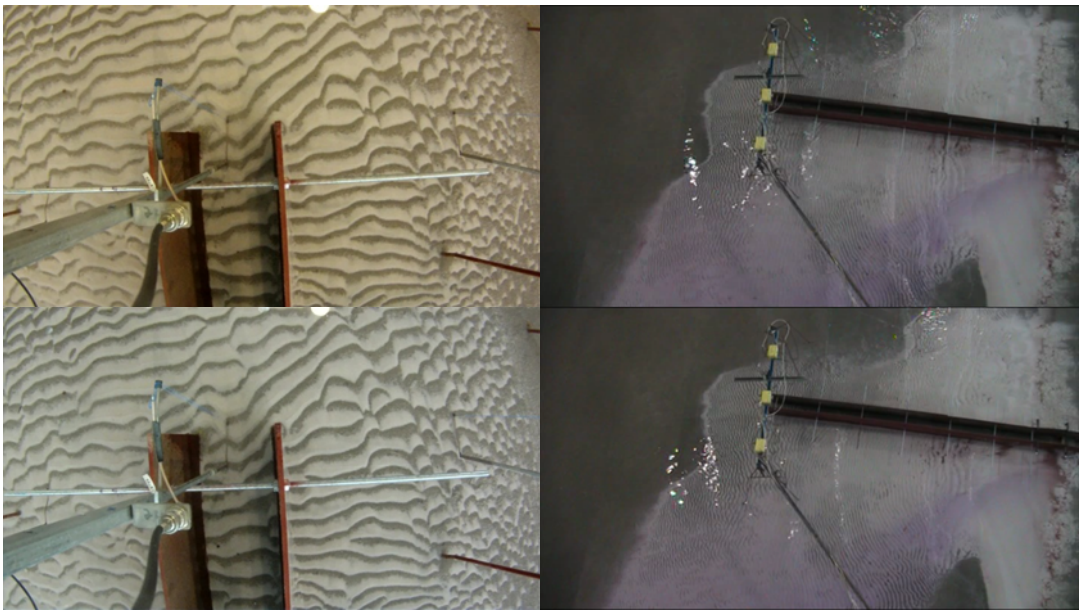

Appendix E

Brief Description of Numerical Model suit - MIKE by DHI

E.1 MIKE

This sub-chapter and those to follow describes the model (MIKE by DHI) used to run the numerical simulation in this study. A general introduction to the full modelling suite is given and then the three models used as one integrated model, is described thereafter.

MIKE developed by DHI is a complete modelling suite that is able to model both inland and coastal scenarios. For the case of this study the focus of MIKE will be drawn to that of the coastal models and the application thereof. Typical applications of the MIKE suite for coastal modelling includes:

- Design data assessment for coastal and offshore structures
- Optimisation of coastal outfalls
- Environmental impact assessment of marine infrastructures
- Coastal flooding and storm surge warnings
- Coastal sediment movement studies

In order to model these scenarios MIKE consist of models including Boussinesq Wave (BW), Mud Transport (MT), Oil Spill, River Channel Design and the three that are relevant to this study, Spectral Waves (SW), Hydrodynamic Flow (HD) and Sediment

Transport (ST) models. MIKE consists of the function to use an integrated flow model where it is possible to model the interaction of some of the above mentioned models. This function, along with a number of pre-processing modules such as the generation of complex sediment tables, allows MIKE to replicate and model complex scenarios in both 2D and 3D.

E.2 Coupled Model Flexible Mesh (FM)

The MIKE 21/3 Coupled Model is a dynamic system which allow the user to integrate a number of MIKE's modules in order to replicate specific scenarios. This system was created with the aim to improve the model accuracy on coastal, estuarine and river environments. The integrated model has the ability to update morphological, hydrodynamic and spectral wave simulations for each specified time step in order to ensure accurate changes in the environment. The MIKE 21 Coupled FM model uses the hydrodynamic model as a base and integrates selected models within its interface according to the modeller's desires. The three modules of interest in this study are the base model namely the Hydrodynamic (HD) model, the Spectral Wave (SW) model and the Sand Transport (ST) model. Using dynamic coupling, the model includes feedback from the two basic computational models, the HD and SW models, in order to replicate realistic sand transport situations.

A short description of each of the three applicable modules will be given next.

E.3 Spectral Waves (SW)

The Spectral Wave module by DHI is a new-generation spectral wind-wave model that has the capability to simulate the growth, decay and transformation of wind generated waves as well as the swell in offshore and coastal areas. The model is both adaptable and flexible in its calculations as it is based on unstructured meshes and includes two different formulations from which the user can chose depending on the modelling situation.

The first of the two formulations is the *Directional decoupled parametric formulation*. It is based on the parameterization of the wave action conservation equation and is determined by creating the parameterization in the frequency domain and then introducing both the zeroth and first order moments of the wave action spectrum as dependant variables (Holthuisjen et al., 1989).

Secondly, there is the *Fully spectral formation* which is based on the wave action conservation equation as described in Komen et al. (1996) and Young (1999), where the directional-frequency is the dependent variable. The model has the ability to calculate wave characteristics in both Cartesian and Spherical coordinates depending on the size and circumstances of the model under consideration.

E.4 Hydrodynamics (HD)

The Hydrodynamic Module consists of continuity, momentum, temperature, salinity and density equations all interacting with the base of the module which is two-dimensional shallow water equations, better defined as the depth-integrated incompressible Reynolds averaged Navier stokes equations. The module can be defined in both Cartesian and Spherical coordinates depending on the modelling situation. The HD model is also capable of incorporating unstructured meshes in the horizontal plane comprising of either triangles or quadrilateral elements. It is also possible to handle discontinuous situations as the computation of the convective fluxes is determined by using an approximated Rienmann solver.

The HD module is thus a powerful tool in the solving of numerical problems within the coastal area.

E.5 Sediment Transport (ST)

The Sediment Transport module of MIKE 21 is a suite that determines the movement of non-cohesive sediment within a certain area. It can calculate sediment transport patterns for both pure current applications or for applications with both wave and current information. The output of this module cannot replace that of a full morphological model but is able to calculate values and visualizations of parameters such as sediment transport rates and initial rates of bed level change.

The module is able to interact with detailed sediment tables generated by MIKE's pre-processing modules to ensure accurate grading of sediment throughout the model area. By using this feature it is possible to implement spatially varying bed material to model the interaction between water systems. The module gives the user a choice of five different sand transport theories in the pure current simulation option including Engelund and Hansen total-load transport theory, Engelund and Fredsoe total-load transport theory, Zyserman and Fredsoe total-load transport formulation, Meyer-Peter and Müller bed-load transport theory and Ackers and White total-load transport

formulation. It however only gives a choice of two simulation theories in the combined wave and current option namely; the application of DHI's deterministic intra-wave sediment transport model or the total-load transport method of Bijker's.

Appendix F

Validation of Scenario 02

The following 6 images are that of Scenario 02 (straight structure with a length of 100 m). These images are referenced in Chapter 5 during the validation of the numerical model.

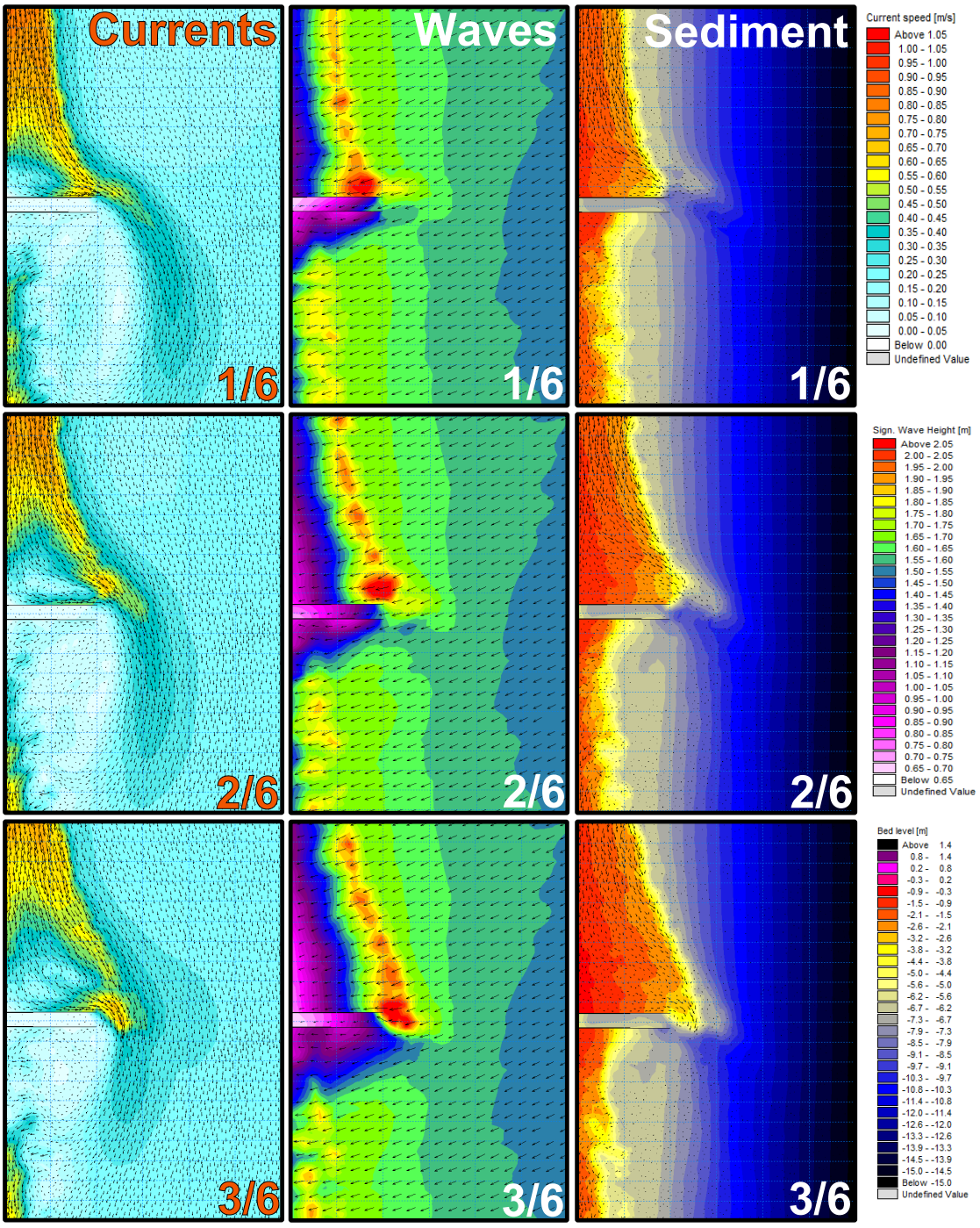

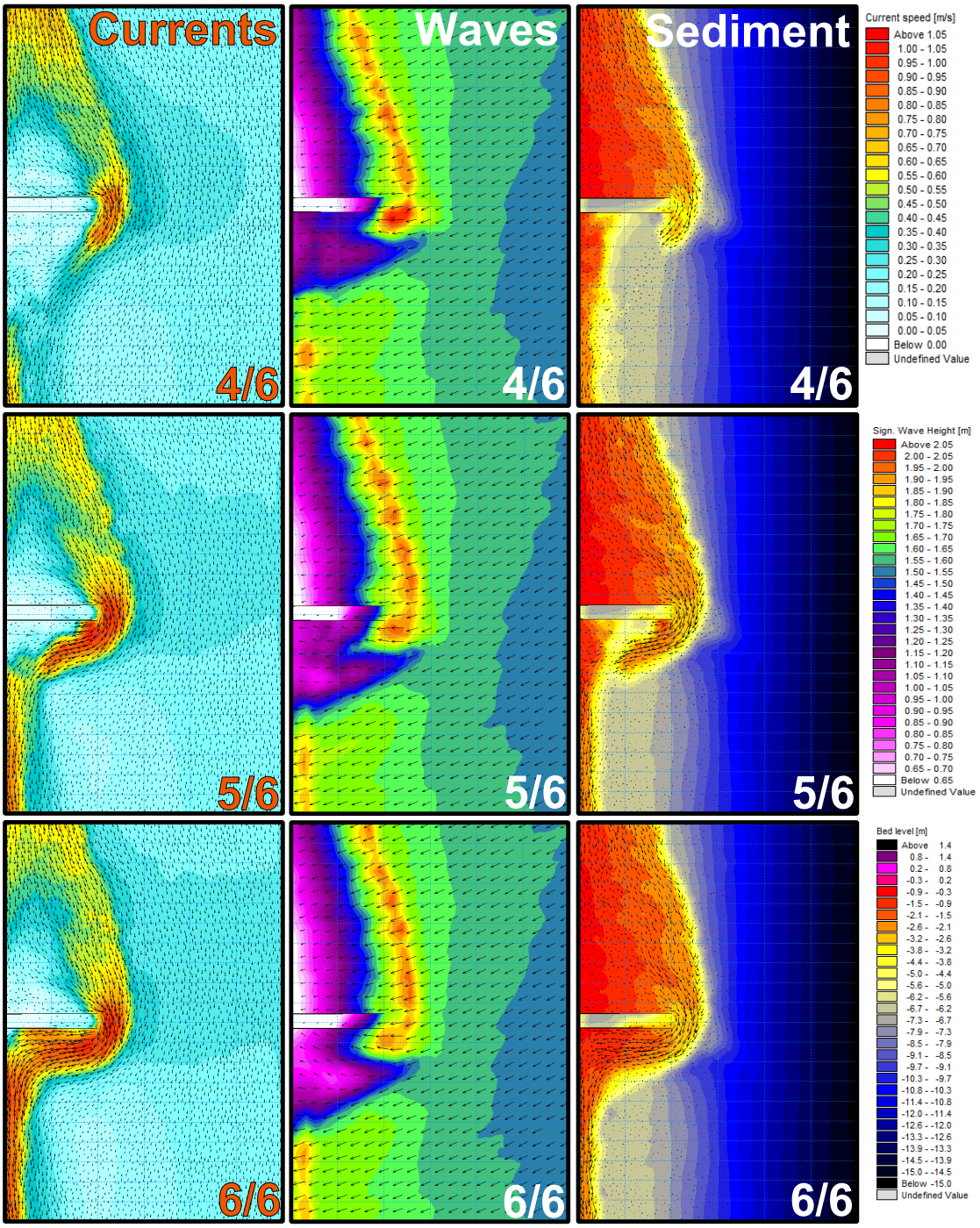

Appendix G

5 Failure Point for Each Scenario

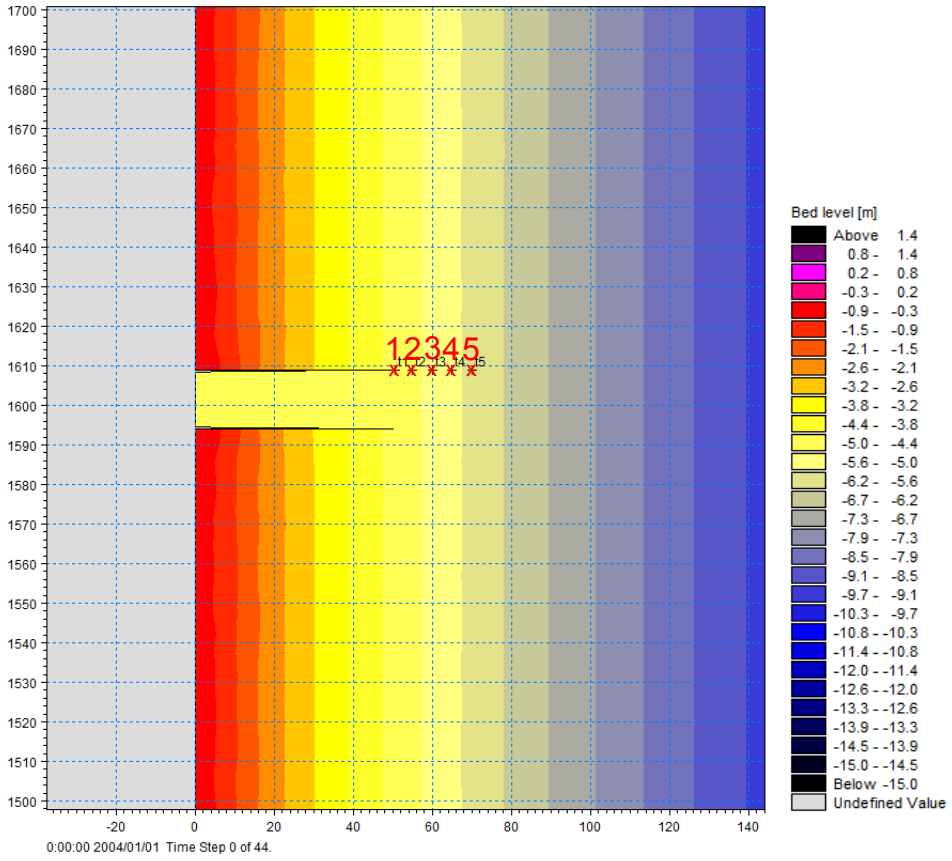

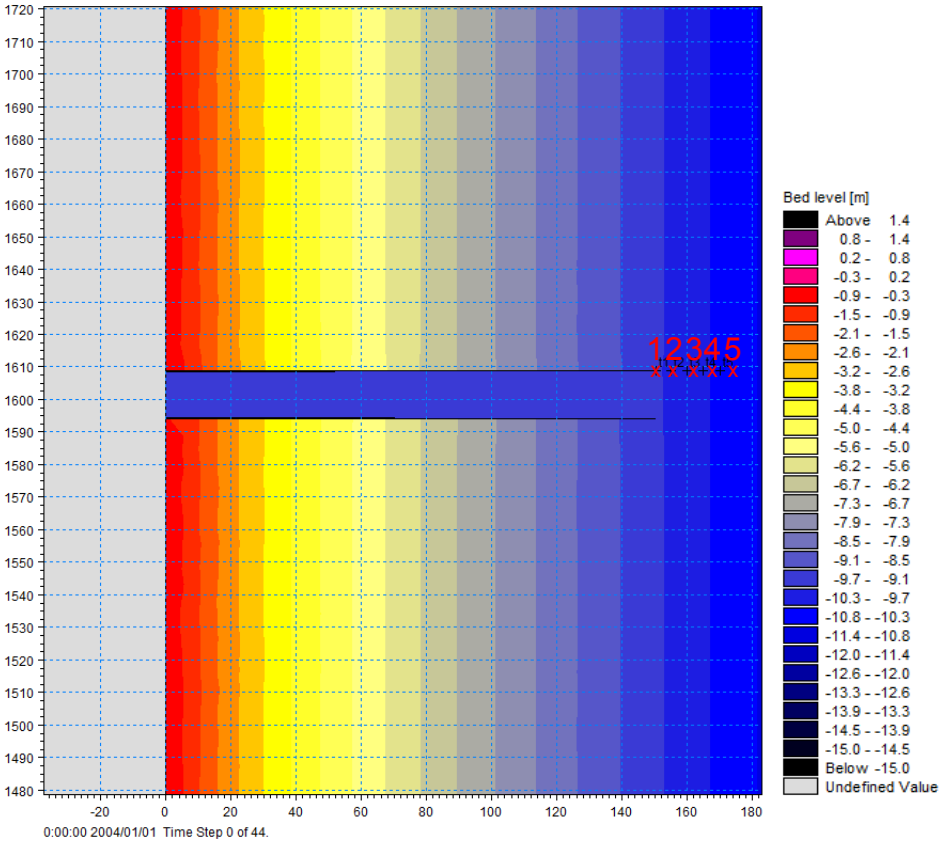

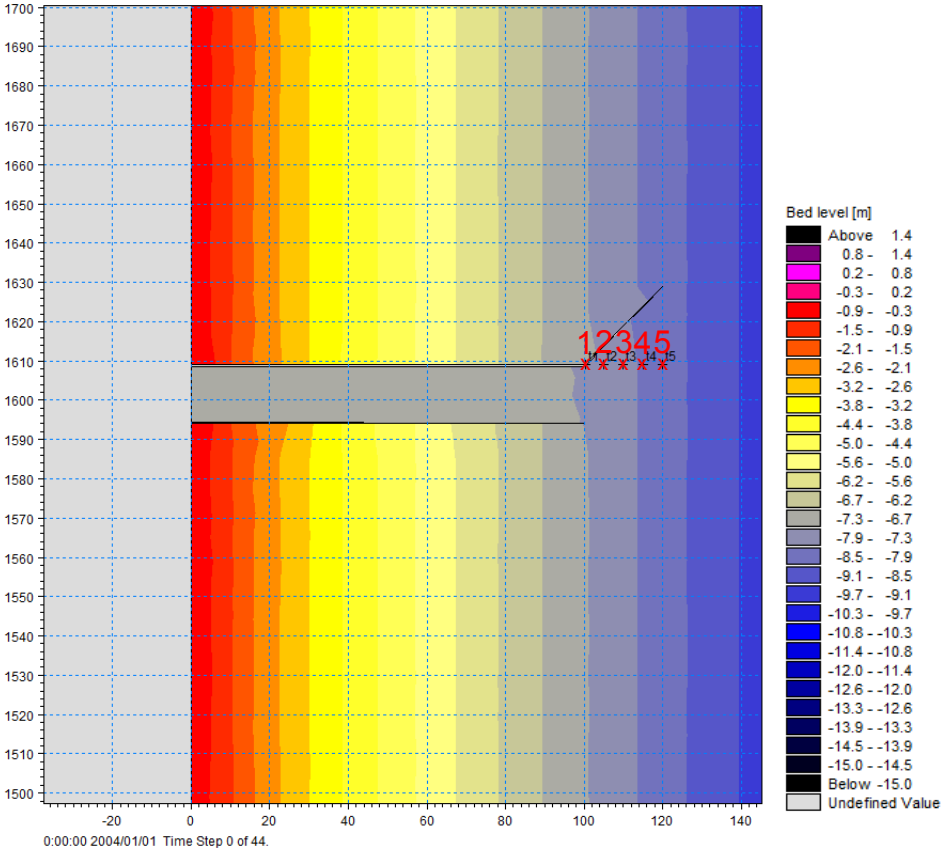

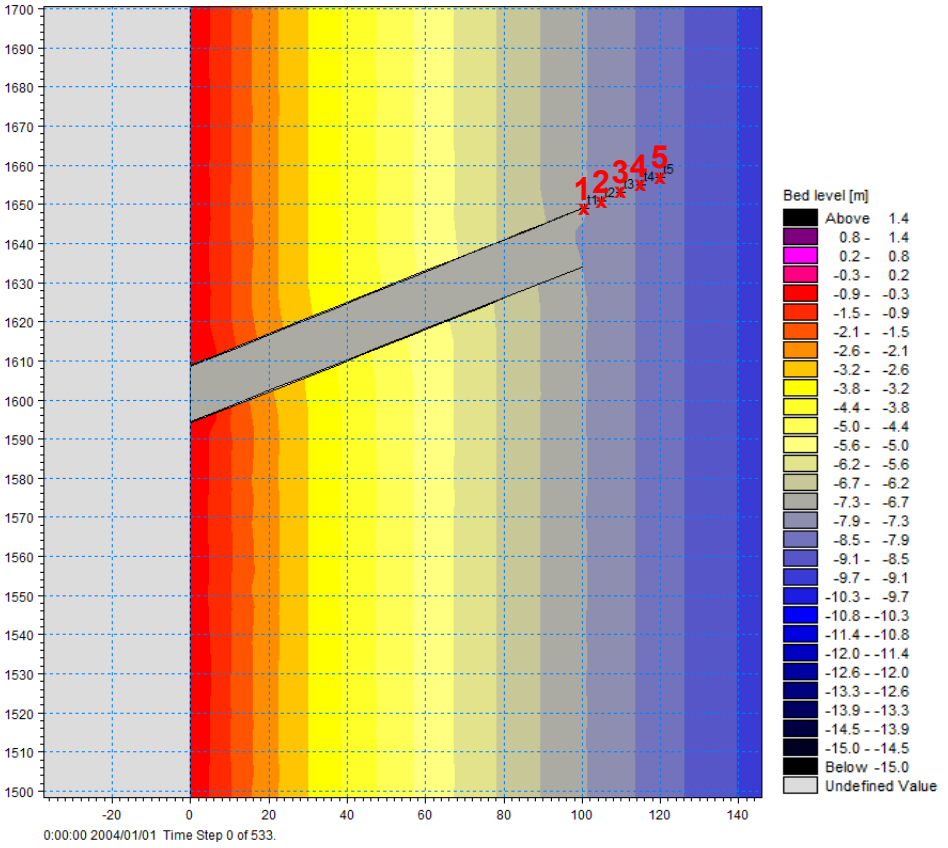

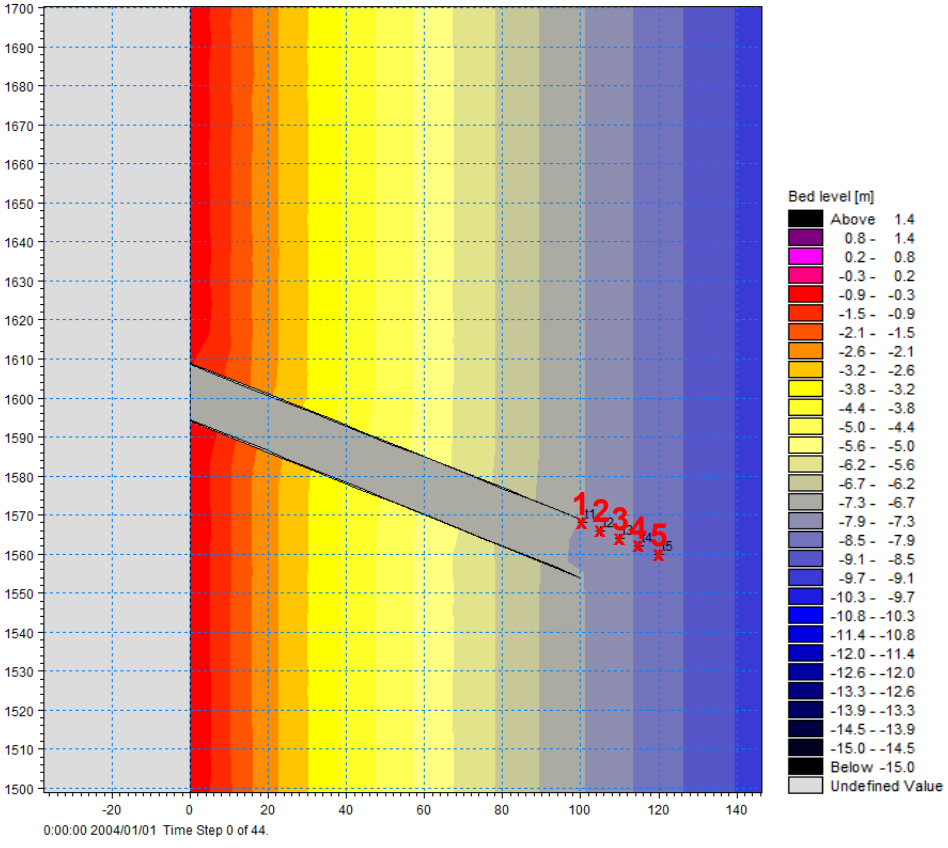

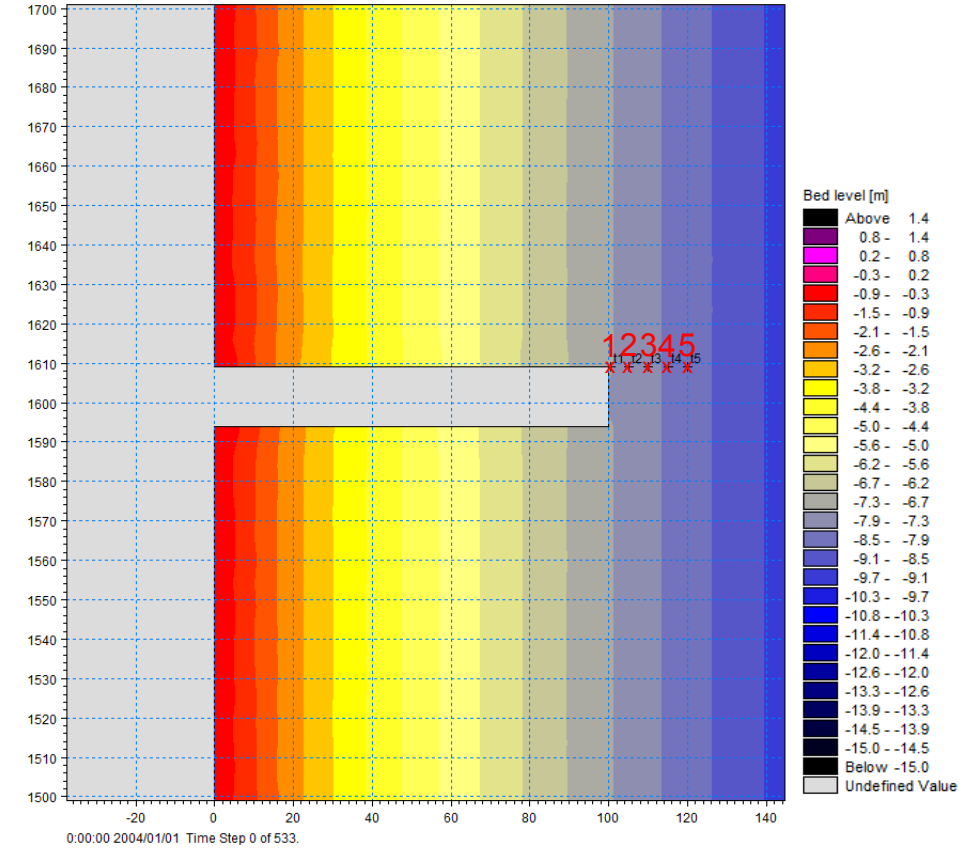

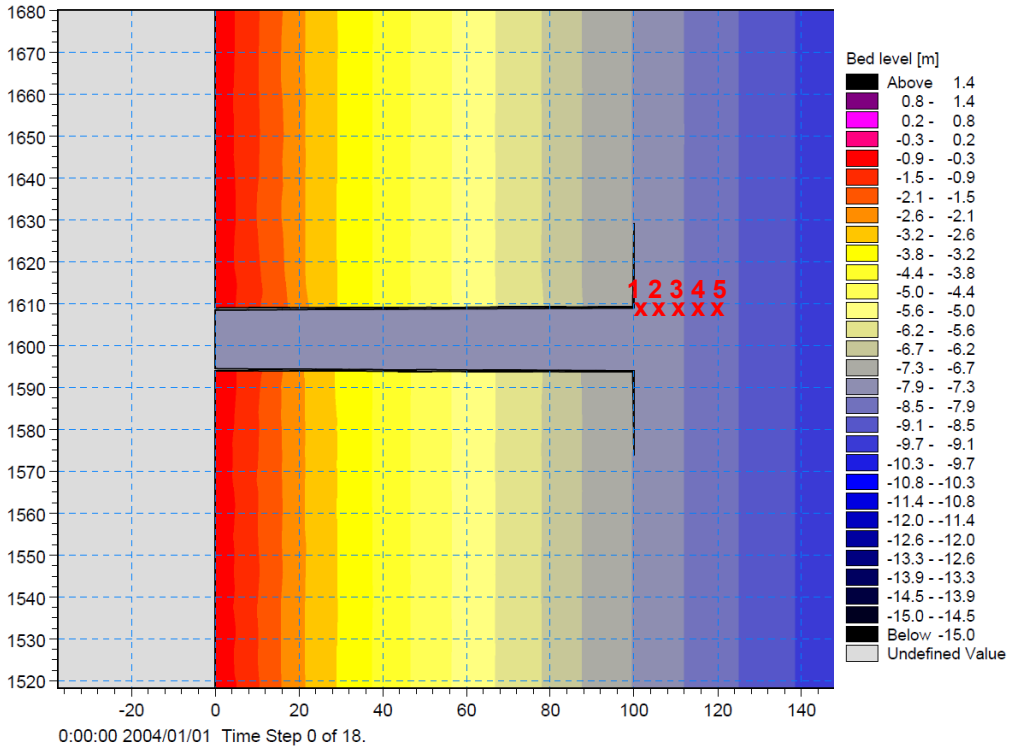

Appendix H

Bed Level Change vs Time Graphs